ELECTRICAL SWITCHING CHARACTERISTICS AND THERMAL PROPERTIES OF TELLURIUM BASED CHALCOGENIDE GLASSY ALLOYS

Thesis

Submitted in partial fulfilment of the requirements for the degree of

DOCTOR OF PHILOSOPHY

by

BRIAN JEEVAN FERNANDES

DEPARTMENT OF PHYSICS

NATIONAL INSTITUTE OF TECHNOLOGY KARNATAKA

SURATHKAL, MANGALORE – 575025

FEBRUARY, 2019

DECLARATION

by the Ph.D Research Scholar

I hereby declare that the Research Thesis entitled **"**Electrical Switching Characteristics and Thermal Properties of Tellurium Based Chalcogenide Glassy Alloys", which is being submitted to the National Institute of Technology Karnataka, Surathkal in partial fulfillment of the requirements for the award of the Degree of Doctor of Philosophy in Physics is a *bonafide report of the research work carried out by me*. The material contained in this Research Thesis has not been submitted to any University or Institution for the award of any degree.

Brian Jeevan Fernandes
Reg. No: 112026PH11F06
Department of Physics

Place: NITK, Surathkal
Date:

CERTIFICATE

This is to *certify* that the Research Thesis entitled **"**Electrical Switching Characteristics and Thermal Properties of Tellurium Based Chalcogenide Glassy Alloys", submitted by Brian Jeevan Fernandes (Register Number: 112026PH11F06) as the record of the research work carried out by him, is *accepted as the Research Thesis submission* in partial fulfillment of the requirements for the award of degree of Doctor of Philosophy.

Chairman-DRPC

Date:

Prof. N.K Udayashankar

Research Guide

ACKNOWLEDGEMENT

The satisfaction that accompanies the successful completion of any task would be incomplete without a mention of the people who have made it possible, and whose constant guidance and encouragement crown all the efforts with success.

I dedicate my sincere thanks to my research supervisor Prof. N. K. Udayashankar, Department of Physics, NITK, for providing me an opportunity to pursue research work. His constant motivation, inspiration and academic support is highly appreciated. I thank him for introducing me to the field of chalcogenide glasses. I shall always cherish the academic freedom that I have enjoyed under his guidance. His views on academics and life have instilled in me the confidence to pursue my research career.

I am highly indebted to Dr. K. Ramesh, Principal Research Scientist, IISC Bangalore, for providing me the opportunity to carry out certain experiments in his lab. I also thank him for taking keen interest in my work and for his constant monitoring and invaluable guidance and support throughout the course of my thesis. I profusely thank him for having patience to clear my doubts and to channelize my efforts. His cheerful disposition made my work all the more enjoyable.

I would like to extend my sincere gratitude to the H.O.D. and all other faculty members of the Dept. of Physics, NITK, for their encouragement and support. I am also thankful to the non-teaching staff for their technical support. I take this opportunity to thank my RPAC members, Dr. Ravishankar, Dept. of Metallurgy and Prof. (Mrs.) H. D. Shashikala, Dept. of Physics, for their valuable suggestions and critical remarks during the progress presentations.

I am also grateful to Dr. Kishore Sridharan for assisting my manuscript writing and data compilation. I thank Dr. Jean Maria Fernandes for her help in compiling the thesis. I am grateful to Mr. Sundaraman and Mr. Harish, Indfurr Superheat Furances, Chennai, for their help in instrumentation and also for funding the filing of our patent. Their goodwill and support is greatly acknowledged. Special thanks to Mr. Lokesh Venkataswamy, CEO and Managing Director and Mrs. Suchetha M. S., Sr.

Consultant and Researcher, Innomantra Consulting Private Limited, Bangalore, for facilitating the patent process.

I am fortunate to have friends like Shivani, Aditya, Saurab, Rathan, Ramyesh, Nishith, Rinuraj, Amrith, Prashanth Preethi, Advithi and Pradeep; their informal support and encouragement has been indispensable. The invaluable help and the memorable company of my lab mates and colleagues, Naveen, Mahendra, Suchitra, Karthik, Achyutha, Bindu, Amudha, Brijesh, Soumalya, Kiran and Ramana will be cherished forever. I would like to particularly acknowledge the contribution from my friends at IISc, Dr. Pumlian Munga, Naresh, Venkatesh and Vivek, in terms of their friendly companionship and valuable suggestions. I humbly acknowledge the assistance provided by the central facilities of NITK for XRD and SEM Analysis.

My deepest gratitude goes to my family members for their unflagging love and support throughout my thesis work. I am indebted to my father Mr. Benedict Fernandes and mother Mrs. Josephine Rodrigues for their love, care and the support during all these years. I fondly recall the continuous encouragement and moral support from my wife Nolita Dolcy Saldanha. I also extend my thanks to my sisters and my in-laws. It is my duty to thank all the teachers who taught me at different stages of my life.

Above all, I give thanks to Lord Almighty with my whole heart for his steadfast love and blessings.

Brian Jeevan Fernandes

ABSTRACT

Chalcogenide compounds have gained considerable research interest in the recent past owing to their capability to transform from an amorphous to crystalline phase and exhibit entirely different electrical properties that can be applied in building new class of memories such as phase-change memories, programmable metallization cells and cross-point devices. The present thesis is focussed on the study of the electrical switching behaviour and thermal properties of Te-based ternary chalcogenide glassy alloys to understand the effect of metallic dopants on switching voltages and their thermal characteristics. A novel approach to prepare chalcogenide glassy alloys has been discussed. In this work, two series of chalcogenide systems, namely Ge-Te-Sn and Si-Te-Bi were chosen to study the electrical and thermal properties of these systems. I-V characteristic studies revealed that all the samples prepared had a smooth memory type switching property. Scanning electron microscopy (SEM) studies on pre- switched and post switched samples revealed the morphological changes on the surface of the sample such as the formation of the crystalline filament between two electrodes during switching. Furthermore, the studies on the sample thickness and temperature dependence on switching voltages revealed the nature of switching mechanism.

Differential scanning calorimetric (DSC) studies have been undertaken for the thermal analysis of Ge-Te-Sn and Si-Te-Bi chalcogenide samples. We have investigated the crystallization kinetics of prepared chalcogenide glassy systems. Thermal parameters such as change in specific heat (ΔC_p), fragility index (F), thermal stability (ΔT), enthalpy (ΔH_c) and entropy (ΔS) are deduced to interpret distinct material behaviour as a function of composition. Structural evaluation like thermal devitrification studies and morphological changes elucidate on restricted glass formability of the Te-based chalcogenide glass system. Finally, the relationship has been established between the thermal parameters and electrical switching characteristics.

Keywords: Chalcogenides, Electrical switching, Metallicity factor, Differential scanning calorimetry (DSC), Thermal devitrification studies.

CONTENTS

LIST OF FIGURES

LIST OF TABLES

NOMENCLATURE

PCM	*Phase change memory*
CD-RW	*Rewritable compact disc*
BD-RE	*Blu-ray disc format*
LRO	*Long range order*
SRO	*Short range order*
GFT	*Glass forming tendency*
GFA	*Glass forming ability*
ChG	*Chalcogenide glasses*
CCNR	*Current controlled negative resistance*
RPT	*Rigidity percolation threshold*
CT	*Chemical threshold*
VAP	*Valence alteration pair*
DSC	*Differential scanning calorimetry*
RPM	*Rotations per minute*
XRD	*X-ray diffraction*
SEM	*Scanning electron microscopy*
FESEM	*Field emission scanning electron microscopy*
EDS	*Energy dispersive x-ray spectrum*
V_T	*Threshold/Switching voltage*
T_g	*Glass transition temperature*
T_c	*Crystallization temperature*
T_m	*Melting temperature*
eV	*Electron volt*
E_F	*Fermi energy*
σ_o	*Pre-exponential factor*
$N(E_F)$	*Density of states*
W	*Hopping energy*
E_A	*Energy in the tail state*
ΔE	*Thermal activation energy*
k_B	*Boltzmann constant*

T	*Temperature in Kelvin*
D	*Sample thickness*
k	*Thermal conductivity*
λ	*External heat conductivity*
ε	*Threshold voltage - activation energy*
E_c	*Onset crystallization activation energy*
E_p	*Peak crystallization activation energy*
ΔT	*Thermal stability*
S	*Saad and Poulin parameter*
H_r	*Hruby parameter*
E_t	*Switching field*
dH/dt	*heat flow measured in mcal sec^{-1}.*
ΔC_p	*Change in specific heat*
ΔH_c	*Change in Enthalpy*
η	*DSC instrumental constant ~ 1.12*
A	*Area under the exothermic curve(crystallization peak)*
m	*Mass of the chalcogenide sample*
F	*Fragility index*
α	*Heating rate of DSC furnace*
R	*Universal gas constant*
ΔS	*Change in entropy*
T_{rg}	*Reduced glass transformation temperature*

CHAPTER 1

INTRODUCTION

This chapter outlines the fundamental aspects of amorphous semiconductors and explains the nature of glassy state and glass forming ability. This chapter also gives an account of electrical switching phenomenon and its correlation with thermal properties. It is then followed by the literature survey. The scope of the present thesis and objectives are mentioned.

1.1 BACKGROUND AND MOTIVATION

The field of amorphous and disordered materials technology constitutes an integral part of Materials Science. Due to its significant impact on the largest and most fundamental areas of global economy, namely the information and energy, this field has been receiving increasing attention since the past few decades. The properties of amorphous and disordered materials enable their use in devices for encoding, switching, transmission and information storage. The first demonstration of switching and memory devices dating back half a century was based on the amorphous semiconductors known as chalcogenide glasses (Ovshinsky 1968a). These glassy chalcogenide semiconductors exhibit a scientifically interesting and technologically important phenomenon known as Electrical Switching which has applications in areas such as information storage, power control, etc.(Asokan and Lakshmi 2012). Information storage devices based on chalcogenides are generally known as phase change memory (PCM) devices. PCM materials exist in at least two structurally distinct solid phases: amorphous and one (or more) crystalline phase and they store information in these phases (Lencer et al. 2011).

It is worth noting that the effects of electrical switching in chalcogenide glassy semiconductors have been actively investigated since the beginning of the 1960s. The beginning of these studies was the discovery of the switching effect by B. Kolomiets and E. Lebedev from the Physico-Technical Institute (Leningrad) in 1960. Ovshinsky was the first to propose that memory effect is related to crystallization. Over the past four decades, attention has been devoted to the material properties of Te - based binary and ternary chalcogenide compounds. Although electrical switching has been

discovered in the year 1960, it has been exploited of late for the development of non-volatile RAM (Reinberg 1998). Rewritable optical storage (CD-RW) introduced in the year 1996 (Kato et al. 1999) holds its position even now in the form of Blu-ray disc format (BD-RE). The phase change memory emerges to be the most promising next generation semiconductor technology due to its multi-bit capability, higher scalability, higher endurance in read/write operations and lower cost and compatibility over existing metal oxide semiconductor technology (Maimon et al. 2001; Zhou 2001). Chalcogenide materials find use in many of the applications which have been shown in the Figure 1.1.

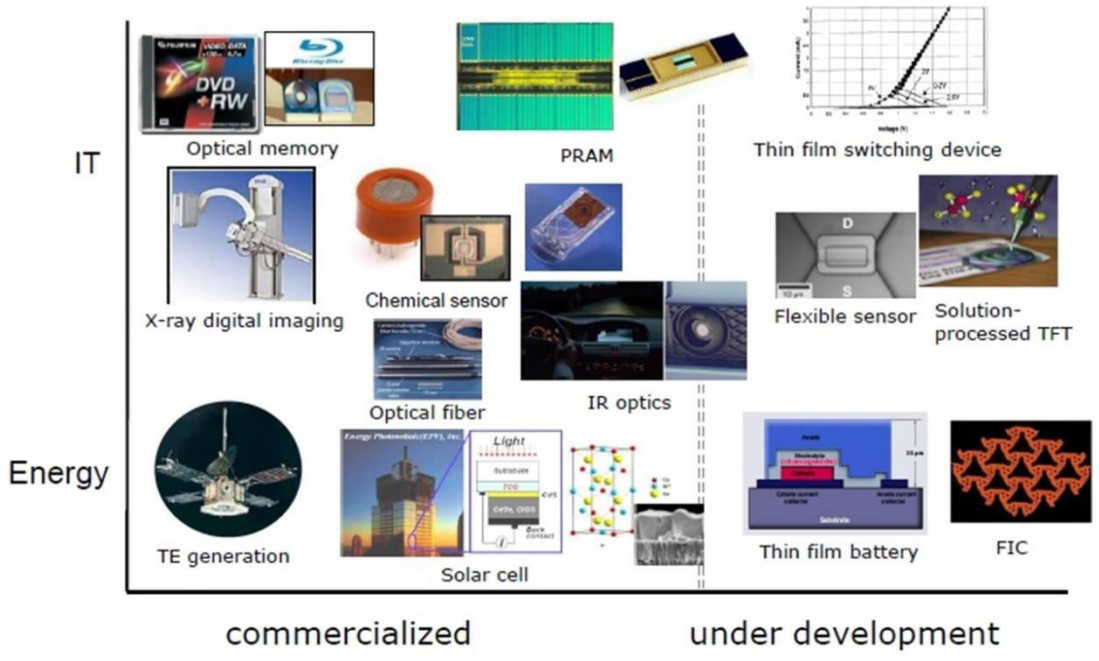

Figure 1.1 Applications of chalcogenide materials

Apart from many of these applications, there exists a wide scope for investigation of switching mechanisms involved in understanding phase change materials. Studies on electrical switching and thermal properties help us in identifying newer chalcogenide glasses which could be used for PCM applications. In order to synthesize suitable memory materials, selection of proper compositions is essential. This can be achieved by studying the compositional dependence of electrical switching parameters and investigating the correlation between switching behavior and other material properties such as thermal properties, glass forming ability, activation energy, etc.

1.2 GENERAL PROPERTIES OF AMORPHOUS MATERIALS

Amorphous or non-crystalline solids represent a unique class of structurally disordered materials. They differ from their crystalline counterparts by the absence of long range periodicity. However, one finds close structural similarities between crystalline and non-crystalline materials, particularly in the nearest neighbor around each atom (Elliott 1991; Zallen 2008). Hence, amorphous materials are known as disordered materials and disorder implies a defective order and not complete randomness. Though there is no long range order (LRO) present in the amorphous solids, they possess a high degree of short range order (SRO) (Elliott 1991). Long range periodic constraints require careful and controlled preparative conditions. As the glassy materials are free from these constraints, they can be prepared in varied compositions with comparatively less cost. According to theoretical consideration, almost all materials can be obtained in amorphous state if they are cooled fast enough from their molten state, so as to arrest the disorder contained in liquid state into the solid state (Debenedetti and Stillinger 2001). Many generic terms such as disordered, amorphous, glassy, etc., are used to refer to non-crystalline solids. Two-dimensional illustrations of arrangements of atoms in the crystalline and non-crystalline (amorphous) materials are as shown in the Figure 1.2.

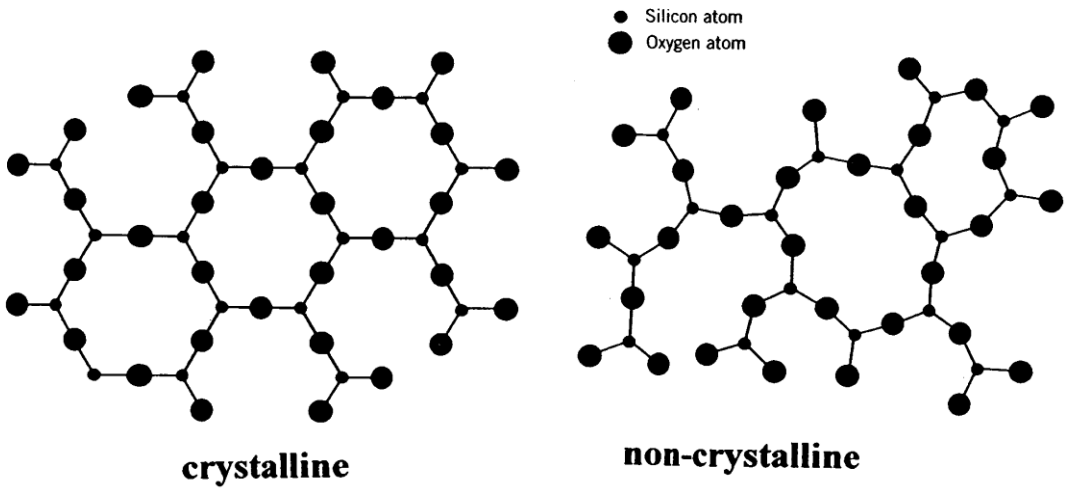

Figure 1.2 Two-dimensional illustrations of arrangements of atoms in the crystalline and non-crystalline (amorphous) materials

Like their crystalline counterparts, non-crystalline materials can be ionic, covalent or metallic bonded materials. Consequently, they can be insulating, semiconducting or metallic in nature (Adler 1971). Glassy alloys prepared by rapid quenching of the melt are excellent conductors of electricity(Gilman 1975). Crystalline and amorphous semiconductors are potential materials in electronic devices. Amorphous semiconductors can be generally classified into two groups, namely tetrahedral semiconductors (a-Si, a-Ge, etc.) and lone-pair semiconductors or chalcogenide semiconductors (GeTe, SiTe, $Ge_2Sb_2Te_5$). Chalcogenide glasses have gained much attention as they exhibit interesting phenomena like switching, memory effects and photo darkening, etc. (Ovshinsky 1968b). Due to the fascinating feature such as electrical switching and its potential applications in memory devices, the field of amorphous semiconductors has become an interesting area of research and development.

1.3 NATURE OF GLASSY STATE

The phenomenon of glass transition can be understood by considering the fact that two events may occur when a material is cooled from the melt. Often, crystallization takes place at the melting temperature T_m, with discontinuous changes in the first order extensive thermodynamic parameters like volume, entropy and enthalpy (Kauzmann 1948). In certain cases, the liquid can become super cooled at temperature below T_m, becoming more viscous with decreasing temperature. At one particular temperature called the glass transition temperature (T_g), these liquids freeze into a solid which is structurally rigid but possesses no long range order. Meanwhile, glassy solids when heated, exhibit glass to super cooled liquid transition at Tg. Unlike the liquid - crystal transition the liquid- glass transition is characterized by a gradual change in volume, entropy and enthalpy (Kauzmann 1948). Although the first order thermodynamic variables are continuous, there are usually sharp changes in second order thermodynamic variables. The typical variations in the thermodynamic parameters at the glass transition are shown in the Figure 1.3.

1.4 GLASS FORMING ABILITY

The glass forming tendency (GFT) or glass forming ability (GFA) has been a subject of much interest due to the technological importance of the composition dependent glassy materials. On the basis of structural, thermodynamic and kinetic factors, various models have been proposed to understand the origin of glass formation. However, there is no structural rule which may be used universally to predict GFA in any given system. Numerous factors are believed to decide the GFA of any particular

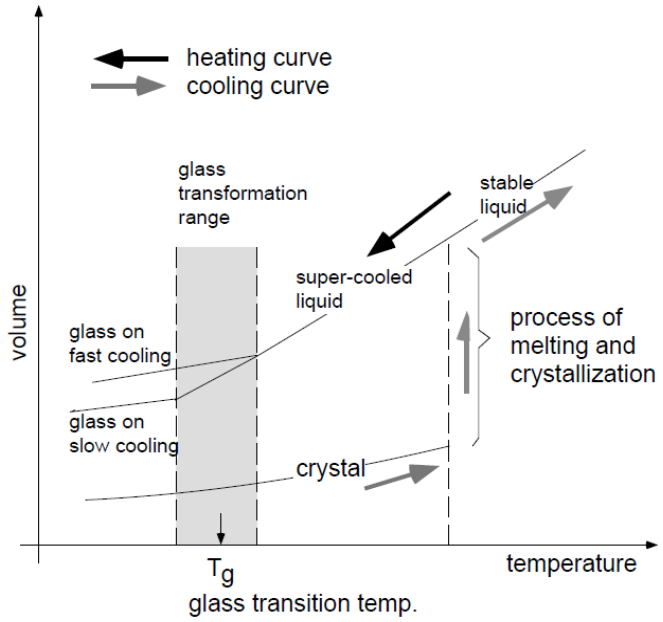

Figure 1.3 Volume vs. temperature curve showing the phenomenon of glass transition and crystallization

glassy material. In the glassy chalcogenide, important parameters like compound formation and the resulting atomic structure, viscosity of the melt, cooling rate and the frustration in a multicomponent melt are found to influence the GFA (Elliott 1991). The GFA is said to increase the covalency of the additive element and decrease with size (Cornet and Rossier 1973). In terms of composition, the GFA decreases with increasing atomic mass. For example, GFA of elements belonging to a particular column in the periodic table follows the following order(Borisova 2013; Hilton 1970).

Si > Ge > Sn > Pb

O > S > Se > Te

P > As > Sb > Bi

Many oxide glasses can be formed even with the cooling rate slower than 1K/ h, whereas most of the metallic glass require cooling rate of the order 10^6 K/s (Elliott 1983). Further, efforts have been made by Phillips to understand the compositional dependency of GFA on the basis of percolation in network rigidity using constraint theory (Phillips 1979; Phillips and Thorpe 1985). It is interesting to note from Figure 1.4 that chalcogenides display wider range of chemical bonds of all types, out of which tellurides are rarely found to bond with trivial ionic or covalent contributions, leading to relatively metallic bond properties (expressed as resonance bonds), heading to exhibit interesting electrical properties (Waser et al. 2010). Meanwhile, in our current study, we have doped $Si_{20}Te_{80,}$ $Si_{15}Te_{85}$ and $Ge_{20}Te_{80}$ with a heavy metal such as Bi and Sn, respectively. It is obvious that excess of heavy metal atoms decreases covalent nature of the bond, adding to their ionic/metallic bond properties. This in turn decreases the viscosity of the molten alloy, leading to the complexity to arrest the molten alloy in vitreous form. Hence, metallicity factor (more metallic in nature), breaking of covalent bonds and growth of microcrystals in the amorphous background restrict the glass formability of Si-Te-Bi and Ge-Te-Sn system to the narrow glass forming region. In this thesis, effort has been made to explain the reason for narrow glass formability and suitable quenching methods to prepare glassy alloys with the help of improved furnace design.

1.5 ELECTRICAL PROPERTIES

The electrical and optical band gaps for chalcogenide glasses (ChG) lie in the range of 1-3 eV, and are thus called amorphous semiconductors. The gap increases in the pattern Te < Se < S, reflecting metallic characters in Te based chalcogenides (Mehta 2006). Structural defects play an important role in electrical properties in ChG. In the amorphous phase, the position of the Fermi level and the presence of defect states within the optical gap (or the mobility gap) have been extensively addressed throughout the course of phase change materials research. Amorphous solids can

exhibit a much wider range of defects, among which charged defects are the most important in chalcogenide glasses (Adler 1980).

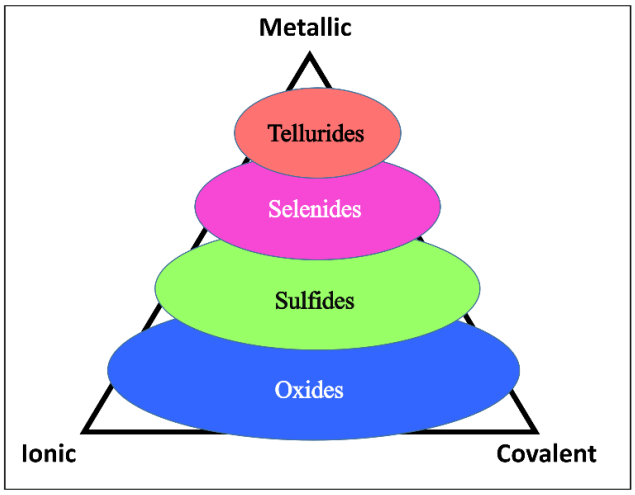

Figure 1.4 Pictorial representation of bond characters of chalcogenides in triangular form displaying wide range of bond types such as, ionic bonds, covalent bonds and metallic bonds (Waser et al., 2010)

Amorphous semiconductor properties such as magnetic properties, opto-electronic behavior, vibrational properties, mechanical characteristics, etc., are controlled by the intrinsic defects which exist in the gap states. This is due to the low creation energy of these defects and hence they can be present in concentrations sufficiently large enough to control the transport behavior (Mott and Davis 1979). Hence, defects turn out to be essential for the conduction properties and electrical switching process. The band of states existing near the centre of the gap arises from specific defect characteristics of the material like dangling bonds, interstitials, etc. Thus, the band structure of the ChG specifically defines its property as shown in the Figure1.5

1.5.1 DC conductivity in chalcogenide glasses

The dc conductivity of chalcogenide glasses can be well understood within the frame work of Davis and Mott model. It predicts three regions of conductivity, (i) extended states conduction, (ii) conduction in band tails and (iii) conduction in localized states at the Fermi energy E_F.

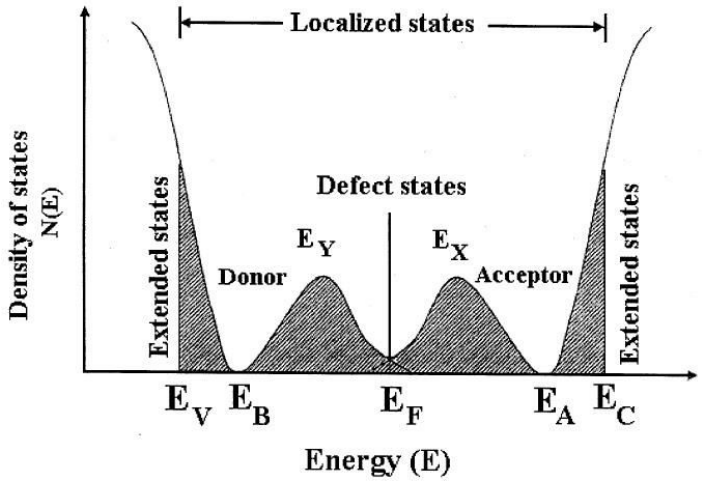

Figure 1.5 Electron band structure model of an amorphous semiconductor, showing band tailing and states within the mobility gap. E_v and E_c are the mobility edges.

(i) Extended state conduction

Conductivity in the extended states is characterized by large mobility, which according to Mott decreases sharply at the mobility edge E_c (or E_v) (Nagels 1979). Assuming a constant density of states and constant mobility, the conductivity was shown to vary as

$$\sigma = \sigma_o exp\left(-\frac{E_c - E_F}{kT}\right) \quad \text{.....(1.1)}$$

where the pre-exponential factor σ_o is

$$\sigma_o = \exp N(E_c) kT \mu_c \quad \text{.....(1.2)}$$

Where $N(E_c)$ is the density of states at mobility edge E_c and μ_c is the mobility. Electrons at and above E_c can move freely while those below it cannot, except through activated hopping.

(ii) ***Conduction in the Band tail***

Conduction via band tails takes place by exchange of energy with a phonon. The conductivity σ is given by

$$\sigma_{hop} = \sigma_{0hop} exp\left(-\frac{E_A - E_F + W}{kT}\right) \quad \text{.....(1.3)}$$

where W is the hopping energy (Nagels 1979) and E_A is the energy in the tail state.

(iii) Conduction in the localized state at the Fermi Energy

In the third region (conduction in the localized states), carriers move between states located at E_F via phonon assisted tunnelling process which is analogous to impurity conduction observed in heavily doped and lightly compensated semiconductors at low temperatures. The temperature dependent hopping conductivity can be expressed as (Mott and Davis 1979)

$$\sigma = \sigma_0 exp\left(-\frac{W}{kT}\right) \quad \text{.....(1.4)}$$

where W is the energy difference between the two localized states ($(W = E_A \sim E_B)$

At room temperature, the dc conductivity of most of these glasses obeys the Arrhenius relation given by equation

$$\sigma = Cexp\left(-\frac{\Delta E}{kT}\right) \quad \text{.....(1.5)}$$

where C is the pre-exponential factor and ΔE is the thermal activation energy for electrical conduction. The value of the conductivity activation energy (ΔE) varies from 0.3 to 1 eV.

1.5.2 Electrical switching in chalcogenide glassy alloys

Electrical switching refers to an electric field driven transition exhibited by amorphous/glassy chalcogenides from a semiconducting OFF state to a conducting ON state which can be of two types, viz.: (1) memory and (2) threshold switching. Memory switching is a phenomenon which involves a structural phase transition (amorphous - crystalline); whereas, threshold switching is a process particular to the amorphous phase and does not involve a structural phase transition. Memory switching refers to crystallization and this distinguishes itself from threshold switching (Lencer et al. 2011). Chalcogenides exhibiting memory switching will retain their crystalline phase even after the input electric field has been removed. However, the OFF state can be restored by applying a short intense pulse with a rapid trailing edge. This process is known as reset process. Hence, they are used as phase change memories (PCM). PCM devices can be programmed by applying an electrical power through applied voltage, which leads to an internal temperature change that can melt and rapidly quench a volume of amorphous material (RESET) or hold this

volume at a slightly lower temperature for recrystallization (SET). A low voltage is applied for sensing the device resistance (READ) without perturbing its state. Current pulses of different states and corresponding I-V plot of a representative sample has been shown in the Figure 1.6 (a) and (b) respectively.

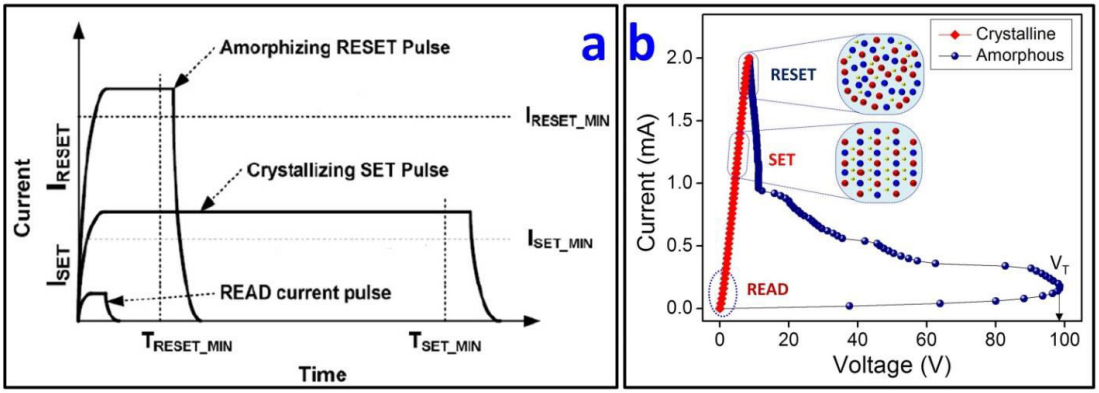

Figure 1.6 (a)Current pulses used in reading, SET and RESET process (b) SET, RESET and READ states are represented by a representative I-V plot of a representative chalcogenide sample

1.5.3 Current Controlled Negative Resistance (CCNR) memory switching behavior

Pictorial representation of current controlled negative resistance (CCNR) switching behavior for a representative chalcogenide $Si_{20}Te_{78}Bi_2$ sample is shown in Figure 1.7. The initial electrical resistivity values of the as prepared glasses are in the range of 10^6 Ω.cm. The voltage across the $Si_{20}Te_{78}Bi_2$ alloy increases linearly with increasing current, indicating an ohmic behavior. Near a threshold voltage V_T, the I-V curve shows a small nonlinearity, after which the voltage across the sample starts to decrease with current, indicating a negative resistance behavior. The negative resistance eventually leads to a low resistance state. As seen from the I-V plots, the samples exhibit swift switching from high resistance state (OFF) to low resistance state (ON). The samples do not revert back to their original high resistance state even after the removal of the applied electrical field. This observation clearly indicates that $Si_{20}Te_{78}Bi_2$ glassy alloy exhibits memory switching behavior at comparatively lower applied currents (≅ 2 mA).

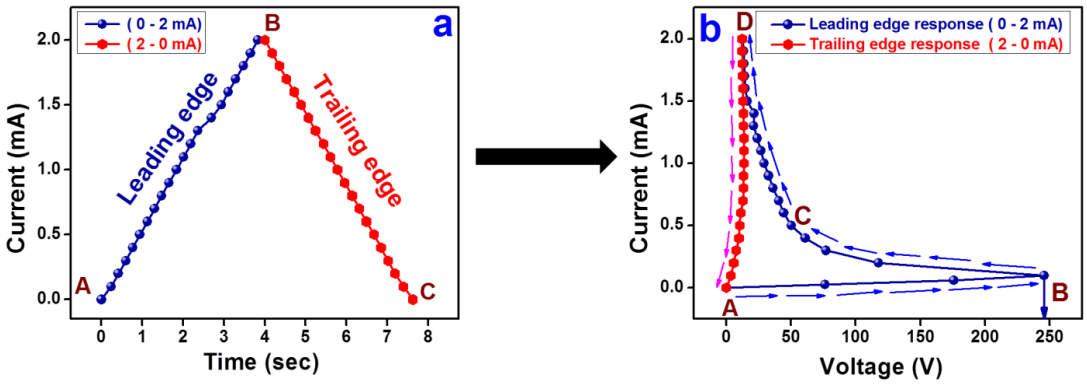

Figure 1.7 Pictorial representation of current controlled negative resistance (CCNR) switching behavior. (a) Triangular current pulse (input signal of maximum amplitude 2 mA) applied on a representative $Si_{20}Te_{78}Bi_2$ chalcogenide glassy alloy. (b) I-V characteristics corresponding to the input (as shown in a), which represents CCNR memory switching behavior. The region AB represents ohmic behavior, BC represents negative resistance region, CD represents low resistance On state and region DA represents sample taking the low resistance path i.e. sample has switched from high resistance (amorphous) state to low resistance (crystalline) state.

1.5.4 The mechanism of electrical switching

In general, the memory switching is believed to be dominated by the thermal process. Memory switching in chalcogenide glasses is considered to be a consequence of a phase transition of the material from amorphous to crystalline state (Adler 1977); in the crystalline state the conduction is higher as the disorder is significantly lesser. It is believed that memory switching occurs in those glassy chalcogenides in which the cross-linking atoms are too few in number. Such glasses have lesser thermal stability (Adler 1977) and application of a high electric field or heating leads to the crystallization of these glasses. The crystallization of the chalcogenide glasses into fine filaments which is responsible for memory switching is believed to be caused by the Joule heating (Fritzsche 1974), and the resultant excess carrier concentration in the current path is due to a larger electric field. The formation of crystalline conducting channel in a memory chalcogenide glass during switching has been confirmed by electron microscope and optical reflectivity investigations (Fritzsche 1974).

Reports so far suggest that switching in chalcogenides is always associated (implicitly or explicitly) with the region of current-controlled negative resistance (CCNR) (Owen and Robertson 1973). CCNR provides a positive feedback mechanism which allows the system to carry the same or larger currents with smaller voltages in the region of instability. On the other hand, thermal mechanisms of switching were first discussed by Warren (Warren 1970), where the current suddenly increases when the voltage reaches V_T, wherein V_T corresponds to the complete filling of the defect states in the chalcogenides. When the defect states are filled, the field dependent mobility or carrier concentration suddenly increases from a low to a high value, thereby decreasing the resistivity (initiation of switching, Threshold voltage V_T) of the material, enabling a larger current to flow through the chalcogenide. The larger current flowing through the sample causes higher joule heating which further reduces the resistance of the sample. Consequently, conductivity of the sample will increase, thereby allowing more current to flow in the sample. This cyclic process (Figure 1.8) can eventually trigger the phase change and memory switching in certain chalcogenide glasses.

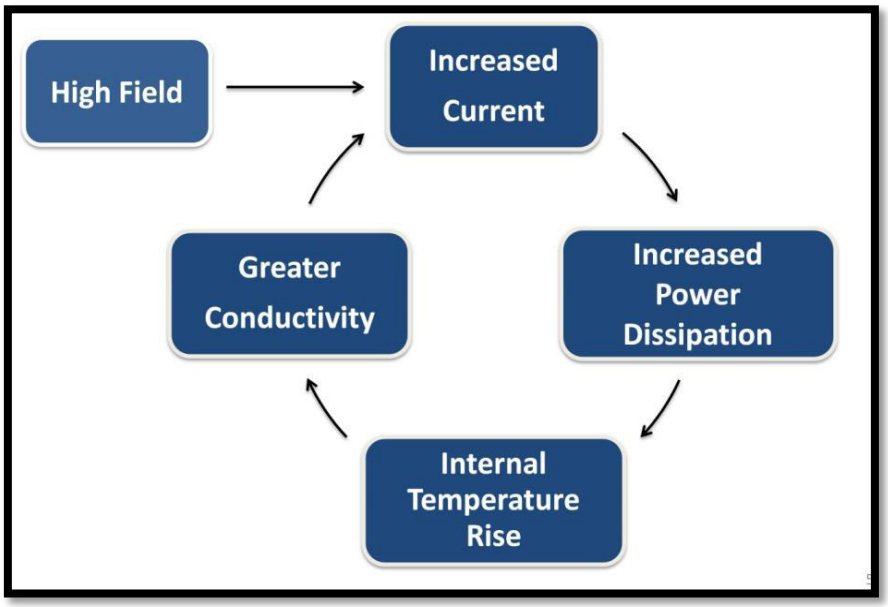

Figure 1.8 The cyclic process which succeeds after the initiation of switching leads to memory switching.

1.5.5 Factors affecting switching voltages of chalcogenide glasses

There are many factors which affect threshold/switching voltage of chalcogenide glasses. Threshold/switching voltage (V_T) is defined as the voltage at which the sample initiates to switch. The threshold/switching voltage is found to vary with composition of the sample as well as with the quantities like thickness of the sample, ambient temperature of the sample, network topology, metallicity of the additives, etc., which are briefly discussed below.

(i) Temperature

Temperature dependence of threshold voltage is an important factor which characterizes the material against thermal degradation and hence, stability of the material for device application. In both threshold and memory samples, V_T is found to decrease with increasing temperature. The temperature dependence of V_T can be expressed as (Shimakawa et al. 1973),

$$V_T = V_0 exp\left(\frac{\varepsilon}{k_B T}\right) \quad \text{.....(1.6)}$$

Where, V_T is the threshold switching voltage, ε is the threshold voltage - activation energy, k_B is the Boltzmann constant (8.617 X 10^{-5} eV K^{-1}) and T is the temperature in Kelvin. At higher temperature, the charged defect centers are filled by thermally excited charge carriers, contrary to the field injected charge carriers, resulting in the decrease in switching voltage (Singh and Shimakawa 2003). The above discussions suggest that there is an increase in electrical conductivity with increase in temperature, confirming the semiconducting nature of the as- synthesized chalcogenide glassy alloys. For memory switching glasses, the reduction of V_T with temperature has been interpreted based on a configurational free-energy diagram. This suggests that the reduction of V_T is due to the reduction in energy barrier required for the crystallization of a sample with elevating temperature (Singh and Shimakawa 2003).

(ii) Thickness of the sample

The sample thickness (d) is a significant parameter and provides a clear perception of the switching mechanism. Literature reports suggest that for samples exhibiting memory switching, the variation of V_T shows linear or square root dependence ($d^{1/2}$) with thickness, whereas for threshold switching, the variation of V_T shows square dependence (d^2) with the sample thickness (Jones and Collins 1979). It is noteworthy to realize that heat loss through the electrode surface is determined by thermal conductivity (k) of the sample and external heat conductivity (λ), leading to the variation in switching voltage (Nakashima and Kao 1979). The development of filament formation in the sample is associated with memory switching. In this case, if the sample is a thin slab, then the loss of heat generated from the filamentary channel to the surface of the electrode is less. Hence, V_T is less dependent on thickness for thin samples.

On the other hand, V_T increases with increase in sample thickness. Increase in V_T is usually observed with thickness greater than 0.30 mm. This is mainly because of large power consumption by the sample for filament formation. Therefore, we use samples of thickness (d = 0.30 mm) for our memory applications, which is optimized for most of the cases. It is very intricate to prepare samples of thickness less than 0.30 mm owing to their brittle nature. In this work, we observe linear increase in the switching voltages as a function of thickness for the studied Ge-Te-Sn and Si-Te-Bi chalcogenide glassy systems.

(iii) Network topology effect

The network topology such as network connectivity and rigidity, topological thresholds - rigidity percolation threshold (RPT) and chemical threshold (CT), etc., have been found to play a crucial role in the electrical switching behaviour. Electrical switching is one of the best characterizing tools for identifying the network topological thresholds, namely the RPT and CT of chalcogenide glassy system. According to Phillips and Thorpe, the optimum glass compositions are those in which the number of constraints exactly equals the degrees of freedom, which is called

rigidity percolation threshold (RPT). The critical value of $< r > = 2.4$ is called RPT (Phillips and Thorpe 1985). At this composition, rigid structures percolate throughout the glass, leading to an isostatic network. The network is flexible with $< r > < 2.4$, and the network is stressed rigid with $< r > > 2.4$. It is exactly isostatic at $< r > = 2.4$. In our present work, glass composition is restricted to a value $< r > \geq 2.48$, which falls in the domain of topological constraint theory, whereas in the over constrained regime($< r > > 2.4$), rigid structures easily percolate throughout the system, resulting in crystallization. The composition at which highest chemical stability occurs is called as chemical threshold (CT) of the glassy system which corresponds to the stoichiometry glass .

Investigations on a wide variety of chalcogenide glasses indicate that the compositional dependence of switching voltages of both memory and threshold switching glasses exhibits anomalies at both RPT and CT of the system. However, we could not probe the influence of RPT and CT on switching voltages for the studied Ge-Te-Sn and Si-Te-Bi chalcogenide glassy system, owing to their narrow glass forming ability. Herein, metallicity factor plays a dominant role over network topology effect and the same has been discussed in the subsequent chapters.

(iv) Metallicity factor

The studies on variation of threshold voltage with composition have revealed that the switching voltage decreases with the addition of metallic dopants. This is because, the addition of metallic impurities increases the conductivity of the sample and decreases the activation energy required for the phase change (Asokan and Lakshmi 2012). Hence, decrease in V_T is expected with the addition of more metallic impurities.

1.5.6 Defect related switching process

Defects in amorphous semiconductors such as structural defects can dominate the switching process. The atomic structure and the electron levels introduced by the defects have been reported to have an influence on the switching behavior in chalcogenides (Waser et al. 2010). David Adler has reported that lowest energy defects are expected in amorphous chalcogenide alloys which are known as Valence Alternation Pairs (VAP) (Adler 1980). Despite the presence of defects and impurities,

chalcogenide materials are highly resistive because the VAP defects pin the Fermi level near the gap center. This property gives a high-resistance OFF state. This is totally different from other semiconductors with comparable energy gaps. Here, switching occurs when the defect states are filled by the field injected charge carriers (by a way of Poole-Frenkel effect) (Xu et al. 2009). This shows that electrical conductivity of the medium is field dependent. When the defect states are filled, the field dependent mobility or carrier concentration suddenly increases from a low to a high value, thereby decreasing the resistivity (initiation of switching, Threshold voltage V_T) of the material, enabling a larger current to flow through the chalcogenide.

1.6 THERMAL PROPERTIES

The fundamental properties of glasses are their thermal properties, and knowledge of the same guides us to select proper glass composition to be used for various applications. Chalcogenide glasses can be classified based on the tendency for vitrification. Glasses with low tendency to crystallize are promising for applications in fiber optics. However, glasses with increased crystallization ability also find their applications in optical switches and storage devices(Adam and Zhang 2014). Owing to the fundamental differences between chalcogenide glasses and their oxide counter parts, understanding the thermal behavior and response of chalcogenide glasses assumes greater importance.

1.6.1 Thermal analysis

Thermal analysis involves a great variety of techniques in which a sample is subjected to a pre-determined temperature profile, and its properties or its reaction products are continuously measured as a function of temperature and time. Such measurements provide qualitative and quantitative information about physical and chemical changes that involve either endothermic or exothermic process (Gill et al. 1993). During any physical or chemical reaction, transfer of heat is involved. Many of the applications involving chalcogenide glasses require precise control over the crystallization process as the most promising properties of chalcogenides have been found to deteriorate drastically with crystallization. Therefore, understanding the crystallization and its

kinetics is an important aspect (Upadhyay and Murugavel 2013). Although tellurium (Te) based chalcogenide glasses have been reported to exhibit tremendous potential for electrical switching device applications, fundamental studies are still required for understanding the thermal stability of different alloy compositions. Various techniques such as electrical resistivity, X-ray diffraction, electron microscopy and differential scanning calorimetry (DSC) have so far been adopted to understand the crystallization of chalcogenide glassy alloys (Raoux and Wuttig 2010). However, out of all the above techniques, DSC analysis is found to be the most powerful tool designed to obtain information about glass structure and its properties over a wide range of length scale and applications.

1.6.2 Differential Scanning Calorimetry (DSC)

DSC is the most often used thermal analysis method, owing to its speed and simplicity. This technique was developed by Watson and O'Neil in 1960. DSC adopts a differential method of measurement in which the difference in the amount of heat required to increase the temperature of a sample and reference is measured as a function of temperature and time. DSC can be performed either in isothermal or non-isothermal mode to study the crystallization kinetics of a material. In isothermal mode, the sample is brought near the crystallization temperature very quickly and the changes in the physical quantities are measured as a function of time. In case of non-isothermal mode, the sample is heated at a fixed rate and physical parameters are recorded as a function of temperature. However, DSC measurements in the non-isothermal mode are usually preferred, since it is impossible to ensure homogeneous furnace temperature during the injection of sample in the isothermal mode (Lafi and Imran 2011). The parameters of crystallization kinetics of a material are generally recorded at the onset of crystallization temperature (T_c), glass transition temperature (T_g), and peak crystallization temperature (T_p). Molecular motions and the rearrangement of atoms in the glassy alloys occurring around the critical transition temperatures reveal their activation energy (Suri et al. 2006). An example of a DSC trace for a multicomponent chalcogenide glass showing the characteristic temperatures of interest is shown in the Figure 1.9.

1.6.3 Crystallization Kinetics

The dynamics involved in the devitrification of amorphous materials corresponding to time and temperature is called as crystallization kinetics (Singh 2013). Crystallization kinetics of chalcogenide glassy alloys is a qualitative/quantitative analysis of the obtained characteristic temperatures and their respective activation energy. Furthermore, kinetics of devitrification studies is interpreted based on thermal parameters such as thermal stability, fragility index, specific heat, etc. Hence, conviction on crystallization kinetics of chalcogenide glassy alloys is important in identifying novel materials for memory applications.

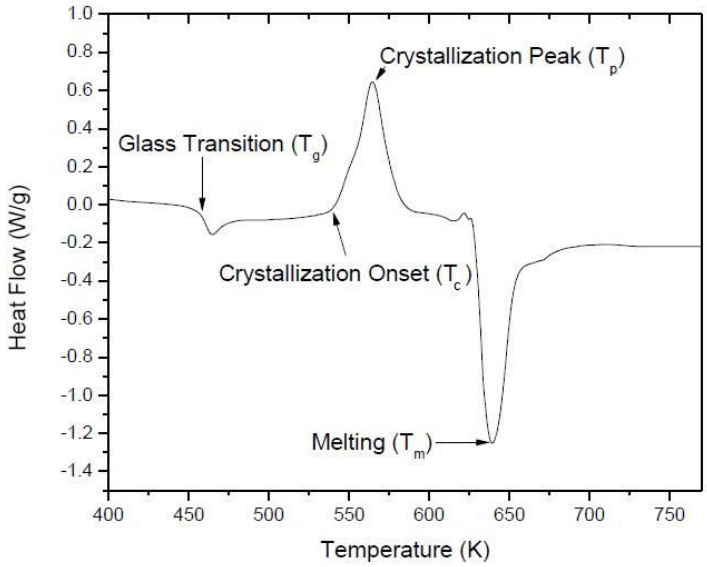

Figure 1.9 Typical DSC thermogram of a chalcogenide glass representing characteristic temperatures.

Based on the Johnson-Moynihan-Avarami (JMA) model, several statistical approximations have been made to evaluate the activation energy. The activation energies of chalcogenide glasses at critical temperatures can be illustrated from parameters, such as glass transition activation energy (E_g), onset crystallization activation energy (E_c) and peak crystallization activation energy (E_p) (Avarami 1941; Johnson and Mehl 1939). Thermal stability and glass forming ability (GFA) of a compound describe its relative ability to adopt an amorphous structure. The GFA

criterion $(\Delta T = T_c - T_g)$, also called the thermal stability parameter was first introduced by Dietzel (Dietzel 1968), which was later improved by Saad and Poulin ('S parameter') (Saad and Poulain 1987). On the other hand, Hruby developed the GFA criterion (H_r) to describe the thermal stability as well as the glass forming ability of amorphous materials (Hrubý 1972). These parameters are very useful in understanding the applicability of the prepared materials in the field of PCM, optical recording, and optical fibre communication.

1.7 SWITCHING VOLTAGE AND THERMAL PARAMETERS

The switching voltages of chalcogenide glasses have a strong correlation with thermal properties such as glass transition temperature, crystallization temperature, activation energy for crystallization and thermal stability of the glass. Evaluation of thermal parameters gives significant information on material behaviour and their impact on switching voltages of chalcogenide glasses (Asokan and Lakshmi 2012). Study of thermal parameters not only helps us to identify newer materials for PCM devices, but also validates the results obtained for electrical properties. In the present work, efforts have been made to correlate the relation between switching voltages and thermal properties.

(i) Glass transition temperature

Glass transition temperature Tg is considered as one of the important parameters as it expresses the strength and rigidity of the glassy alloys. Increase in the value of Tg indicates an increase in the network connectivity, thereby increasing the switching voltage and vice versa. Empirical relation between switching field (E_t) and T_g is given as (Prakash et al. 1994)

$$E_t^2 = C_1 \exp[C_2 * k(T_g - T)/kT] \quad \text{.....(1.7)}$$

where C_1, and C_2 are constants, T is the ambient temperature and k is the Boltzmann constant. Aforementioned relation states that variation of T_g is directly proportional to the change in switching field (E_t), thus establishing a relationship between T_g and E_t.

(ii) Crystallization temperature

When a compound (glassy material) attains systematic patterns, it releases energy in the form of heat and this is called as an exothermic reaction. The phase change corresponding to exothermic reaction is called crystallization of a compound (Singh 2012). Higher value of T_c indicates strong glasses. However, lower values of T_c favor easy crystallization, leading to memory switching. Hence, it can be concluded that high electric field is required for the strong glasses compared to those having lower values of T_c (Asokan and Lakshmi 2012). In the present work, we have observed decreasing values of T_c with respect to V_T for the Ge-Te-Sn and Si-Te-Bi chalcogenide glassy systems.

(iii) Activation energy for crystallization (Ec)

In addition to the crystallization temperature, activation energy measured for the crystallization sheds light on the material behavior as a function of composition. Here, activation energy for crystallization represents energy barrier requisite for the devitrification (Naqvi and Saxena 2011). Hence, we can anticipate direct relationship with the activation energy and switching voltage. A decreasing trend of V_T in parallel with E_c has been displayed for the studied Ge-Te-Sn and Si-Te-Bi chalcogenide glassy system which reveals the correlation between them. Furthermore, lower values of E_c also imply rapid crystallization, leading to better switching speed.

(iv) Thermal stability of the glass

As discussed in the mechanism of electrical switching, the phenomenon of memory switching is thermal in nature which involves the formation of conducting crystalline channel in the sample. The formation of crystalline channel is favourable in those chalcogenide glasses which are easily prone to devitrification (Nakashima and Kao 1979). Devitrification refers to the crystallization tendency of the material. The devitrification process in turn depends on the thermal stability of the sample. Thermal stability$\left(\Delta T = T_c - T_g\right)$ indicates resistance offered by the vitreous chalcogenides to crystallization. Glasses with lower thermal stability have higher devitrification ability. Samples which are prone to an easy devitrification are expected to show the memory behaviour even at lower 'ON' state currents.

1.8 LITERATURE SURVEY

It is difficult to date the origin of the field of chalcogenide glasses. For a long time, the vitreous glass state was limited to oxygen compounds and their derivatives. Schulz- Sellack was the first to report data on oxygen free glass in 1870. Investigations of chalcogenide glasses as optoelectronics materials in infra red systems began with the rediscovery of arsenic trisulfide glass (Frerichs, 1950, 1953) when Frerichs reported his work. During the period 1950-1970, the glasses were made available as commercial devices.

In 1968, Ovshinsky and his co-workers discovered that some chalcogenide glasses exhibited memory and switching effects. After this discovery, it became clear that the electric pulses switch the phases in chalcogenide glasses back and forth between amorphous and crystalline state. Based on the theory of electronic processes in non-crystalline chalcogenide glasses, Mott et al.(1979) and Kawamura et al. (1983) discovered xerography. The switching device applications were introduced by Bicerono et al. 1985 and Ovshinsky 1994. Boolchand et al. 2001 discovered intermediate phase in chalcogenide glasses. Further, several investigators have reported the use of chalcogenide glasses in infrared transmission and detection, threshold and memory switching applications. (Selvaraju et al. 2003)

Anbarasu et.al. (2006) reported Differential scanning calorimeter studies on As-Te-Si glasses. These studies were carried out in order to understand the thermal behavior and the compositional dependence of thermal parameters of $As_{40}Te_{40-x}Si_x$ glasses. Daniele (2008) presented modeling of switching phenomenon in phase change memory (PCM) devices. He reported recent progress in the physical modeling of threshold and memory switching in phase-change memory (PCM) devices.

The decrease in switching voltages with the addition of more metallic impurities has been observed in chalcogenide systems including $Cu_xGe_{15}Te_{85-x}$, $Ag_xGe_{15}Te_{85-x}$, $Si_{15}Te_{85-x}Sb_x$, $Ge_{18}Te_{82-x}Bi_x$, and $Ge_{17}Te_{83-x}Tl_x$ glasses with composition, thus indicating the effect of resistivity/metallicity of the constituents. Earlier investigations

reveal that binary Si-Te glasses (Murthy et al. 2005) and ternary samples in bulk glassy and amorphous thin film forms containing Si including As-Te-Si (Anbarasu et al. 2005) and Ge-Te-Si (Anbarasu 2007) exhibit electrical switching phenomenon. Zhang et al. (2008) investigated crystallization kinetics of $Si_{15}Te_{85}$ and $Si_{20}Te_{80}$ chalcogenide glasses using non-isothermal crystallization approach. It was found that $Si_{20}Te_{80}$ amorphous has higher thermal stability and higher glass formation ability compared to $Si_{15}Te_{85}$.

Lokesh et al. (2009) studied the electrical switching behavior of melt quenched bulk $Si_{15}Te_{85-x}Sb_x$ glasses. Studies have been undertaken in order to understand the effect of Sb additions on the electrical switching behavior of $Si_{15}Te_{85-x}$ based glass. Chandasree et al. (2010) prepared bulk, melt quenched $Ge_{18}Te_{82-x}Bi_x$ glasses ($1 \leq x \leq 4$). It has been found that these glasses exhibit memory type electrical switching behavior. Asokan et al. (2011) reported studies on electrical switching and other properties of chalcogenide glasses. Srinivasa et al. (2012) investigated thermodynamic, Raman and electrical switching characteristics of $Si_{15}Te_{85-x}Ag_x$ ($4 \leq x \leq 20$). Upadhyay et al. (2013) investigated crystallization behavior, electrical switching and structure of the bulk Ge_xTe_{100-x} glasses to ascertain the role of composition on phase change behavior.

Sherchenkov et al. (2014) have reported on the non-isothermal method for estimating the kinetic parameters of crystallization for the phase change memory (PCM) materials. Farid and Atyia (2015) studied the crystallization kinetics of $Se_{90}Bi_{10}$ and $Se_{85}B_{i5}Te_{10}$ chalcogenide glasses using Differential Thermal Analysis (DTA) under a non-isothermal condition at different heating rates. Pumlianmunga et al. (2016) studied electrical switching in $(GeTe_4)_{100-x}(As_2Se_3)_x$ glasses in the range ($0 \leq x \leq 40$) having fixed network connectivity with average coordination number ($Z_{av} = 2.4$) . In the same year Pumlianmunga and Ramesh reported electrical switching and aluminum speciation in Al-As-Te glasses. They have observed a change in switching type from memory to threshold with the increase of Al. Pumlianmunga and K Ramesh (2017) reported electrical switching in Sb doped $Al_{23}Te_{77}$ glasses. Those glasses also exhibited changeover of switching type as a function of composition.

The literature survey mentioned herein clearly suggests that memory type electrical switching has been observed in Te-rich chalcogenide glasses. They also suggest a strong correlation between electrical switching and thermal properties of chalcogenide system. Accordingly, metal dopant chalcogenides show interesting electrical switching and thermal properties. Tin (Sn) and Bismuth (Bi) are two such additives with fascinating material characteristics. This has given us the motivation to carry out studies on electrical switching and thermal properties on newer chalcogenide materials such as Ge-Te-Sn and Si-Te-Bi.

1.9 SCOPE AND OBJECTIVES OF THE PRESENT WORK

Chalcogenide glassy alloys are one of the important semiconductor materials exhibiting distinct electrical properties. The feature which enables them to be used for memory devices has made them technologically and scientifically important among materials of the semiconductor family. The present work essentially deals with studies on electrical switching and thermal properties of Tellurium based chalcogenide glassy alloys. In this work, two series of chalcogenide systems, namely Ge-Te-Sn and Si-Te-Bi were chosen to study the electrical and thermal properties of these systems. A detailed study has been undertaken on electrical switching studies on these glasses to know the dependence of switching voltages on composition of the glasses and the effect of metallicity factor on switching voltages. Furthermore, thickness and temperature dependence on switching voltages studied herein reveals the nature of switching mechanism.

Differential scanning calorimetric (DSC) studies have been undertaken for the thermal analysis of Ge-Te-Sn and Si-Te-Bi chalcogenide samples. The information obtained from thermal parameters such as glass transition and crystallization temperatures, specific heat capacity, relaxation enthalpy, thermal stability, etc., has been used to correlate it with the switching characteristics. A novel approach to prepare chalcogenide glassy alloys has been discussed here. The present experimental unit has a few modifications regarding the working chamber of the furnace and also the design of ampoule holder for rapid quenching of the melt purposes

The main research objectives are :

1) The synthesis of Ge-Te-Sn, Si-Te-Bi ternary chalcogenide glassy alloys.
2) The study of compositional dependence of electrical and thermal properties of synthesized chalcogenide glassy alloys.
3) The study of investigation on the thickness and temperature dependence on switching voltage.
4) The study of the relation between electrical and thermal properties of chalcogenide glassy (Ge-Te-Sn, Si-Te-Bi) alloys.

1.10 ORGANIZATION OF THE THESIS

The research work in this thesis is divided into 5 chapters

Chapter 1 and its sub-sections provide the background and motivation for the present work. This chapter also outlines the fundamental aspects of amorphous semiconductors and explains the nature of glassy state and glass forming ability. This chapter gives an account of electrical switching phenomenon and its correlation with thermal properties. It is then followed by the literature survey. The scope of the present thesis work and objectives are mentioned.

Chapter 2 provides the details of the experimental techniques used in the present work. In this chapter, the preparation of chalcogenide glassy alloys using melt quenching is described. The characterization of the prepared samples using x-ray diffraction (XRD), scanning electron microscopy (SEM), energy dispersive x-ray analysis (EDAX), I-V and differential scanning calorimetry(DSC) is also explained. The investigation of electrical switching characteristics at ambient and high temperatures is discussed. Details of the indigenously fabricated high temperature melt quenching system is also discussed.

Chapter 3 presents the investigation of electrical switching and thermal studies of $Ge_{20}Te_{80-x}Sn_x$ chalcogenide glassy alloys. In this chapter, we report on the studies of memory type electrical switching behavior and thermal properties of a ternary $Ge_{20}Te_{80-x}Sn_x$ ($0 \leq x \leq 4$) chalcogenide glassy alloys.

Chapter 4 presents the investigation of electrical switching and thermal studies of Si-Te-Bi chalcogenide glassy alloys in the two composition tie lines $Si_{15}Te_{85-x}Bi_x$ ($0 \leq x \leq 2$) and $Si_{20}Te_{80-x}Bi_x$ ($0 \leq x \leq 3$).

Chapter 5 summarizes the conclusions drawn from the present work. Next, the scope for further work in this field is mentioned. An appendix followed by list of references and a brief profile with publications in international journals and conferences are presented at the end of the thesis.

CHAPTER 2

EXPERIMENTAL TECHNIQUES

In this chapter, the preparation of chalcogenide glassy alloys using melt quenching is described. The characterization of the prepared samples using x-ray diffraction (XRD), scanning electron microscopy (SEM), energy dispersive x-ray analysis (EDAX), I-V and differential scanning calorimetry(DSC) is also explained. The investigation of electrical switching characteristics at ambient and high temperatures is discussed. Details of the indigenously fabricated high temperature melt quenching unit is also discussed.

2.1 SYNTHESIS OF BULK CHALCOGENIDE GLASSY SAMPLES

There are different methods to obtain materials in the amorphous form. Bulk glasses studied herein, namely Ge-Te-Sn and Si-Te-Bi are prepared by conventional melt quenching technique. Chalcogenide glasses generally have high vapor pressures around their melting temperatures (Lezal 2003) and a tendency to react with oxygen, especially at high temperatures. Therefore, chalcogenide glasses are normally prepared by melting the constituent high purity elements in quartz ampoules sealed under high vacuum conditions (at a pressure of the order 10^{-5} - 10^{-6} torr). The condition for synthesizing these glasses generally depends on the glass composition, glass forming region and glass forming ability (GFA).

Glass formation depends on the rate of cooling. When the sample is quenched, heat has to quickly conduct. Compared to other chalcogens, tellurium based glasses are difficult to prepare. Hence, the following steps are taken to ensure the formation of glass.

Reduction of ampoule holder: When the ampoule diameter is less, rate of cooling increases. In this thesis, ampoules of 8 mm outer diameter and 6 mm inner diameter are used.

Weight of the sample: Glass formation is easier when the weight of the starting material is less. Due to lower mass, the amount of heat that has to be conducted away is reduced. The weight of the starting material is optimized between 0.5 - 1.0 gm.

Flattening of the sides of the ampoule: To ensure that a significant portion of the sample is exposed to the cooling medium, the sides of the quartz tubes are flattened, which reduces the diameter further.

Apart from these necessary steps, it is very important to achieve rapid quenching of the quartz ampoule containing chalcogenide melt into ice bath. In order to achieve rapid quenching, we have indigenously fabricated a high temperature melt quenching system for the preparation of chalcogenide glasses (details are discussed in the following section 2.6).

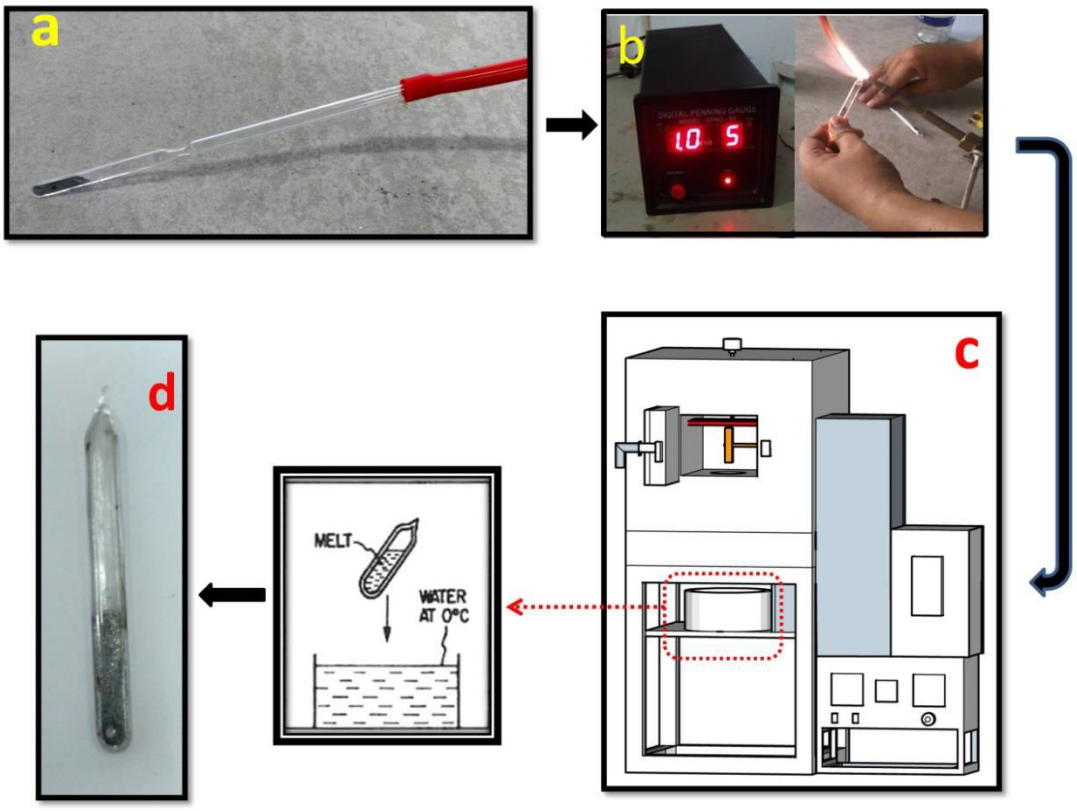

Figure 2.1 (a)-(d) Synthesis procedure of chalcogenide glassy alloys. (a) Starting material has been transferred to the pre-cleaned quartz ampoule and kept for vacuum sealing. (b) Ampoules have been sealed at high vacuum at the pressure of 10^{-5} torr (c)

Sealed ampoules have been transferred to the furnace for heat treatment and then quenched rapidly to the ice bath. (d) Quenched ampoule containing chalcogenide glassy alloy.

Figure 2.1 shows the steps involved in preparing chalcogenide glasses. Appropriate quantities of the constituent elements (99.99% purity) were weighed according to their atomic percentage using electronic balance accurate to 0.0001mg and were sealed in flattened quartz ampoules having inner and outer diameter 6 and 8 mm, respectively, under a vacuum of about 10^{-6} torr. The sealed ampoules were loaded inside the indigenously fabricated electric furnace (*Indfurr* India: patent pending) and heated slowly beyond the melting point of the constituent elements. The furnace temperature is gradually increased at the rate of 100 K/h to reach the melting temperature of the constituents (around 1273 to 1473 K). The sealed ampoules were maintained at this temperature for about 24-36 hours and to ensure the homogeneity of the melt, a constant rotation was given at the rate of 10 rpm. The ampoules were subsequently quenched by dropping them in a bath of NaOH+ ice-cold water and they were then broken carefully to retrieve the synthesized glass sample.

2.1.1 Preparing samples for electrical switching experiments

Melt quenched chalcogenide retrieved by carefully breaking the ampoule yielded many small chunk pieces without a regular shape (as seen in Figure 2.2a). Out of these, one big chunk pellet piece (as shown in the inset of Figure 2.2a) was thinned and polished on both sides using two different grade (1200 grade paper for initial thinning of the sample, 3000 grade paper for the fine polishing of the sample) emery papers. Digital Vernier callipers having a least count of 0.01 mm was used to measure the thickness. In order to obtain a precise value, the thickness was measured at regular intervals of time while the sample is polished. Polishing was stopped when the thickness of the sample reaches 0.30 mm (as seen in Figure c). An experimental error of ± 0.01 mm can be expected rarely. Flat, finely polished chalcogenide glass samples of thickness 0.30 mm (as shown in Figure b) were employed for switching experiments.

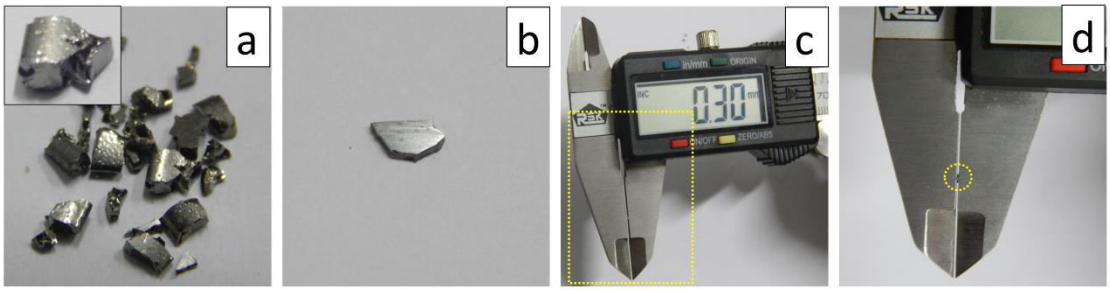

Figure 2.2 Bulk chunk pieces collected after melt quenching (a), is polished (b) and thinned down to 0.30 mm which is measured using a digital Vernier caliper (c). The sample held between the Vernier calipers in (c) is focused in (d) in which the area marked by a circle clearly indicates the presence of the sample.

For electrical switching experiments, it is essential to have a sample (pellet) of uniform thickness with flat surfaces on both the sides. This is because, in electrical switching, the switching area depends on the area of the sharp electrode tip (2 mm in diameter) targeted at the sample center.

2.2 X-RAY DIFFRACTION

Diffraction is a scattering phenomenon where the atoms scatter incident X-rays in all directions. In some directions, the scattered beams will be in phase and hence, they reinforce, giving rise to high intensity diffracted beam. The technique began when von Laue in 1912 discovered that crystals diffract X-rays. Since then, it has been applied to chemical analysis, stress and strain measurement, measurement of particle size as well as crystal structure [Whittaker 1981]. X-rays have wavelength comparable with interatomic spacing and hence results in the interference of deflected rays. The diffraction of X-rays by crystal is defined by Bragg's law (Figure 2.3) given as

$$n\lambda = 2d \sin\theta \tag{2.1}$$

where, d is the distance between two planes, λ is the X-ray wavelength, θ is the angle which the incident photon makes with the crystal plane. Different 'd' spacing of the crystal satisfies Bragg's condition at different angles, giving rise to XRD spectrum which is the fingerprint of the sample. Each crystal has many planes and alignment of

these planes determines the crystal structure. These relationships are used in X-ray diffraction to determine specific properties about the specimen.

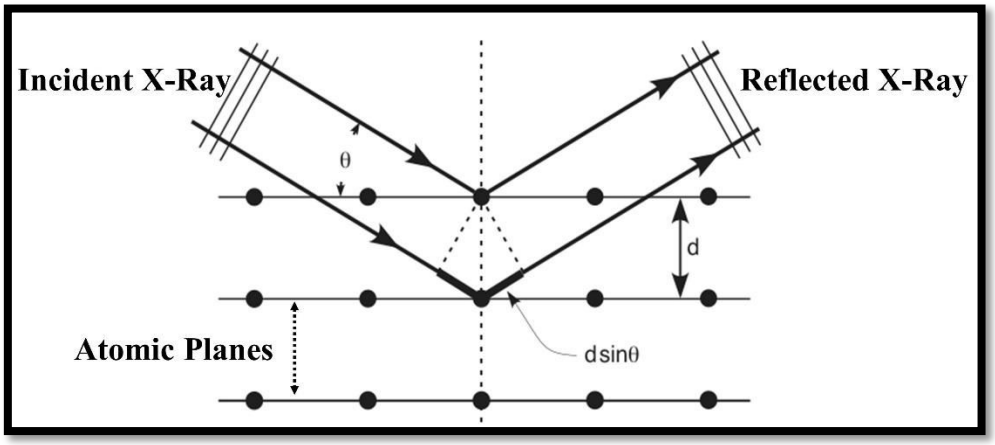

Figure 2.3 Bragg's law for X-Ray diffraction

To confirm the amorphous nature of the synthesized bulk samples indicated above, X-ray powder diffraction study has been employed. Powder X-ray diffraction (XRD) uses X-rays to investigate and quantify the crystalline nature of materials by measuring the diffraction of X-rays from the planes of atoms within the material. It is sensitive to both the type of atoms and relative position of atoms in the material as well as the length scale over which the crystalline order persists. It can therefore be used to measure the crystalline content of materials, identify the crystalline phases and determine spacing between lattice planes and length scales over which they persist. The schematic diagram of powder X-ray diffractometer is shown in Figure 2.4 (a)

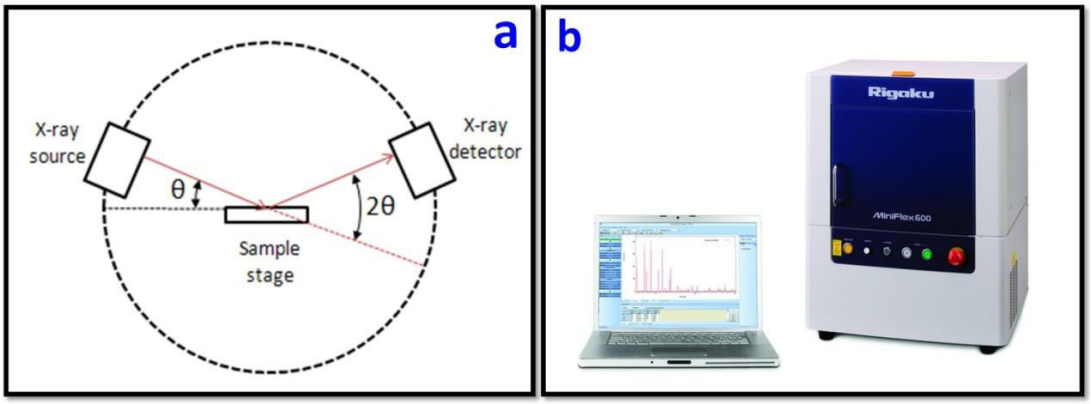

Figure 2.4 (a) Schematic diagram of powder X-ray diffractometer (b) Image of the Rigaku MiniFlex600 used for the XRD measurement

As mentioned earlier, non-crystalline materials are characterized by the absence of diffraction peaks and the XRD patterns of as-quenched samples are obtained to confirm this. The XRD patterns are collected by scanning 2θ from 20°-80° at a rate of 2°/minute. The absence of any sharp diffraction peaks in the XRD patterns confirms that the as-prepared samples are amorphous in nature. XRD patterns obtained for annealed samples at their crystallization temperatures gives structural information of the prepared materials. Image of the Rigaku MiniFlex600 used for the XRD measurement is shown in the Figure 2.4 (b)

2.3 SCANNING ELECTRON MICROSCOPY (SEM)

The SEM studies have been undertaken to study the micro structural changes in the sample. SEM uses electrons rather than light to form images. It provides a great combination of magnification (100,000x), greater resolution (few nm), larger depth of view and ease of sample preparation and observation. The fundamental principle behind SEM is the scanning of a finely focussed electron beam over the surface of the specimen to study the micro structural features of the material. Normally in SEM, electrons are either thermoionically emitted from a tungsten (or lanthanum hexaboride) cathode and accelerated towards the anode or generated by field emission. The high energy (upto 100keV) electron beam is focussed and scanned over a rectangular surface of the specimen. The interaction/energy exchange between the electron beam and the specimen leads to several phenomena like back scattering, emission of secondary electrons and X-rays etc., leading to a range of imaging techniques and analytical modes to measure the composition and nature of the specimen.

2.3.1 Energy Dispersive X-ray Analysis (EDAX)

EDAX is a technique used to analyze elemental composition of the material. It is based on the investigation of a sample by means of interactions between electromagnetic radiation and matter. The X-rays emitted by the matter in response to being hit by electromagnetic radiation are analyzed. The fact that each element has a unique atomic structure allows emitted X-rays that are characteristic of an element's atomic structure to be identified uniquely from each other.

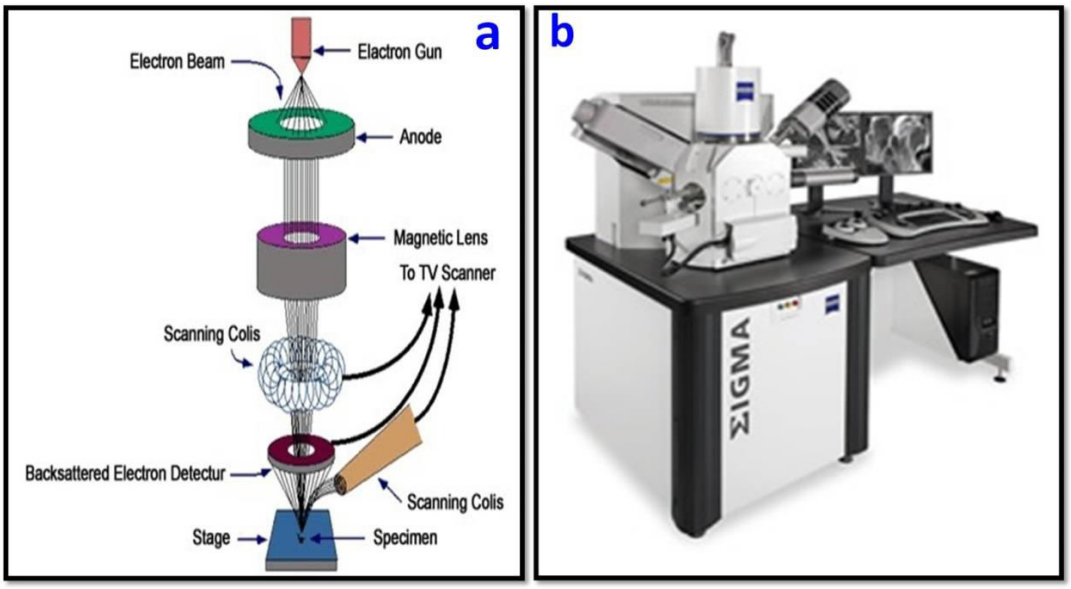

Figure 2.5 (a) Principle of scanning electron microscope (SEM). (b) Image of the Rigaku MiniFlex600 used for the XRD measurement

To stimulate the emission of characteristic X-rays from a specimen, a high energy beam of charged particles such as electrons or a beam of X-rays is focused on the sample being studied. At rest, an atom within the sample contains ground state electrons in discrete energy levels or electron shells bound to the nucleus. The incident beam may excite an electron from an inner shell, ejecting it from the shell and creating a vacancy. This positive vacancy is eventually occupied by a higher energy electron from an outer shell and the difference in energy between the higher energy shell and lower energy shell may be released in the form of an X-ray as shown in Figure. 2.6. The amount of energy released by the transferring electron depends on which shell it is transferring from and which shell it is transferring to. The energy of the X-rays emitted from a specimen can be measured by an energy dispersive spectrometer. Since the emitted X-ray is characteristic of the difference in energy between the two shells and of the atomic structure of the element from which they are emitted, it allows the elemental composition of the specimen to be measured. The position of the peak gives information about the composition of the sample. The data generated by EDAX analysis consists of spectra showing peaks corresponding to the elements, making up the true composition of the sample being analyzed. Elemental mapping of the sample and image analysis are also possible.

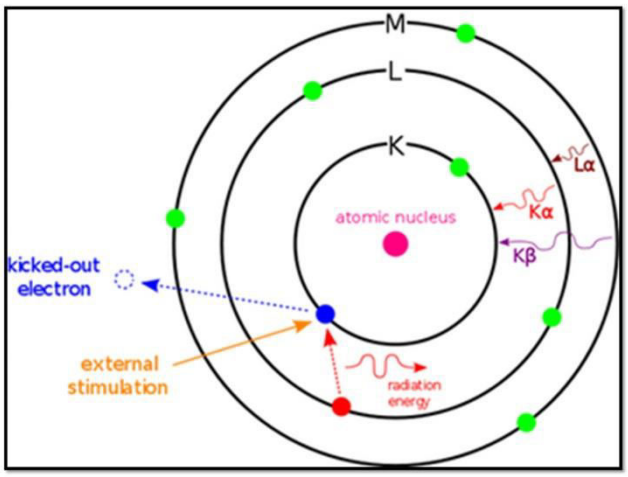

Figure 2.6 Principle of EDAX

2.4 ELECTRICAL SWITCHING ANALYZER

The current-voltage characteristic of a solid can be studied either by scanning along the voltage axis with variable voltage source and measuring the current induced in the sample, or by scanning the current axis with the variable current source and measuring the voltage developed across the sample. The selection of the source depends on the characteristics to be measured. In the case of ohmic samples, either of these methods produces the same result. In the case of amorphous semiconductors, on the other hand, the behavior is different from crystalline samples. In these materials, the current increases linearly with voltage only up to a threshold voltage (V_T). At V_T, the resistance drops either drastically (switching) or gradually, indicating a distinct negative resistance behavior. If the voltage source is used directly across the sample, the decrease in resistance leads to the flow of very high current. To limit the flow of this high current, a series resistance (R_s) has to be connected in the circuit. The incorporation of R_s will adversely affect the characteristics to be measured (Saheb et al., 2003). Hence, in the present study, the I-V characteristics and switching behavior of the as prepared chalcogenide glasses are studied by sourcing current and measuring the voltage developed across the sample. Schematic diagram of the PC based switching analyzer system used to study the electrical switching behavior of the chalcogenide glasses is shown in the Figure. 2.7. It consists of two main parts:

(i) Source meter :- A Keithley Source - Meter (Model 2410) controlled through IV Lab Tracer 2.0 is used as an excitation source to study the I-V characteristics. It can deliver a maximum current of 20mA at a compliance voltage of 1100V. Here, the 1A, 20V and 20mA, 1kV magnitudes are nominal values of current and voltage respectively. The maximum output magnitudes of the Source-Meter are 1.05A, 21V and 21mA, 1.kV. The current source mode of this instrument is employed for the switching analyses as it is possible to obtain the complete I-V curve in this mode.

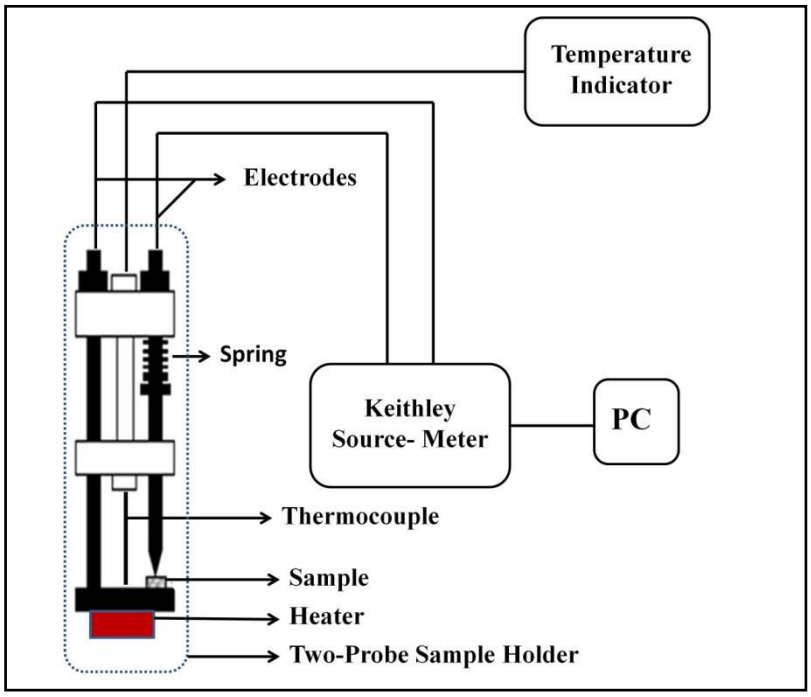

Figure 2.7 Schematic of PC controlled switching set-up used for I-V characteristic and electrical switching studies of the chalcogenide glasses

(ii) Sample holder:- The sample whose I-V characteristic is to be studied is placed in a sample holder cell. Basically, the design comprises of an inter changeable two probe holder assembly comprising of a four hole high purity Alumina Sheathing with overall diameter not exceeding 8mm. This is integrated with alumina plates of diameter not exceeding 20mm at the bottom with suitable holding assembly on which the specimen to be tested is placed. The brass electrodes are inserted through the holes of the alumina sheathing for making contact with that of the sample. The design is such that the measuring probes will run through the individual holes of the Alumina sheathing duly fitted with a spring loading system provided at the top. By just

applying adequate hand pressure on the spring loading system, the contacts between the probes and the specimen are developed. To study the I-V characteristics, point contacts are taken from the two electrodes as shown in Figure. 2.7.

To study the temperature effects on the switching parameters, the sample holder is introduced into a fabricated stainless steel circular vessel with a flange with provision for mounting the same on a heating jacket. Necessary ports are also provided on the cover assembly for introducing inert atmosphere as and when necessary. The vessel is covered with a pre-heating segment employing Kanthal A1 heating coils for preheating of the specimen to a maximum of 500°C. This segment is provided with a separate Chromel/Alumel thermocouple to act as sensor. The preheating segment is designed for operation at 230 Volts single phase AC Mains, and power rating of 2.5 KW. Experimental setup used for electrical switching studies is shown in Figure. 2.8.

2.5 DIFFERENTIAL SCANNING CALORIMETRY(DSC)

The thermal studies presented in this thesis have been performed using a differential scanning calorimeter (DSC). DSC is a thermal analysis technique that measures the heat flow into or out of a sample as a function of temperature and is used to detect thermodynamic transitions such as glass transition, crystallization or melting. A DSC measures the temperature difference between the sample under study (S) and an inert reference (R). Thus, DSC is a calorimetric method in which differences in energy are measured. Generally, the temperature program for a DSC analysis is designed such that the sample holder temperature increases linearly as a function of time. The reference sample should have a well-defined heat capacity over the range of temperatures to be scanned. The DSC operates under the simple assumption that the heat flow rate between two points is proportional to the temperature difference between those two points. The Figure 2.9 shows the schematics of a DSC and the image of the instrument used in the present work The calorimeter consists of a sample holder and a reference holder (beneath their respective pans) as shown in Figure 2.9. Both are constructed of platinum to allow high temperature operation.

Figure 2.8 Image of the experimental setup used for electrical switching studies

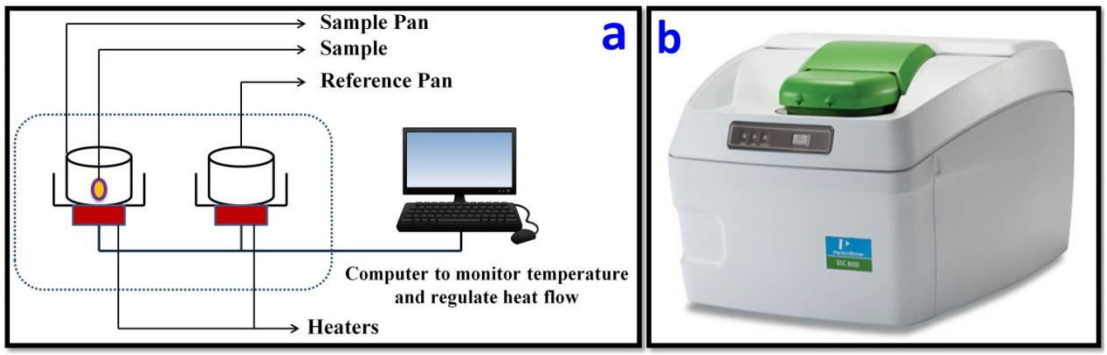

Figure 2.9 (a) Schematics of a Differential Scanning Calorimeter. (b) Image of the Perkin Elmer DSC 8000 used for thermal studies.

Under each holder is a resistance heater and a temperature sensor. Currents are applied to the two heaters to increase the temperature at a selected rate. The difference in the power to the two holders is necessary to maintain the holders at the same temperature. A flow of nitrogen gas is maintained over the samples to create a reproducible and dry atmosphere. The nitrogen atmosphere also eliminates air oxidation of the samples at high temperatures. The sample is sealed into a small aluminum pan. The reference is an inert material such as alumina or just an empty aluminum pan. The pans hold up to about 10 mg of material. Since the DSC is at constant pressure, heat flow is equivalent to enthalpy changes:

$$\left(\frac{dq}{dt}\right)_p = \frac{dH}{dt} \tag{2.2}$$

Here dH/dt is the heat flow measured in mcal sec^{-1}. The heat flow difference between the sample and the reference is:

$$\frac{\Delta dH}{dt} = \left(\frac{dH}{dt}\right)_{sample} - \left(\frac{dH}{dt}\right)_{reference} \tag{2.3}$$

and can be either positive or negative. In endothermic processes such as most phase transitions, heat is absorbed and therefore, heat flow to the sample is higher than that to the reference. Hence, ΔdH/dt is positive. For example, as a solid sample melts into a liquid, it requires more heat flowing to the sample to increase its temperature at the same rate as the reference. This is due to the absorption of heat by the sample as it undergoes the endothermic phase transition from solid to liquid. In an exothermic process such as crystallization, some cross-linking processes, oxidation reactions, and some decomposition reactions, the opposite is true and ΔdH/dt is negative. When the sample undergoes exothermic processes (such as crystallization), less heat is required to raise the sample temperature. By observing the difference in heat flow between the sample and the reference, differential scanning calorimeters are able to measure the amount of heat absorbed or released during such transitions. DSC may also be used to observe more subtle physical changes, such as glass transitions.

Glass transitions may occur as the temperature of an amorphous solid is increased. These transitions appear as a step in the baseline of the recorded DSC signal. This is due to the sample undergoing a change in heat capacity; no formal phase change occurs.

As the temperature increases, an amorphous solid becomes less viscous. At some point, the molecules may obtain enough freedom of motion to spontaneously arrange themselves into a crystalline form. This is known as the crystallization temperature (T_c). This transition from amorphous solid to crystalline solid is an exothermic process, and results in a peak in the DSC signal. As the temperature increases, the sample eventually reaches its melting temperature (T_m). The melting

process results in an endothermic peak in the DSC curve. The ability to determine transition temperatures and enthalpies makes DSC a valuable tool in producing phase diagrams for various chemical systems.

2.5.1 Measurements in DSC

DSC parameters such as *Tg, Tc, Tp and Tm* are measured accurately by plotting the acquired data using Origin software. Pyris program (compatible software for the Perkin Elmer DSC 800 Instrument) is used to calculate the thermal parameters such as ΔC_p and ΔH_c.

2.5.1.1 Calculation of thermal parameters (ΔC_p and ΔH_c)

The specific heat capacity shows a jump in the glass transition (T_g), which is a characteristic feature of all glassy alloys. Change in specific heat (ΔC_p) is the difference in the heat capacity between the glassy state (solid) and the super-cooled liquid as shown in the Figure 2.10.

$\Delta C_p = C_p$(solid state) - C_p(super-cooled liquid state)

In our experiments, values of ΔC_p were calculated using the automated feature available in the compatible software (*Perkin Elmer Pyris*^{TM}), The auto-slope function is selected from the preferences menu to enable all runs to be automatically shifted and sloped to zero based on the final heat flow points of the highest and lowest temperature isotherms.

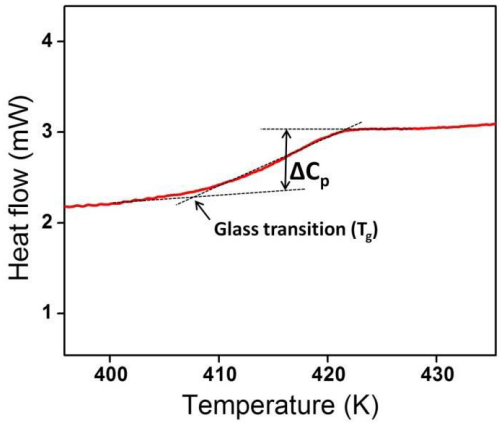

Figure 2.10 The baselines are extrapolated between before (liquid like) and after (solid like) the glass transition (T_g) (as shown by dotted lines). ΔC_p is the difference

in the heat capacity between the glassy state (solid) and the super-cooled liquid (as shown by arrows)

For converting to C_p units, the iso-aligned baseline data is subtracted from the single curve C_p by selecting the Calculate/Specific Heat menu. The resulting specific heat curve plotted as a function of temperature can be saved for further analysis. The representative Figure 2.11(screen shot of the *Pyris* Software) is shown as a guide to the eye for demonstrating the calculation of specific heat.

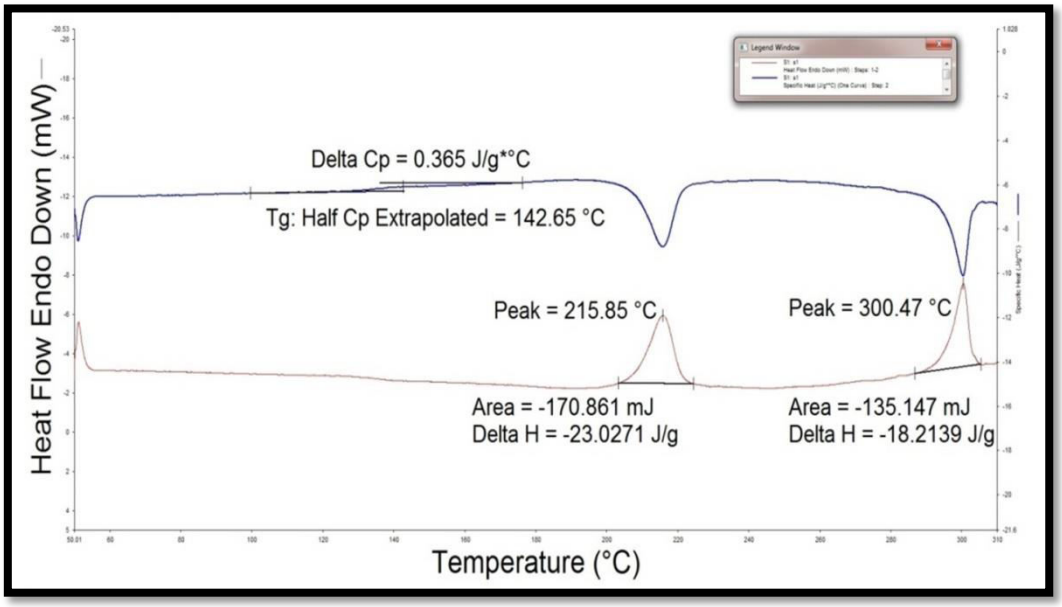

Figure 2.11 Representative image of *Perkin Elmer Pyris*^{TM} showing the calculation of ΔC_p and ΔH_c

The value of ΔH_c during the crystallization process has been estimated by measuring the area under the exothermic peak as,

$$\Delta H_c = \frac{\eta A}{m} \tag{2.4}$$

where η is an instrumental constant – found to be 1.12; A is the area under the crystallization peak and m is the mass of the sample. In our experiments, we enter the mass of the sample and then execute the program. Once the thermogram was obtained, the area under the crystallization peak was calculated. By choosing inbuilt

option in the compatible software the values of ΔH_c were calculated. The representative Figure 2.11(screen shot of the *Pyris* Software) is shown as a guide to the eye for demonstrating the calculation of ΔH_c.

2.6 INDIGENOUSLY FABRICATED HIGH TEMPERATURE MELT QUENCHING UNIT TO PREPARE CHALCOGENIDE GLASSY ALLOYS

In this section, we discuss an indigenously fabricated high temperature melt quenching system to prepare glassy alloys. This comprises a high temperature furnace with a vertically rotating ampoule holder assembly and a speed control system. The vertically rotating ampoule holder assembly is provided to hold at least one ampoule tube having the sample. The vertical rotation of the ampoule tube ensures uniform mixing of the sample composition. The embedded heating elements maintain heat within the furnace and allows the sample to melt at high temperature. The system incorporates a quenching unit provided with a cooling medium. Here, the quenching unit is thermally insulated and vertically placed below the high temperature furnace so as to receive the ampoule tube at a rapid speed freely under gravity. This enables quenching of the sample composition in the ampoule tube, leading to the obtention of desired amorphous samples of glassy alloys.

2.6.1 Need for the improved design of high temperature melt quenching unit

The Synthesis of chalcogenide glasses is a challenging task as it requires rapid quenching of the ampoule containing chalcogenide melt from high temperature (1000°C - 1200°C) to a low temperature ~ 10°C within a fraction of a second. This involves dropping of the ampoule into a low temperature ice bath. The sudden drop into the ice bath arrests the chalcogenide melt in glassy/amorphous form. Chalcogenide melt is the combination of chalcogens and metal elements in it. It is basically metalloid or metal mix. Arresting this in amorphous form needs to be done quickly, else the same will result in crystalline form. Continuous rotation while heating should also be maintained to ensure proper mixing of the material.

Conventionally used high temperature furnaces make use of horizontal type rotation, tilting, and the like.. Some of the typically known methods for the preparation of chalcogenide glasses employ a horizontal mode of rotation which leads to improper mixing of sample composition. Further, in such methods, heating samples are placed inside a ceramic tube, resulting in a temperature gradient on samples during heating process. Furthermore, quenching process is slow since the samples are pushed through the length of the tube, thereby leading to temperature gradient problems before the actual quenching begins.

All ampoule holders, till date, are typically designed to rotate inside a ceramic tube – mostly horizontally. There are a number of factors a horizontally rotating ampoule holder is subjected to, namely:

1. If the speed of rotation is slow, the reduced speed and the friction present between the interior of the ceramic tube and the exterior of the quartz ampoule holder will lead to the following consequence: the holder will be carried along the inner curvature of the tube to a certain position and then will slide off to the bottom portion of the horizontally rotating ceramic tube when the gravitational pull becomes marginally greater than the frictional resistance. This will, in all practical purposes, not allow for proper mixing of the chemicals inside the ampoule.
2. If the speed of rotation is relatively medium-high, then the ampoule will be raised to half of the diameter of the tube and will then fall back, in air, to the bottom portion of the ceramic tube. This will in effect cause the ampoule to break at elevated temperatures. Repeated process of this kind of experiments will also lead to the ceramic tube failure.
3. If the speed of rotation is high to very high ($\geq$ 20 rpm), then due to centrifugal force acting on the chemicals inside the ampoule, there will not be any kind of mixing taking place .

Moreover, with the present system available, it was observed that, after the heating process is complete and when the sample needs to be quenched, it either needs to be pushed through the complete length of the tube or the whole furnace needs to be

rotated 90°. to ensure self-falling of ampoule due to gravity and "frictional force" between the walls of the ceramic tube and quartz ampoule. In summary, although conventional methods of preparation of chalcogenide glasses by horizontally rotating, tilting type furnaces yielded results, it was a big motivation to prepare and achieve far better-quality glasses by simplifying the process system and also implementing better safety norms. Further, there is also a need for an improved ampoule holder which achieves uniform mixing and also removes all the problems of horizontal rotating ampoule holder. Therefore, the fabricated high temperature melt quenching system enabled the preparation of glassy alloys required for all our subsequent experiments.

2.6.2 Design specifications of the fabricated high temperature melt quenching system

Horizontal muffle type furnace with opening in the front capable of enduring continuous operating temperatures up to 1300ºC and occasional maximum temperature of 1400ºC is designed. The bottom of the furnace has an opening of 50mm diameter which aligns with the quenching tank placed vertically below the hot zone of the furnace. This hole enables the ampoule to drop through without any interference. As the Quartz ampoule needs to be rotated inside the heating chamber for proper mixing of sample composition, a specially designed ampoule holder is fabricated, which enables vertical rotation of the ampoule as opposed to the horizontal rotation. The ampoule holder and guide rod system are connected to a set of bearings and pulleys which in turn connect to a motor system where speeds can be controlled from 10 RPM to 90 RPM. A separate RPM indicator is also provided and calibrated to be used with a proximity sensor. After the achievement of proper thermal characteristics, the quartz ampoule with samples are allowed to fall free in to the quenching tank with a cooling medium to obtain the amorphous samples. Figure 2.12 illustrates a front view of high temperature melt quenching unit and the corresponding functional units are as follows:

1) Furnace doors,
2) Heating elements,
3) Inconel sample holder,

4) Quenching tank
5) Extended closure for motor and mechanical drive pulley system
6) Electronic motor drive and speed indicator,
7) Control systems for main furnace

2.6.3 Design specifications of ampoule holder

The complete holder system is designed in such a way that the ampoules do not fall off until necessary by ensuring that the free side portions are sealed and only one opening with cap is given to insert or remove the ampoule at any point of time. Figure 2.13 illustrates the design of the holder system and its corresponding features are as follows

1) Inconel centre rod,
2) Bearing assembly,
3) Bearing base mount,
4) Machined Inconel rod in square form so as to aid rotation,
5) Inconel sample holder,
6) Inconel cap

A box type Inconel holder is designed with a drop on type cap having an inner working volume of 12mm W X 12mm L X 100mm H. On one of the outer sides of the Inconel ampoule holder, a 30mm long square rod is extended. A fitting rod machined with a small clearance (tolerance) is also machined so as to fit the square portion of the holder. A square shape is selected so that it will enable the rotation without slip and guide the holder easily. The other side of the square machined rod is fit tightly into a bearing assembly and attached with a pulley and belt system, which connects to a motor. The motor is three phase geared unit capable of speed adjustments from 10 to 100 RPM by variations in the frequency fed to the motor, done using an imported motor drive. The speed indication is displayed by an RPM indicator coupled with a proximity sensor. The cap is attached to the holder with fine grade temperature tolerant wires tied around the holder, positioning the cap so that the ampoule will not fall off the holder even while the holder rotates vertically. A small

amount of ceramic fibre is also placed in the holder so that the metal end of the holder will not cause any damage to the quartz at high temperatures.

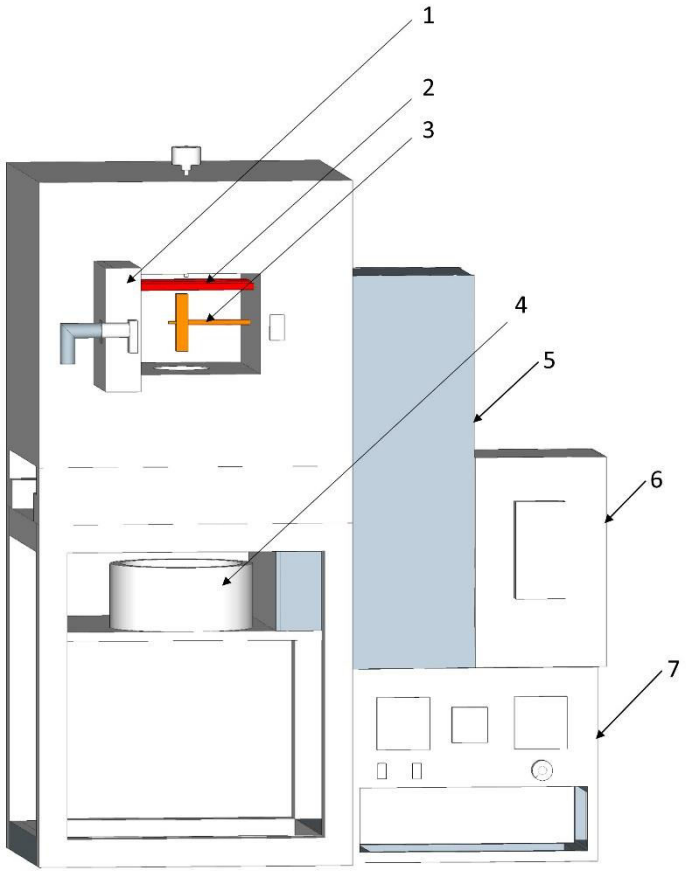

Figure 2.12 Front view of high temperature melt quenching system (complete patent has been filed : **Patent application No: 201641044209**)

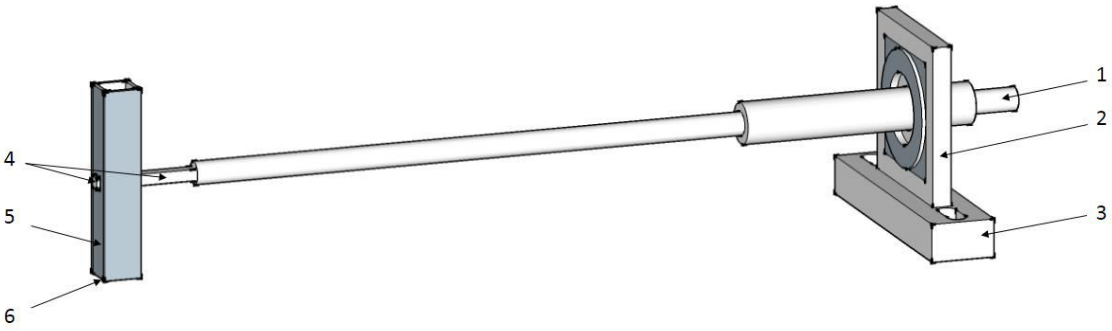

Figure 2.13 Isometric view of an ampoule holder system

2.7 ADVANTAGES OF HIGH TEMPERATURE MELT QUENCHING UNIT.

1) The new holder design can synthesize 4 samples at a time. Further increase in the holder volume will increase the number of samples to be prepared.
2) The arrangement of the holder enables quenching of the ampoule rapidly at gravity pull.
3) Identification and alignment of the sample holder in such a way that mold will be collected at the bottom of the ampoule .
4) During the quenching process even if the door is open for a small period of time, the ampoule will not suffer thermal instability.
5) Operating temperature of the furnace can be maintained up to 1300°C
6) Though we have focused on preparing chalcogenide glassy alloys, this unit can also be used for the preparation of various semiconductor alloys.
7) The present system is basically a two in one system owing to the ability of removing holder assembly from the furnace with ease, which allows us to use the same furnace system for other practical applications whenever required.
8) The uniform mixing is claimed due to the vertical rotation system. This rotation is set up in such a way that it provides agitation to the sample while mixing.

CHAPTER 3

ELECTRICAL SWITCHING AND THERMAL STUDIES OF $Ge_{20}Te_{80-x}Sn_x$ CHALCOGENIDE GLASSY ALLOYS

In this chapter, the studies of memory type electrical switching behavior and thermal properties of a ternary $Ge_{20}Te_{80-x}Sn_x$ ($0 \leq x \leq 4$). chalcogenide glassy alloys are presented. This chapter comprises of detailed study on composition, thickness and temperature dependence of chalcogenide glasses on switching voltage. Investigations using X-ray diffraction (XRD) and scanning electron microscopy (SEM) revealed the formation of a crystalline channel that acts as the conduction path between the two electrodes in the switched region. Furthermore, thermal studies carried out using DSC technique and crystallization kinetics are discussed. Glass forming ability of the said composition has been estimated by thermal crystallization. Thermal parameters are correlated with the electrical switching studies to get an insight into the phase change mechanism. Results of the calculated thermal parameters reveal that the GFA of the synthesized $Ge_{20}Te_{80-x}Sn_x$ ($0 \leq x \leq 4$) glassy alloys has a synchronous relationship with their thermal properties studied through differential scanning calorimetry, indicating their potential for phase-change memory device applications.

3 .1 INTRODUCTION

Electrical switching is one of the scientifically interesting and technologically important phenomenon exhibited by non-crystalline semiconductors that was first observed by Ovshinsky (Ovshinsky 1968). Chalcogenide glassy alloys are typical semiconductor materials capable of exhibiting electrical switching. By applying a suitable electric field, chalcogenide compounds can be switched from a high resistance (OFF/RESET) amorphous to a low resistance (ON/SET) crystalline state and the voltage at which switching occurs is called threshold or switching voltage (V_T). In general tellurium (Te) rich chalcogenides exhibit memory switching behavior (Lokesh et al. 2010). Out of many Te rich chalcogenides, Ge-Te is a system that has been extensively studied. It has a well-understood atomic structure and relatively simple binary chemical composition (Murthy et al. 2005). Switching studies on metal doped Ge-Te chalcogenides with additives such as Sn, Bi, Tl, As (Das et al. 2011, 2012;

Prakash et al. 1996; Rahman et al. 2011), have shown that the V_T reduces with increase in additive concentration, which has been attributed to the increase in the metallicity factor and thus to the conductivity of the material. However, the selection of additives and controlling their concentration is a critical factor. Tin (Sn) has been incorporated as an additive in different chalcogenide systems such as, Se-Te, $Pb_9Se_{71}Ge_{20}$ and Ge-Se-Te, whose physical and electrical properties improved drastically in comparison to the host matrix (Abdel-Wahab 2011; Heera et al. 2012; Modgil and Rangra 2014). Bi-layer chalcogenide films formed by interfacing Sn-Te with Ge-Te favored phase transition in Ge-Te and also yielded optimum phase change characteristics (Campbell and Anderson 2007). Furthermore, inclusion of Sn-Te in Ge-Te produces an ohmic contact with better adhesion between the layers which assisted in exhibiting excellent PCM characteristics. Although Sn plays a major role in improving material properties, literature report gives clear evidence to show that Sn containing bulk chalcogenides form a very narrow region of chalcogenide glass formation. Aforementioned reasons motivated us to investigate the interaction of heavy metal like Sn with Ge-Te chalcogenides.

For the present study, a ternary chalcogenide system with $Ge_{20}Te_{80-x}$ as the host matrix and Sn as the additive was synthesized, which yielded composition $Ge_{20}Te_{80-x}Sn_x$ ($0 \leq x \leq 4$). Electrical switching behavior and thermal properties of $Ge_{20}Te_{80-x}Sn_x$ ($0 \leq x \leq 4$) chalcogenides were studied for understanding the effect of Sn on switching. Switching studies were also carried out by varying the temperature and thickness of the chalcogenides. An attempt was made to understand the chalcogenide glass formation based on the results of thermal crystallization studies and composition dependence of surface morphology. Furthermore, a correlation between the thermal parameters and electrical parameters is established to validate the results in order to further understand the applications of $Ge_{20}Te_{80-x}Sn_x$ ($0 \leq x \leq 4$) glassy alloys in PCM devices.

3.2 EXPERIMENTAL TECHNIQUES

3.2.1 Sample Preparation

A total of eight different ternary chalcogenide compounds having a composition $Ge_{20}Te_{80-x}Sn_x$ ($0 \leq x \leq 4$) were prepared using vacuum sealed melt-quenching approach by varying 'x' as 0, 1, 1.5, 2, 2.5, 3, 3.5 and 4, respectively. In a typical synthetic process, suitable quantities of elemental precursors namely Ge, Te and Sn (99.99% pure) were weighed and transferred into a flattened quartz ampoule. The ampoule containing the precursors was evacuated to a pressure of ~10^{-5} Torr (*Avac Vacuum*, made in India) and was held for 30 min, after which it was sealed under vacuum. The sealed ampoule was loaded into a custom built electric furnace (*Indfurr*, made in India) and was slowly heated to 1000°C at a heating rate of 100°C/h. The ampoule was maintained at this temperature for 24 h under continuous rotation at 10 rpm to ensure homogeneity of the melt. The ampoules were subsequently quenched in an ice water bath mixed with NaCl for obtaining the ternary chalcogenides.

3.2.2 Structure, morphology, electrical switching and thermal studies

X-ray diffraction (XRD) patterns of the synthesized compounds were recorded using an X-ray diffractometer (Rigaku MiniFlex 600-Benchtop XRD, Made in Japan) with Cu Kα radiation (λ = 1.54056 Å). Morphology and energy dispersive X-ray spectroscopy (EDS) studies were performed using a JEOL JEM 6380AL high-resolution scanning electron microscope (SEM). The samples for SEM were prepared by sputter coating gold to avoid charging effect. The electrical switching studies on the as-synthesized $Ge_{20}Te_{80-x}Sn_x$ ($0 \leq x \leq 4$) ternary chalcogenide samples were performed using a programmable dc source-meter (Keithley 2410-C, made in Canada). The samples (0.30 mm thickness) were mounted on a two probe sample holder in between a flat bottom electrode and a pointed electrode using a spring load mechanism. A current of 0 – 2 mA was passed and the voltage developed across the sample was measured. Temperature dependence on the switching voltage was studied in the range of 30-110°C using a custom built heater cell (Indfurr, made in India) installed with a thermocouple.

DSC experiments were carried out using a DSC 8000 Instrument (*Perkin Elmer*, USA). The samples had masses in the range 10-20 mg, and the experiments to record the thermal parameters T_g, T_c and T_m were undertaken in the temperature range of 323-673K K at a scan rate of 10 $Kmin^{-1}$. The changes in the specific heat and enthalpy were estimated and their interdependence was studied as a function of glass composition. Perkin Elmer Pyris is a compatible software employed to calculate parameters like ΔC_p and ΔH_c.

3.3 RESULTS AND DISCUSSIONS

3.3.1 XRD Studies

Since electrical switching behavior can only be shown by amorphous semiconductors, it is important to confirm the non-crystalline nature of as-synthesized $Ge_{20}Te_{80-x}Sn_x$ ternary chalcogenides. Figure 3.1 shows the XRD pattern of the as-prepared $Ge_{20}Te_{80-x}Sn_x$ $(0 \leq x \leq 4)$ glass samples. The amorphous nature of as-prepared samples is proved by the absence of sharp diffraction peaks in the XRD patterns.

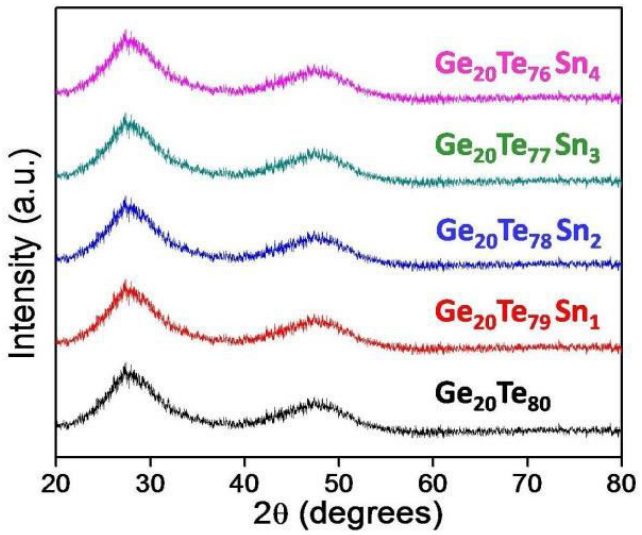

Figure 3.1 X- Ray diffraction patterns of as-prepared $Ge_{20}Te_{80-x}Sn_x$ $(0 \leq x \leq 4)$ chalcogenide glassy alloys. Absence of the sharp peaks in the XRD pattern indicate their amorphous nature.

3.3.2 I-V characteristics of $Ge_{20}Te_{80-x}Sn_x$ chalcogenides and thermal mechanism

I-V characteristics of eight chalcogenide samples in the series $Ge_{20}Te_{80-x}Sn_x$ ($0 \leq x \leq 4$) are presented in Figure 3.2. It is clear from the plots that at lower applied current, the samples exhibit an ohmic behavior and at a certain critical voltage called threshold voltage V_T, the samples exhibit a rapid switching from amorphous (high resistance OFF state) to crystalline (a low resistance ON) state. It was found that samples did not revert back to their original OFF state resistance even after removing the applied electric field. This observation indicates that memory switching behavior occurs at a comparatively lower applied current (2 mA) in $Ge_{20}Te_{80-x}Sn_x$ ($0 \leq x \leq 4$) chalcogenide compounds. Literature reports suggest that tellurium rich chalcogenides exhibit a clean electrical switching without any fluctuations in the I-V plots during their transition to the ON state(Lokesh et al. 2010). But, rapid variation of electrical conductivity is also reported to influence the switching behavior (Warren 1970). However, out of the many factors which determine memory switching in chalcogenides, the formation of a crystalline channel (filament) between the electrodes is quite significant.

In principle, filament formation can be provoked by thermal or electronic fluctuations that lead to redistribution of current, leading to switching (Adler et al. 1978). Initiation of threshold supports filament formation due to the inability to arrest switching at any point within the region of negative resistance. Reports so far suggest that switching in chalcogenides is always associated (implicitly or explicitly) with the region of current-controlled negative resistance (CCNR) (Owen and Robertson 1973). CCNR provides a positive feedback mechanism which allows the system to carry the same or larger currents with smaller voltages in the region of instability. On the other hand, thermal mechanisms of switching were first discussed by Warren (Warren 1970), in which the current suddenly increases when the voltage reaches V_T, wherein V_T corresponds to the complete filling of defect states in chalcogenides. Defects in amorphous semiconductors such as structural defects can dominate the switching process. The atomic structure and the electron levels introduced by the defects were reported to influence the switching behavior in chalcogenides (Waser et al. 2010).

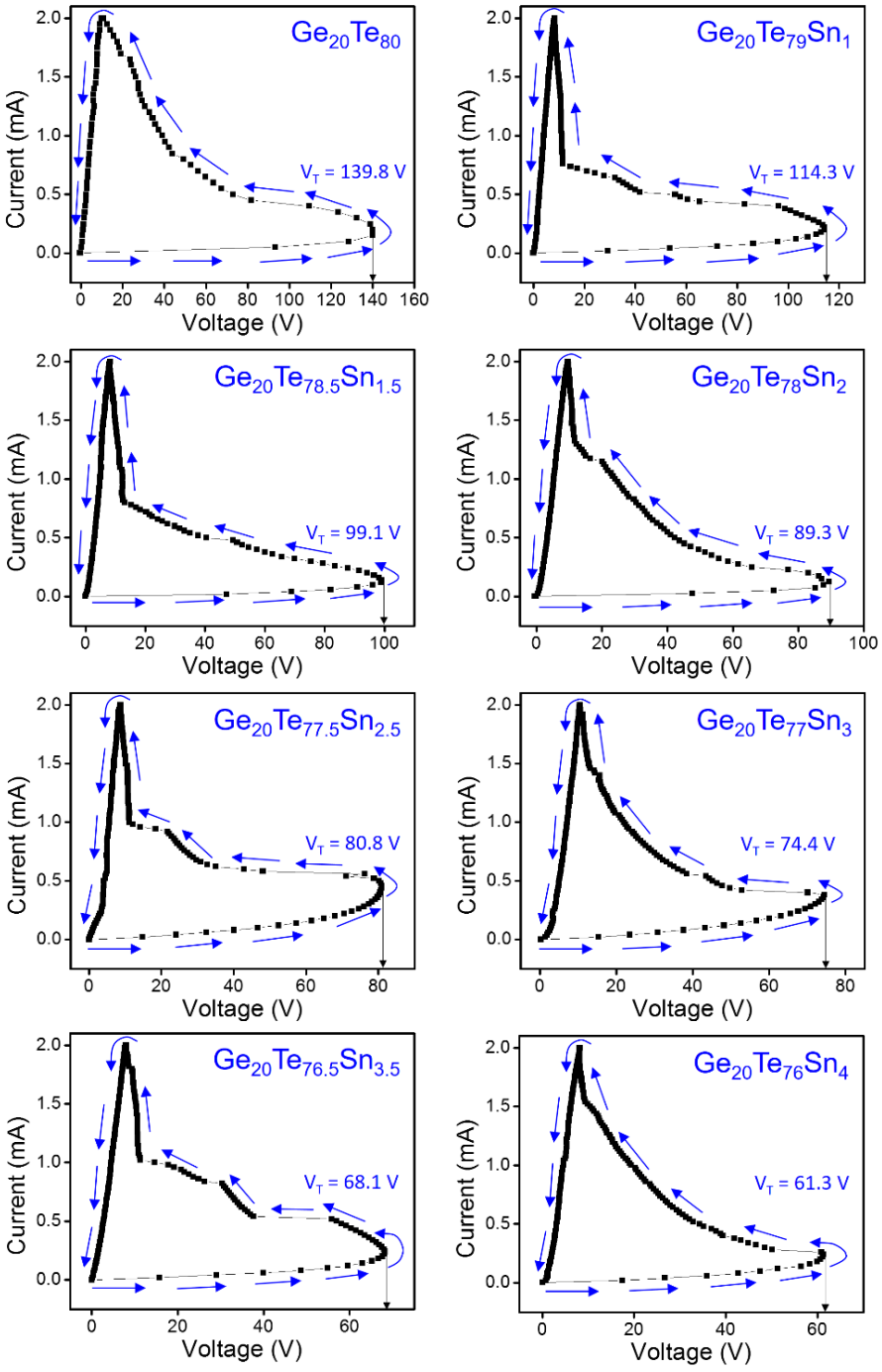

Figure 3.2 I-V characteristics of $Ge_{20}Te_{80-x}Sn_x$ chalcogenide compounds in the composition range x = 0 to 4. As seen from the plots the switching voltage (V_T) decreases remarkably with respect to increase in Sn content. The arrow marks in the I-V plots are guide to the eye representing the direction of current sweeping.

Adler(1980) has reported that lowest energy defects known as a Valence Alternation Pair (VAP) are expected in amorphous chalcogenide alloys, in which switching occurs when the defect states are filled by the field injected charge carries (by a way of Poole-Frenkel effect). This essentially indicates that electrical conductivity of the medium is field dependent. When the defect states are filled, the field dependent mobility or carrier concentration would suddenly increase (owing to the change of phase from amorphous to crystalline) from low to high value, thereby decreasing the resistivity (initiation of switching, Threshold voltage V_T) of the material and enabling a larger current to flow through the chalcogenide. In general, the chalcogenides studied herein are p–type semiconductors with a high resistance OFF state due to the dominance of holes (h^+) as charge carriers, whereas, electrons (e^-) are responsible for the dynamic low resistance ON state. In the OFF state (high resistance cold layer of the material) both of these charge carriers (e^- and h^+) are trapped in the localized state owing to which the charge carrier free path is very small (only about 10^{-9} m = 1 nm) and their lifetime at extended states is very low. However, their relaxation time is reported to be longer than diffusion length lifetime or recombination time (Savransky 2005). Hence, the high resistance OFF state of the chalcogenides studied herein is associated to dielectric relaxation. It is important to note that switching occurs by dielectric breakdown (O'Dwyer 1969).

At V_T, the lifetime of the current increases longer than the relaxation and hence a sudden drop in voltage is observed. Based on the thickness and material composition, the lifetime is reported to vary (Popescu 1975). Usually memory switching is observed in poorly connected Te rich amorphous chalcogenides, owing to their greater conductance, resulting in greater power dissipation which eases the formation of conducting channel. The formation of conducting paths is more drastic in those chalcogenide compositions which devitrify easily, and compounds with lower thermal diffusivity are likely to exhibit memory switching which is attributable to their thermal origin (Stocker 1970).

3.3.3 Compositional dependence of threshold voltage (V_T)

The variation in the switching voltages and starting electrical resistance of $Ge_{20}Te_{80-x}Sn_x$ ($0 \leq x \leq 4$) chalcogenide compounds with respect to the composition is presented in Figure 3.3. The plot indicates a stepwise decrease in both V_T and starting electrical resistance with increase in atomic percentage of Sn. Previous studies have revealed that the composition dependent switching voltage is determined mainly by the metallic factor of the additives and the connectivity or rigidity of the network (Asokan and Lakshmi 2012). According to the network constraint theory (Phillips 1979), the addition of higher coordinated atoms increases the network connectivity and complexity of the structural reorganization required for memory switching owing to which there is an increase in the switching voltages.

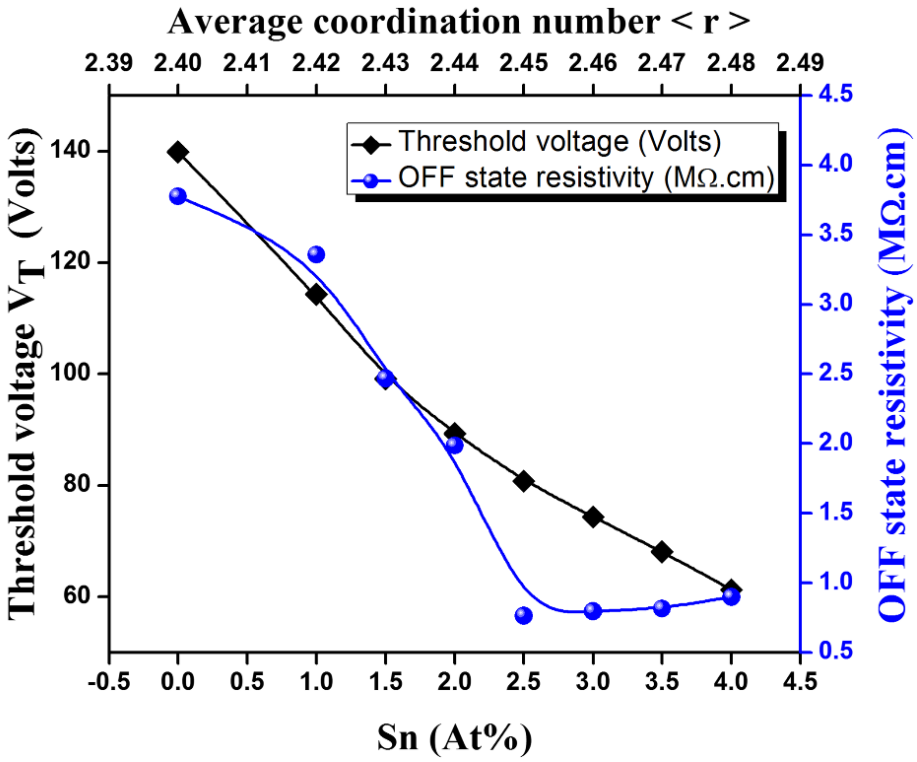

Figure 3.3 Compositional dependence of threshold voltage (V_T) and OFF state resistivity of $Ge_{20}Te_{80-x}Sn_x$ ($0 \leq x \leq 4$) chalcogenide compounds as a function of atomic percentage of Sn. Both V_T and OFF state resistivity are found to decrease with increase in Sn concentration

The most interesting outcome of the present work is the significant decrease in V_T with increase in Sn content. As mentioned in the experimental section, herein the chalcogenides with composition $Ge_{20}Te_{80-x}Sn_x$ ($0 \leq x \leq 4$) are synthesized by the addition of Sn metal to the host matrix ($Ge_{20}Te_{80}$), making it more metallic in nature. Since the inclusion of Sn happens at the expense of Te, there is a remarkable decrease in V_T which can be attributed to the increase in conductivity in the chalcogenide system, owing to the lower resistivity value of Sn in comparison to Te ($\rho_{Sn} = 11.5 \times 10^{-8}$ Ωm and $\rho_{Te} = 10 \times 10^{-5}$ Ωm). The addition of metallic additives such as Cu, Ag, Bi and Tl (Das et al. 2011; Rahman et al. 2011; Ramesh et al. 1999) to Ge-Te system exhibit a decrease in V_T indicating that the present results are in accordance with literature reports. Furthermore, during memory switching process the lower resistivity allows higher currents to flow through the samples which in turn raises the temperature due to Joule heating assisting the structural transformation. These observations indicate that the metallicity of the dopant plays a dominant role in decreasing V_T in $Ge_{20}Te_{80-x}Sn_x$ ($0 \leq x \leq 4$) chalcogenide systems in comparison to intrinsic network connectivity and rigidity. As observed from Figure 3.3, in addition to V_T, the starting electrical resistivity (OFF state resistivity) values also decrease with the increase in Sn content in the chalcogenide compound. Previous studies have already established a direct correlation between V_T and electrical resistivity which support our results. Average coordination number <r> varies with respect to the composition of the chalcogenides. The average coordination number <r> for the composition $Ge_{20}Te_{80-x}Sn_x$ ($0 \leq x \leq 4$) can be given as (Phillips 1979),

$$\langle r \rangle = \frac{\alpha N_{Ge} + \beta N_{Te} + \gamma N_{Sn}}{\alpha + \beta + \gamma} \tag{3.1}$$

where, α, β and γ are concentration (At%) of Ge, Te and Sn, respectively and their coordination number are $N_{Ge} = 4$, $N_{Te} = 2$ and $N_{Sn} = 4$, respectively. Increase in the average coordination number reveals the compactness of the compound. Herein, it is intricate to explain the effect of network topological thresholds such as rigidity percolation on the composition dependence of V_T of $Ge_{20}Te_{80}Sn_x$, since the composition of chalcogenide formation is restricted to a narrow range of average coordination number ($2.40 \leq < r_c > \leq 2.48$).

3.3.4 Thickness and Temperature dependence of switching voltages

Sample thickness (d) is an important parameter that can provide an insight into the switching mechanism. In general, for samples exhibiting memory switching, the variation of V_T shows linear or square root dependence ($d^{1/2}$) with thickness and in case of threshold switching, variation of V_T shows square dependence (d^2) with sample thickness (Jones and Collins 1979). Thermal conductivity (k) of the sample and external heat conductivity (λ) determine the heat loss through the electrode surface and based on the sample thickness V_T varies. Herein, the variation in V_T with respect to the thickness (d = 0.10 - 0.60 mm) of a representative $Ge_{20}Te_{77}Sn_3$ chalcogenide sample is plotted in Figure 3.4. The overall features of I-V characteristics of $Ge_{20}Te_{77}Sn_3$ are not altered by varying its thickness. However, V_T is found to increase linearly with increase in thickness of $Ge_{20}Te_{77}Sn_3$. It is apparent that a linear relationship between switching voltage and sample thickness is relevant, but this result appears to exclude a purely thermal theory which predicts that the switching voltage should have a square root dependence ($d^{1/2}$) on sample thickness (O'Dwyer 1969). The formation of filament in memory switching is well known (Nakashima and Kao 1979). If the sample is a thin slab ($\lambda d >> 2k$), then the loss of heat generated from the filamentary channel to the surface of the electrode is less.

Therefore, for thin samples, V_T is less dependent on the thickness while for bulk samples thicker than 0.3 mm, V_T increases with increasing thickness (see Figure 3.4), indicating that the power required for the filament formation is directly associated with the volume of the channel (Nakashima and Kao 1979). Therefore, it is a common practice to have an optimum thickness (d = 0.3 mm) for memory applications. However, achieving a pellet with thickness less than 0.3 mm for switching experiments is hardly possible, owing to the brittle nature of the bulk samples.

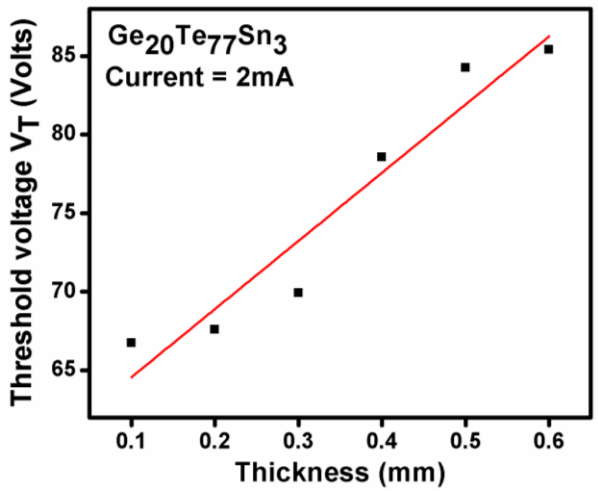

Figure 3.4 Variation of switching voltage (V_T) with respect to thickness of a representative $Ge_{20}Te_{77}Sn_3$ chalcogenide.

I-V characteristics of a representative $Ge_{20}Te_{78}Sn_2$ chalcogenide sample at different temperatures are shown in Figure 3.5. Although the I-V plots in Figure 3.5 become broader and sluggish at higher temperatures, the nature of the switching curves remain the same. The region of the switching slope is narrowed down at higher temperatures since the activation energy required for the phase change reduces, resulting in the decrease of V_T. Memory type materials during switching at elevated temperature are reported to undergo reduction in the energy barriers for crystallization (Murugavel and Asokan 1998). The moderate decrease in V_T of the chalcogenides with respect to the increase in temperature suggest their limited thermal stability and their semiconducting nature is confirmed from the increase in the electrical conductivity with respect to increase in temperature.

The temperature dependence on the threshold switching voltage can be expressed as (Shimakawa et al. 1973),

$$V_T = V_0 \exp\left(\frac{\varepsilon}{K_B T}\right) \tag{3.2}$$

Where, V_T is the threshold switching voltage, ε is the threshold voltage–activation energy, K_B is Boltzmann constant (8.617×10^{-5} eV. K^{-1}) and T is temperature in Kelvin. The threshold voltage–activation energy at elevated temperatures calculated from the

above expression is tabulated in Table 3.1. It can be noticed that the value of the activation energy decreases with increase in the temperature which can be directly related to the decrease in V_T observed at elevated temperatures.

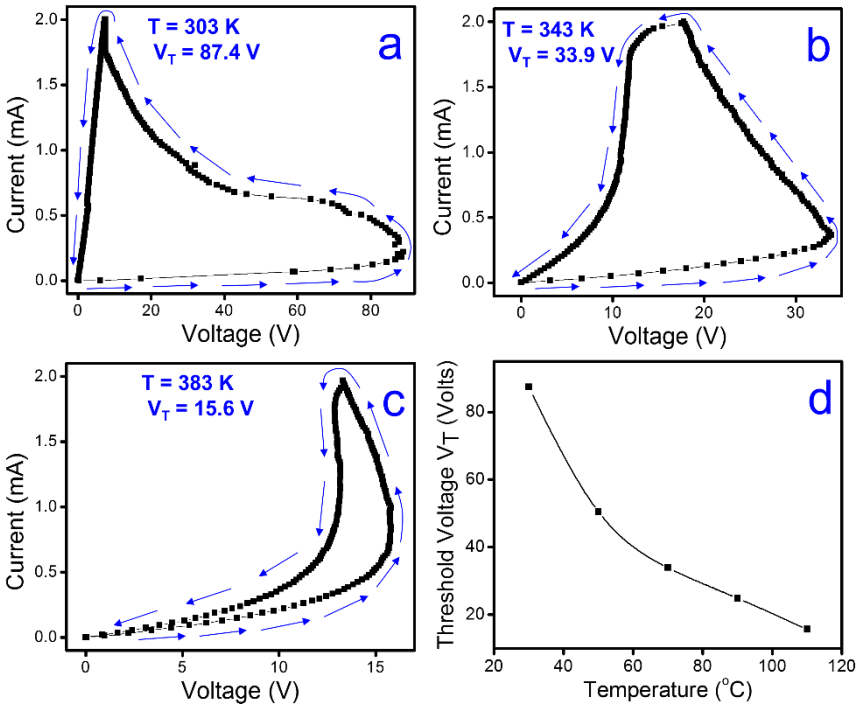

Figure 3.5 I-V characteristics of a representative $Ge_{20}Te_{78}Sn_2$ chalcogenide measured at different temperatures, (a) 303K (b) 343K and (c) 383K. Increase in temperature exhibited a remarkable decrease in V_T which is plotted in (d). The arrow marks in (a), (b) and (c) are guide to the eye representing the direction of current sweeping.

Table 3.1: The values of activation energy (ε) at different temperature range.

Temperature Range (K)	Activation energy ε (eV)
303-323	0.22
323-343	0.19
343-363	0.16

3.3.5 Microscopic study of the switched region

As an additional experimental evidence for confirming the memory switching process, SEM analysis was carried out on a representative $Ge_{20}Te_{78}Sn_2$ chalcogenide sample for analyzing the microstructural changes before and after switching studies. Chalcogenide samples even after the removal of voltage causing memory switching are known to retain their crystalline phase and the crystallized area in a switched sample is called conducting filament (Karuppannan et al. 2011). It is interesting to observe and identify the conducting (current carrying) filament from the SEM micrograph of the switched sample shown in Figure 3.6c and 3.6d, which look like a linear crystalline melt. On the other hand, the morphology of the region other than the conducting filament in Figure. 3.6c look identical to the amorphous phase of unswitched sample shown in Figure. 3.6a.

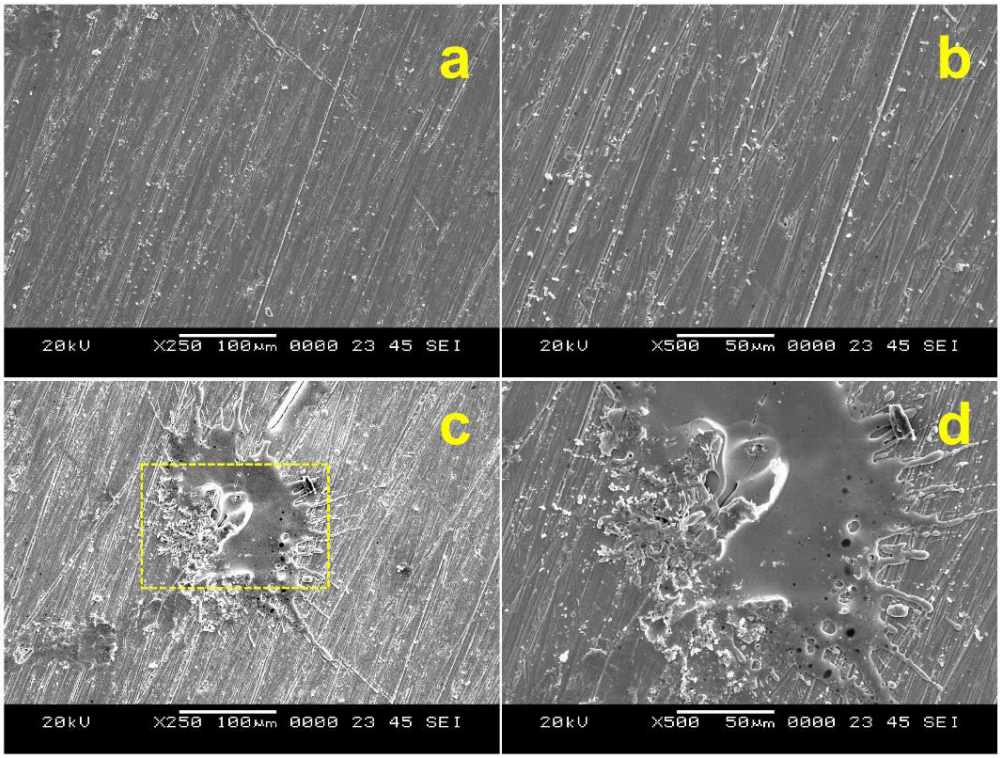

Figure 3.6 SEM micrographs of unswitched (a, b) and switched (c, d) $Ge_{20}Te_{78}Sn_2$ chalcogenide. SEM image in (d) is the magnified area marked in (c), which clearly shows a crystallized melt representing the conducting filament formed during switching.

3.3.6 DSC studies – Compositional dependence of thermal parameters

The dependence of the composition on the thermal parameters provides important information regarding crystallization kinetics of the $Ge_{20}Te_{80-x}Sn_x$ ($0 \leq x \leq 4$) chalcogenide glasses under study and their suitability for phase-change mechanism. The total heat flow curve of one representative $Ge_{20}Te_{78}Sn_2$ glass sample is shown in Figure 3.7. The first peak (endothermic peak) in Figure 3.7a denoted as a circle (expanded in Figure 3.7b), indicates glass transition temperature (T_g) which represents the glassy nature of the prepared material. Further, the sharp peak (exothermic peak) appearing at 500 K in Figure 3.7a indicates the crystallization (T_c), and the peak appearing at about 660 K is the characteristic melting temperature (T_m). The variation of characteristic temperatures, T_g, T_c and T_m for the studied $Ge_{20}Te_{80-x}Sn_x$ ($0 \leq x \leq 4$) glasses is tabulated in Table 3.2. As observed from the thermograms, single T_g accompanied by a single T_c indicates that the prepared glasses are homogeneous. T_g is a very important thermal parameter which is indicative of the connectivity of the glassy network (Wright et al. 1991). The rise in the value of T_g with the introduction of Sn to the base matrix ($Ge_{20}Te_{80}$) can be attributed to the relatively hard metallic or semi-metallic character of Sn with hydrogen like weak bonding in the alloy stoichiometry as reported previously in other chalcogenide glassy alloys (Phillips 1979, 1981). As a consequence, a rise in activation energies for $Ge_{20}Te_{80-x}Sn_x$ was observed in comparison to pristine $Ge_{20}Te_{80}$ base matrix. Furthermore, the addition of Sn attributes to the domination of metallicity factor (more metallic in nature) leading to reduced amorphous network connectivity and rigidity (Fernandes et al. 2016), which resulted in a decline in the value of T_g for $Ge_{20}Te_{80-x}Sn_x$. On the other hand, a similar trend of decrease in the values of T_p and T_c in Sn doped $Ge_{20}Te_{80}$ glassy alloys was observed. Lower values of T_c is indicative of the existence of weak homoploar and heteropolar bonds in glassy configuration. The observed sharp and continuous crystallization process reported herein for Ge-Te-Sn chalcogenide alloys exists between T_c and T_p, owing to continuous breaking of rigid heteropolar bonds, causing generation of greater amount of heat energy in the specimen (Singh 2012). It can be seen that the T_g decreases moderately with increase in Sn concentration (Table 3.2), indicating the disruption of

the covalent bonds caused by the decrease in the chain length, owing to the addition of Sn in Ge-Te, resulting in a reduced structure (Asokan and Lakshmi 2012).

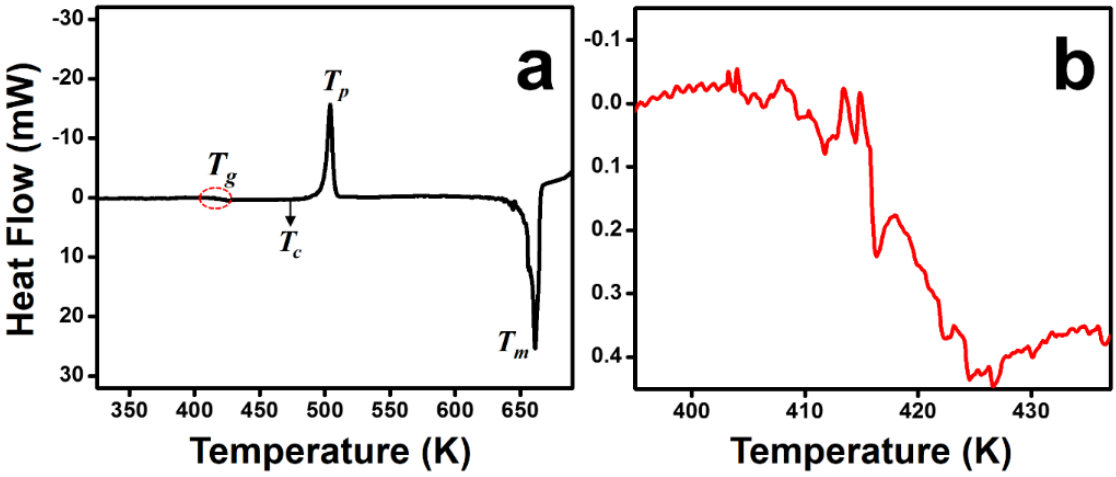

Figure 3.7 (a) Total heat flow curve of a representative $Ge_{20}Te_{78}Sn_2$ glass sample indicating characteristic temperatures such as glass transition temperature (T_g), peak crystallization temperature (T_p) and melting temperature (T_m). The enlarged glass transition temperature region in (a) is expanded in (b).

The specific heat capacity (C_p) measured at T_g is an important parameter to characterize a given glassy material, since it represents the heat stored in molecular motions. The change of state of a glassy matrix from viscous liquid to structurally arrested state is associated with T_g, wherein it is the temperature above which a glassy matrix will attain various structural configurations. Hence, when the glass is heated in a DSC furnace, it must exhibit an increase in the specific heat C_p value at T_g. A change in the specific heat capacity during glass transition (ΔC_p) suggests the occurrence of an extended stiffness transition. Liquids that show large changes in ΔC_p are fragile liquids and those which exhibit small changes in ΔC_p are strong liquids (Angell 1985). Based on the obtained values of ΔC_p listed in Table 3.2, it is clear that the addition of Sn to Ge-Te glasses produces ternary alloys obtained from strong liquids. Similar results have been reported in the case of Sn doping to Se–Sb glasses, which confirms our discussions (Imran 2011; Lafi and Imran 2011).

Table 3.2: Characteristic temperatures and specific heat measurements of Ge-Te-Sn Chalcogenides at a heating rate of 10 $Kmin^{-1}$.

Sample	$T_g(K)$	$T_m(K)$	$T_c(K)$	$T_p(K)$	ΔC_p (J/g K)
$Ge_{20}Te_{80}$	401.24	661.08	487.02	515.8	0.278
$Ge_{20}Te_{79}Sn_1$	415.04	668.31	487.07	502.67	0.238
$Ge_{20}Te_{78}Sn_2$	414.62	661.26	482.82	503.89	0.286
$Ge_{20}Te_{77}Sn_3$	410.99	659.62	476.8	494.19	0.234
$Ge_{20}Te_{76}Sn_4$	408.78	644.09	474.3	490.14	0.344

3.3.7 Crystallization kineics

Generally, the crystallization kinetics of chalcogenide materials is described in terms of the activation energies of amorphous and crystalline transformation (Málek 2000). The dependence of T_g on heating rate (α) has been discussed on the basis of three approaches reported in literature (Das et al. 1972; El-Mously and El-Zaidia 1978; Kissinger 1957; Kotkata and El-Mously 1983; Moynihan et al. 1976). The first empirical relationship is of the form

$$T_g = A + Bln\alpha \qquad (3.3)$$

where A and B are constants for a given glass compositions. According to the equation, a useful assignment of T_g can be obtained by extrapolating the heating rate to $\alpha = 1K/min$, i.e. $T_g = A$. Additionally, the constant B reflects the rate dependence of configurational changes in super cooled liquids (Debenedetti and Stillinger 2001). This dependence can provide information on the kinetics of the glass transition (Moynihan et al. 1976). Values of the constants A and B are obtained by fitting the experimental data to the least square as shown in Figure 4.8b. These values are listed in the Table 3.3.

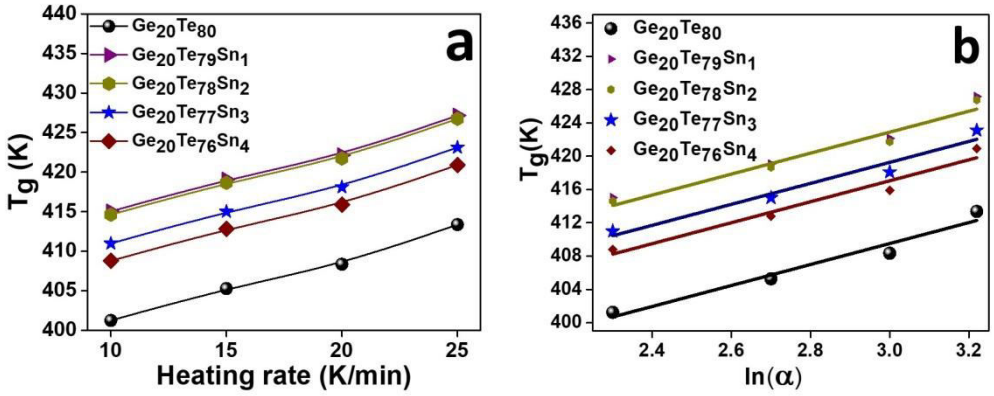

Figure 3.8. Plots showing the (a) dependence of heating rate on the glass transition temperature T_g and (b) glass transition temperature T_g against $ln(\alpha)$.

Table 3.3: Lasocka parameters (A and B), Fragility index and the glass transition activation energy determined using the Moynihan model and the Kissinger equation.

Composition	Lasocka parameters		Activation Energy (E_g) (kJ/mol)		Fragility index (F)
	A(K)	B	Moynihan	Kissinger	
$Ge_{20}Te_{80}$	371.73	12.59	131.86	123.73	16.10
$Ge_{20}Te_{79}Sn_1$	385.53	12.59	127.21	118.43	14.90
$Ge_{20}Te_{78}Sn_2$	385.11	12.59	112.07	104.51	13.16
$Ge_{20}Te_{77}Sn_3$	381.48	12.59	112.07	104.51	13.28
$Ge_{20}Te_{76}Sn_4$	379.27	12.59	108.01	95.94	12.25

It is useful to compare the values of glass transition activation energy (E_g) determined using the different models. Evaluation of E_g using the theory of structural relaxation was first developed by Moynihan et al. (Easteal et al. 1974; Grenet et al. 1981; Howell et al. 1974; Kasap and Juhasz 1986; Larmagnac et al. 1981; Moynihan et al. 1974, 1976; Moynihan and Gupta 1978), from the heating rate dependence of glass transition temperature given as;

$$\ln(\alpha) = -\frac{E_g}{RT_g} + C \qquad (3.4)$$

The plots of $\ln(\alpha)$ against $(10^3/T_g)$ are plotted for various compositions as shown in Figure 3.9a and the slopes of these plots have been used to calculate the activation energy of glass transition (listed in Table 3.3). On the other hand, Kissinger formulation (Kissinger 1957) is also used for the evaluation of the activation energy for glass transition (E_g). Despite the fact that Kissinger equation is basically used for the determination of activation energy for crystallization process, it has been shown that (Chen 1978; Colmenero and Barandiaràn 1979; Macmillan 1965; Shelby 1979) the same equation can be used for the evaluation of glass transition activation energy (E_g), and can be written as;

$$ln\left(\frac{\alpha}{T_g^2}\right) = -\frac{E_g}{RT_g} + C \qquad (3.5)$$

E_g is calculated from the slope of the plot of $ln(\alpha/T_g^2)$ against $(10^3/T_g)$ shown in Figure 3.9b. The glass transition activation energy (E_g) reflects the endothermic energy of the material which is produced due to the unsaturated or hydrogen like bond breaking at the pre crystallization critical temperature (Ozawa 1970). This is based on the assumptions that E_g is associated with the internal energy of the system arising from the relative positions and interactions of its parts, which can be changed by transfer of matter or heat or by doing work (Kumar and Singh 2012). From Table 3.3, it is observed that activation energy of glass transition (E_g) decreases with the increase in Sn content in the samples. Commotion of covalent bonds of Ge-Te network on further addition of Sn leads to the increase in internal energy of the system, thereby channelling to the decrease in E_g values. Similar results on the decrease of E_g with the addition of metallic dopants validate our conclusion (Deepika et al. 2012; Imran et al. 2001; Lafi et al. 2013)

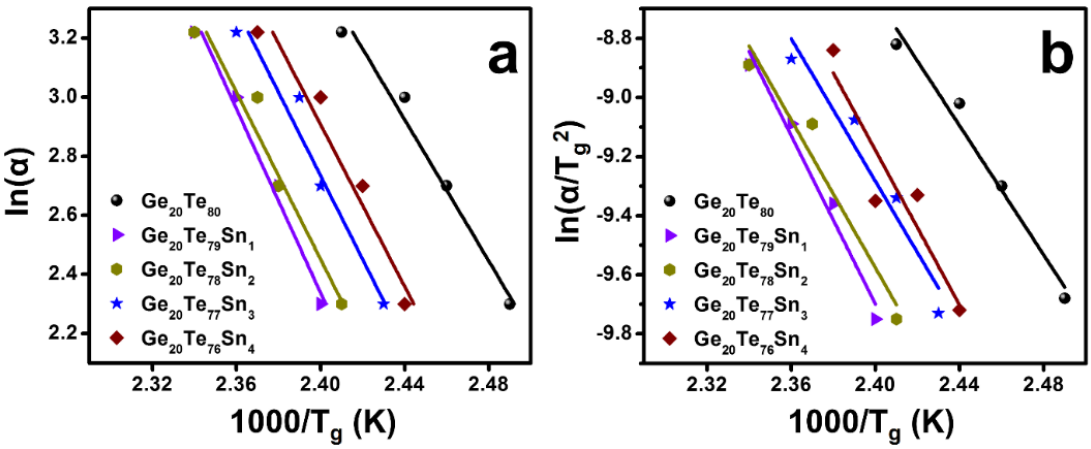

Figure 3.9 Plots exhibiting the variation of glass transition with respect to heating rate in $Ge_{20}Te_{80-x}Sn_x$ ($0 \leq x \leq 4$) chalcogenide glasses based on (a) Moynihan [$ln(\alpha)$ versus $1000/T_g$] and (b) Kissinger [$ln(\alpha/T_g^2)$ versus $1000/T_g$] models.

The fragility is calculated using the following relationship (Böhmer et al. 1993)

$$F = \frac{E_g}{2.303RT_g} \tag{3.6}$$

According to Vigils (Vilgis 1993), glass forming liquids exhibiting an approximate Arrhenius temperature dependence of relaxation time are defined as strong liquids and are specified with a low value of F ($F \approx 16$), while the limit for fragile glass-forming liquids is characterized by a high value of F ($F \approx 200$) (Böhmer and Angell 1994). The values of F for all samples have been listed in Table 3.3. Since the values of F are within the limit of 16, it is reasonable to state that the prepared $Ge_{20}Te_{80-x}Sn_x$ ($0 \leq x \leq 4$) glassy alloys are obtained from strong glass-forming liquids.

According to the Johnson-Mehl-Avarami (JMA) model, several methods can be used to deduce E_c. The first method was suggested by Kissinger (Kissinger 1957), and is based on the fact that the crystallization rate reaches its maximum value at the peak temperature of crystallization (T_p). According to this approach, the variation of T_p with the heating rate (α) is given by,

$$ln\left(\frac{\alpha}{T_p^2}\right) = -\frac{E_p}{RT_p} + C \tag{3.7}$$

The second approach is the one which was developed by Takhor (Takhor 1972) by monitoring the variation of T_p with respect to heating rate (α), which can be written in the form

$$ln(\alpha) = -\frac{E_p}{RT_p} + C \tag{3.8}$$

The third approach to find the crystallization activation energies is Augis-Bennett (Augis and Bennett 1978) approximation method as given by the following equation.

$$ln\left(\frac{\alpha}{T_p}\right) = -\frac{E_p}{RT_p} + C \tag{3.9}$$

Finally, the crystallization activation energies for the studied glasses were also deduced using the following equation, derived by Ozawa (Ozawa 1965, 1971) as shown below:

$$\ln(\alpha) = -\frac{E_c}{RT_c} + C \tag{3.10}$$

This equation describes the variation of onset crystallization temperature T_c with the heating rate (α). Depending on the equations 3.7- 3.10, the data for glassy $Ge_{20}Te_{80-x}Sn_x$ $(0 \leq x \leq 4)$ alloys were fitted to linear functions using the least square fitting function as shown in Figure 3.10a-d, respectively, and the activation energy of the samples were evaluated from the corresponding slopes as listed in Table 3.4.

The activation energy for crystallization (E_c) is a measure of the potential for crystallization, as it indicates the rate of crystallization (Mullin 2001). The observed values of E_c calculated through various theoretical models differ slightly from each other owing to the different approximations used. For example, onset crystallization temperature (T_c) has been used in Ozawa model where the crystallization just begins,

while the other three models use peak crystallization temperature (T_p) at which 62% of crystallization is complete (Lafi et al. 2014). However, the variation in the values of E_c confirms the validity of the studied models as a means for evaluating E_c. As observed from Table 3.4, the activation energy of crystallization (E_c) is found to decrease with respect to increase in Sn content. The decrease in E_c can be attributed to the decrease in viscosity of the medium of the studied glasses, which aids crystallization and causes T_c and T_p to occur at lower temperatures. The estimated values of E_c thus indicate why the atoms of the studied glasses require less energy to switch from amorphous to crystalline form.

3.3.8 Thermal stability and Glass Forming Ability

The Thermal stability $(\Delta T = T_c - T_g)$ and glass forming ability are two important parameters that determine the utility of chalcogenide alloys as recording materials, since phase change optical recording and erasing techniques are based on laser induced thermal amorphization and crystallization of chalcogenide glasses. Therefore, the origin of thermal stability and glass forming ability is of great practical interest. T_g represents the strength or rigidity of a glassy structure, it offers valuable information on its thermal stability. However, information on the glass forming ability cannot be obtained from T_g alone, owing to which the knowledge of crystallization temperature (ΔT) of a glassy material is essential. It has been reported that unstable glasses show onset crystallization temperature close to that of the T_g (Dietzel 1968). Stability of the glassy material towards hot forming processes represents its ability to deform without affecting its amorphous nature. A higher value of ΔT indicates a delay in nucleation process and as the rule of thumb suggests, a minimum value of ΔT of 100 K is needed to provide a sufficient temperature window for applications such as fiber drawing (Rocca et al. 2009). On the other hand, lower values of ΔT represent the ability of the glasses to devitrify easily, signifying the suitability of these materials for PCM devices. The calculated values of ΔT for $Ge_{20}Te_{80-x}Sn_X$ $(0 \leq x \leq 4)$ samples listed in Table 3.5, indicate a consistent decrease with respect to increase in the atomic percentage of Sn, which reveals their easy devitrifiable nature, suggesting their suitability for PCM applications.

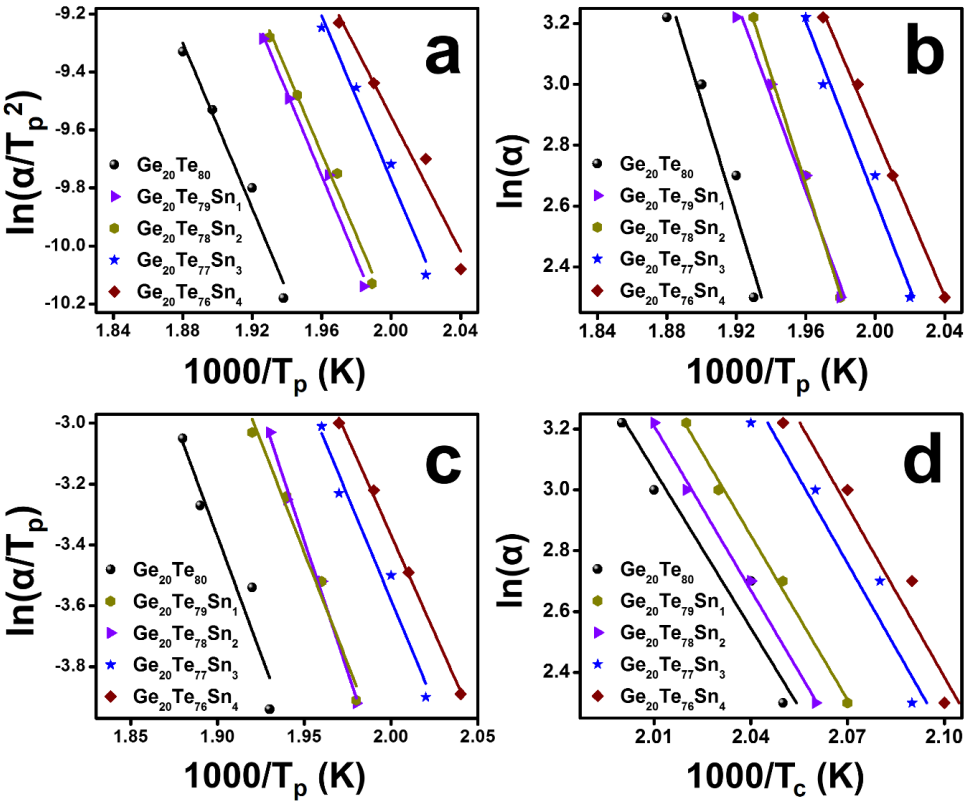

Figure 3.10 Plots of (a) $ln(\alpha/T_p^2)$ versus $1000/T_p$, (b) $ln(\alpha)$ versus $1000/T_p$, (c) $ln(\alpha/T_p)$ versus $1000/T_p$ and (d) $ln(\alpha)$ versus $1000/T_c$ for $Ge_{20}Te_{80-x}Sn_x$ ($0 \leq x \leq 4$) chalcogenide glasses corresponding to Kissinger, Takhor, Augis-Bennett and Ozawa models for calculation of the crystallization activation energy.

Table 3.4 Calculated values of crystallization activation energies (E_c) using Kissinger, Takhor, Augis-Bennett, and Ozawa model

Composition	**Activation energy (E_c) (kJ/mol)**			
	Kissinger	**Takhor**	**Augis-Bennett**	**Ozawa**
$Ge_{20}Te_{80}$	118.73	127.39	128.62	134.49
$Ge_{20}Te_{79}Sn_1$	117.37	132.38	116.68	149.09
$Ge_{20}Te_{78}Sn_2$	119.44	132.38	123.88	157.69
$Ge_{20}Te_{77}Sn_3$	117.35	118.96	114.02	144.02
$Ge_{20}Te_{76}Sn_4$	95.56	110.74	106.61	144.02

Saad and Poulin (Saad and Poulain 1987) suggested another important parameter for thermal stability defined as,

$$S = (T_p - T_c)(T_c - T_g)/T_g \tag{3.11}$$

where T_p is the peak crystallization temperature and the difference $(T_p - T_c)$ is related to the rate of devitrification transformation of the glassy phases. The value of the S parameter listed in Table 3.5 shows a decreasing trend, which is in agreement with the values of ΔT as seen in Figure 3.11 .

Furthermore, it has been reported that the enthalpy ΔH_c released during the crystallization process of a glass is associated with its stability, i.e. glasses with the lowest value of ΔT will have a maximum value of ΔH_c (Mahadevan et al. 1986; Predeep et al. 1997). The value of ΔH_c during the crystallization process has been estimated by measuring the area under the exothermic peak as,

$$\Delta H_c = \frac{\eta A}{m} \tag{3.12}$$

where η is an instrumental constant – found to be 1.12; A is the area under the crystallization peak and m is the mass of the sample. The obtained values of ΔH_c for $Ge_{20}Te_{80-x}Sn_x$ ($0 \leq x \leq 4$) glasses listed in Table 3.5 clearly illustrate an increase with increase in Sn content.

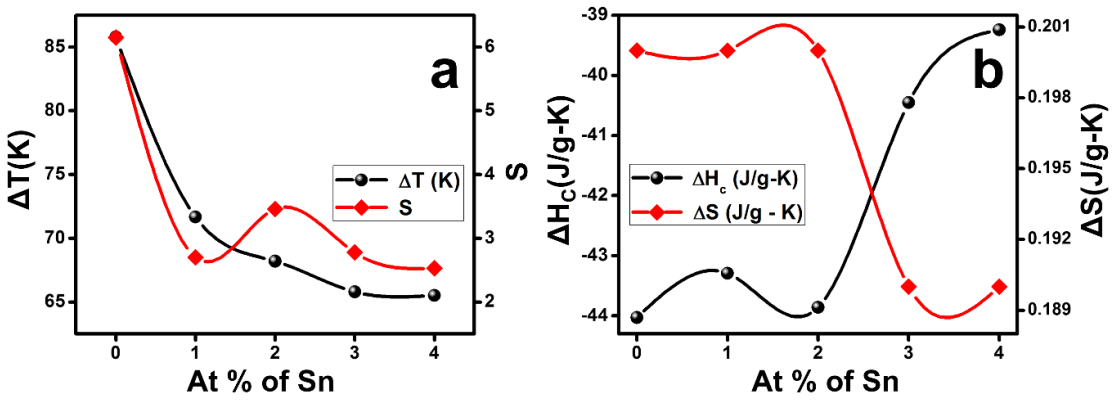

Figure 3.11 (a) Variation of thermal stability $(\Delta T \; and \; S)$ of $Ge_{20}Te_{80-x}Sn_x$ glasses with respect to increase in Sn content indicates a decreasing trend, signifies the easy devitrifiability of the synthesized glasses. (b) Variation of $\Delta H_c \; and \; \Delta S$ with respect to the composition showing a symmetric decreasing trend indicates the presence of disorder in the amorphous system.

The degree of disorder in the amorphous structure is called as entropy (ΔS), which can be deduced during the amorphous to crystalline phase transitions (Aji and Johari 2010; Kumar et al. 2011). Higher values of ΔS are an indicator of a stable glassy state as it posseses a huge energy unstable atomic configuration. The entropy change during the crystallization process can be calculated as (Dalvi et al. 2003),

$$\Delta S = \frac{\Delta H_c}{T_c} \tag{3.13}$$

As observed from Figure 3.11b, the values of ΔH_c and ΔS exhibit a clearly decreasing trend with respect to the increase of Sn content in $Ge_{20}Te_{80-x}Sn_x$ ($0 \leq x \leq 4$) glasses. From the estimated values of $\Delta H_c, \Delta S, \; \Delta T$ and S parameter listed in Table 3.5, it clear that the thermal stability of Ge-Te-Sn decreases with increasing Sn content.

It is well known that thermal stability and glass forming ability (GFA) are related, but they are independent properties for a given glass. GFA of a glassy alloy correlates to the ease by which the melt can be cooled while avoiding crystal formation. However, efforts have been made to study and relate the thermal stability and GFA of chalcogenide glasses with their composition due to their importance in determining the utility of chalcogenide alloys for certain applications. Nasciemento et al. (2005) suggested that GFA is related to the rate of crystallization, wherein a high GFA is associated with a small crystallization rate. The first parameter introduced to estimate the GFA is the reduced glass transformation temperature, T_{rg} given as (Kauzmann 1948), $T_{rg} = T_g/T_m$, which varies between 0.3 and 0.85 for any glass former and is inversely related to the nucleation rate for a variety of materials (Kauzmann 1948). Materials with T_{rg} value larger than ~ 0.7 feature low nucleation rates and can be

quenched into a glassy state without crystallization even during a slow cooling and hence they are called as easy glass formers (Waser et al. 2010). On the other hand, relatively low values of T_{rg} feature higher nucleation rate, implying their poor glass formability. It should be noted that T_{rg} values are too simplistic for exclusively describing crystallization kinetics. As seen from Table 3.5, the value of T_{rg} for $Ge_{20}Te_{80-x}Sn_x$ ($0 \leq x \leq 4$) glasses range from 0.33 to 0.36, which is almost a constant .Therefore, it can be understood that the values of T_{rg} have negligible effect on GFA among various compositions of the studied glasses. Hence, it is important to look for another parameter of the GFA that effectively explains the crystallization kinetics at different compositions of Ge-Te-Sn. Hruby (Hrubý 1972) has introduced a parameter, H_r which combines both nucleation and growth aspects of phase transformations and is given as,

$$H_r = \frac{T_c - T_g}{T_m - T_c} \tag{3.14}$$

where T_m is the melting temperature. The values of the Hruby number (H_r) for different concentrations of Sn at a heating rate of 10 K/min are shown in Table 3.4. According to Hruby, it is found that the difference ($T_c - T_g$) is directly proportional to the GFA. The calculated values of H_r for all compositions of Ge-Te-Sn are found to decrease with increasing Sn content, as shown in the Table 3.5. From the available data, it is observed that synthesized samples have moderate thermal stability.

Table 3.5 Listed values of thermal parameters: Enthalpy, Entropy, Thermal stability, Hruby parameter, reduced glass transition.

Composition	ΔH_c ***(J/g-K)***	***ΔS (J/g-K)***	ΔT ***(K)***	**S**	H_r	T_{rg}
$Ge_{20}Te_{80}$	-44.027	0.20	85.78	6.15	0.78	0.33
$Ge_{20}Te_{79}Sn_1$	-43.293	0.20	71.67	2.70	0.52	0.35
$Ge_{20}Te_{78}Sn_2$	-43.856	0.20	68.2	3.46	0.56	0.36
$Ge_{20}Te_{77}Sn_3$	-40.451	0.19	65.81	2.78	0.50	0.35
$Ge_{20}Te_{76}Sn_4$	-39.242	0.19	65.52	2.53	0.52	0.36

3.3.9 Thermal crystallization and structural studies

Memory switching can be observed only in those systems which have the ability to change states from amorphous to crystalline. Low resistance state of a memory material comprises the crystallized region representing the conducting filament and observing the memory state in it is a kinetically controlled process (Nakashima and Kao 1979). Thus, it is necessary to study the thermal behavior of the chalcogenides samples for understanding the switching process. The samples were prepared by annealing under vacuum (10^{-3} Torr) at their melting temperature (T_m = 400 ºC) for 4 h after which their XRD spectra was recorded. It is known that thermal stability and thermal diffusivity are the key factors in the filament formation. Since filament formation is thermal in nature Joule heating is associated in the process. On applying a high electric field, the current carried between the electrodes in the chalcogenide sample with low resistivity value will experience a higher Joule rating (I^2R), which implies that Joule heating is directly proportional to the drop in resistivity value in the ON-state and the corresponding rise in current (Upadhyay and Murugavel 2013). Typically the energy dissipated by a current pulse is found to be 10^{-5} J, which is sufficient to cause melting (phase change) in the material (Stocker 1970).

The XRD pattern of a representative $Ge_{20}Te_{78}Sn_2$ sample annealed under vacuum at T_m = 400°C for 4 hours shown in Figure 3.12 can be indexed to trigonal Te (JCPDS card no. 01-089-4899) and hexagonal Ge-Te (JCPDS card no. 01-078-3709) phases . However, phases corresponding to elemental Sn or Sn compounds (with Ge and Te) were not detected. In case of host matrix composition $Ge_{20}Te_{80}$, all four fold coordinated Ge atoms bond with two fold coordinated Te atoms, owing to which Ge–Te has a very high binding energy. While Sn atoms are doped into the host matrix, they are expected to change the network by replacing Te atoms, forming a composition $Ge_{20}Te_{80-x}Sn_x$. The addition of dopant to a host matrix with a binary system can happen in two ways viz., (i) it can form its own structural units without participating in forming a network in the system or (ii) it can interact and participate in the network formation with the host and improve the network connectivity and improve the mechanical stability of the chalcogenides (Borisova 2013).

However, when it forms its own structural units, it acts as an impurity and remains as a micro-inclusion which hardly interacts with the host matrix (Singh 2012). On the other hand, since the atomic radius and electronegativity values of Ge and Sn are similar, the addition of Sn may result in a random substitution of Ge by Sn. In such a case, there will be no net increase in the general network connectivity owing to the reasons (the addition of dopant into host matrix) discussed above.

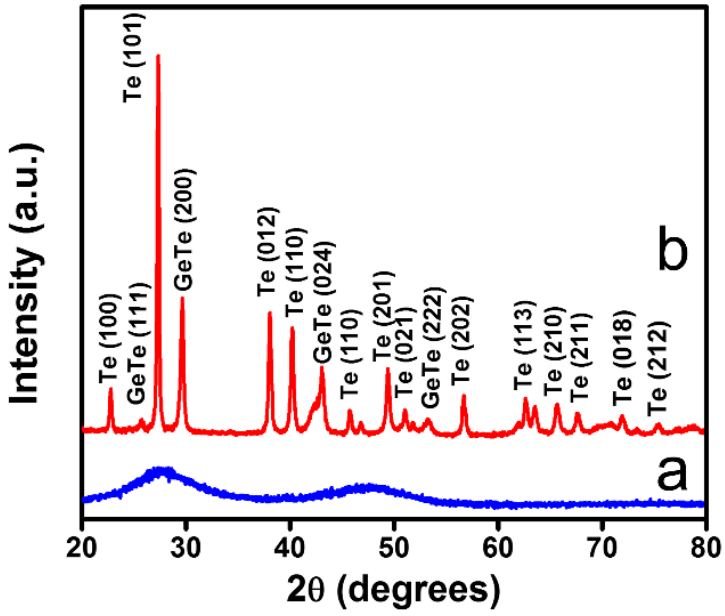

Figure 3.12 X-ray diffraction patterns of (a) as-synthesized and (b) vacuum annealed $Ge_{20}Te_{78}Sn_2$ chalcogenide. The sharp diffraction peaks in (b) indicate the phase change from amorphous to crystalline.

Thermal crystallization studies indicate that Sn does not take active participation in the formation of non-crystalline chalcogenides. However, it is extremely important to perceive how the Sn interacts with the host matrix. SEM and XRD analysis were conducted on $Ge_{20}Te_{80-x}Sn_x$ chalcogenides with different compositions (x = 0, 2, 4, 5 and 7) to explore the behavior of Sn. SEM images in Figure 3.13 indicate a radical change in the surface morphology with respect to increase in the atomic percentage of Sn. As observed from the SEM images, $Ge_{20}Te_{80}$ (host matrix) shows a disordered surface structure, whose amorphous phase is confirmed from the corresponding XRD pattern and EDS results clearly indicate its proper elemental composition (see Appendix I). Doping of Sn (x = 2, 4 %) in the host matrix decreases the rate of disorder in the

surface structure which can be attributed to the metallicity of Sn. But, at such low concentrations, Sn tends to appear as particles (as seen from SEM images corresponding to $Ge_{20}Te_{78}Sn_2$ and $Ge_{20}Te_{76}Sn_4$) distributed over the amorphous background as confirmed from their corresponding XRD patterns and EDS results (see Appendix III and Appendix V).

These particles are the electron rich constituents (Te and Sn) that can efficiently scatter the electron beam in comparison to the other regions in the samples, owing to which they appear bright. On the other hand, at higher doping concentrations of Sn (x = 5 and 7%) which are confirmed from the corresponding EDS results (see Appendix VI and Appendix VII) , the SEM images of $Ge_{20}Te_{75}Sn_5$ and $Ge_{20}Te_{73}Sn_7$ indicate a rough and dry surface revealing the crystalline nature of the samples which were also confirmed from their corresponding XRD patterns. From these observations, it can therefore be concluded that only a maximum of 4% Sn can be doped in $Ge_{20}Te_{80}$ host matrix for obtaining chalcogenides with non-crystalline phase towards memory switching studies.

3.3.10 Correlation between electrical switching and thermal properties

In the present work, the glass formation, crystallization and thermal stability of chalcogenide glasses were investigated in order to ascertain their potential for phase change memory applications. Since T_g is an indicator of the glassy network connectivity, an increase in T_g represents the increase in network connectivity. On the other hand, the addition of dopants decreases T_g, which has been attributed to nano-phase separation caused by the segregation of homo-polar bonds (El-Mously and El-Zaidia 1978). Further, T_g is indicative of the energy required for the phase change from amorphous to crystalline state during memory switching. Based on a configurational free energy model, an empirical relation between the switching fields and T_g has been suggested in the literature (Prakash et al. 1994) as,

$$E_t^2 = C_1 \exp[C_2 * k(T_g - T)/kT] \quad (3.15)$$

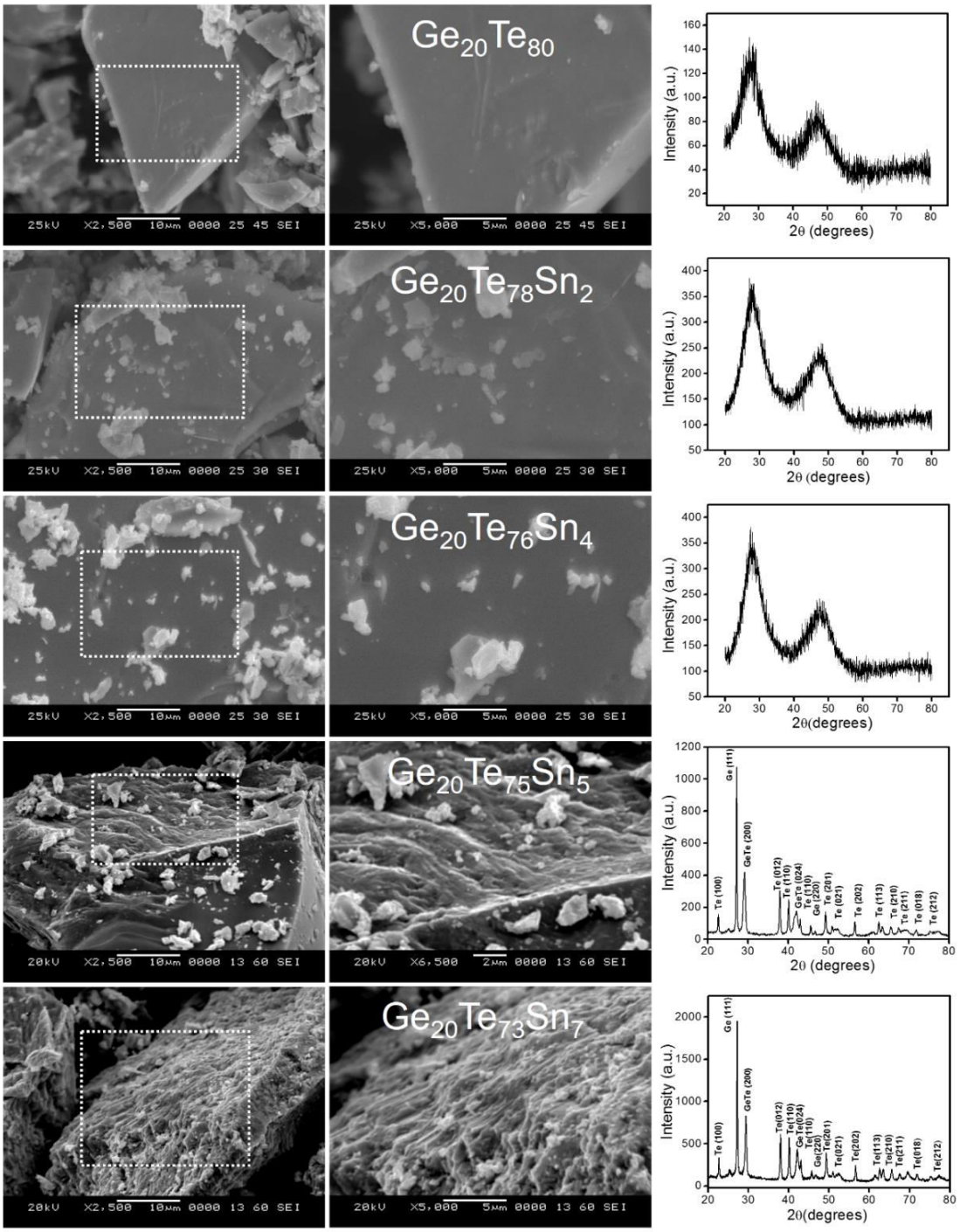

Figure 3.13 SEM images and corresponding XRD patterns of Ge20Te80 (host matrix), $Ge_{20}Te_{78}Sn_2$, $Ge_{20}Te_{76}Sn_4$, $Ge_{20}Te_{75}Sn_5$ and $Ge_{20}Te_{73}Sn_7$.

where E_t is the switching field, C_1, and C_2 are constants, T is the ambient temperature and k is the Boltzmann constant. The results of E_t are directly proportional to the variation of T_g and herein we notice the decrease in T_g with respect to the stepwise decrease in the switching voltage (V_T), which confirms the validity of this relation. In a glassy system, as the network gets more rigid, T_c generally increases and consequentially, V_T is expected to increase. Thus the downward trend and the lower values of T_c result in the decrease of V_T. The crystallization temperature and the activation energy for crystallization (E_c), which denote the energy barrier to overcome crystallization are indicators of the ease of devitrification. As such, a relation between V_T and E_C for crystallization can be expected for memory switching samples. A clear correlation is noticed from the obtained results, wherein we have observed a decrease in the T_c, T_g, E_c and V_T. Similar results have been observed in Ge-Te-Bi system (Das et al. 2011). Further, a low value of E_c could also mean fast crystallization, leading to a good switching speed.

3.4 CONCLUSIONS

Memory type electrical switching behavior of the chalcogenides was observed from their current-voltage characteristics. The metallicity factor of Sn is attributed to the remarkable decrease in V_T from 140 to 61 V with increase in Sn doping concentration. Temperature and thickness dependence of V_T suggest that thermal effects play a key role during switching process. Experimental investigations using XRD and SEM confirm the thermal role in switching through observations on the formation of conducting filament on the surface after switching. Studies on the crystallization mechanisms of melt quenched $Ge_{20}Te_{80-x}Sn_x$ ($0 \leq x \leq 4$) chalcogenide glassy alloys were conducted using differential scanning calorimetry and T_g, T_c, T_p, T_m, E_g, E_c were evaluated. DSC thermograms show that each composition has a single T_g and single T_c value. Various quantitative methods based on Johnson-Mehl-Avarami model were employed for evaluating the values of E_g and E_c, which are observed to be in close agreement with each other. ΔT and ΔH_c of the base $Ge_{20}Te_{80}$ glass are found to decrease with the addition of Sn. Glass forming ability of the Ge-Te decreases with the increase of Sn, resulting in a narrow range of glass forming region. Furthermore, the obtained

thermal parameters of Ge-Te-Sn glasses indicate that the moderate thermal stability and easy devitrifiability are favorable for phase-change memory device applications. XRD and SEM investigations also reveal that Sn hardly contributes in forming amorphous chalcogenide network and remains phase separated from the host matrix, owing to which the maximum composition was restricted to $Ge_{20}Te_{80-x}Sn_x$ to Sn $\leq$ 4%. A relationship has been established between the obtained thermal parameters and electrical switching characteristics. Herein, the decreasing trend in the values of V_T has a coherence with the variation in the values of obtained thermal parameters such as T_c, T_g, E_c and ΔT .

CHAPTER 4

ELECTRICAL SWITCHING AND THERMAL STUDIES OF $Si_{15}Te_{85-X}Bi_X$ AND $Si_{20}Te_{80-X}Bi_X$ CHALCOGENIDE GLASSY ALLOYS.

In this chapter, we report electrical switching and thermal crystallization behavior of $Si_{15}Te_{85-x}Bi_x$ ($0 \leq x \leq 2$) and $Si_{20}Te_{80-x}Bi_x$ ($0 \leq x \leq 3$) glasses. We observe a significant decrease in the threshold voltage (V_T), indicating that in Si-Te-Bi glasses, the resistivity of the additive element Bi plays a dominant role over network connectivity/rigidity. The variation of V_T with respect to thickness and temperature of the sample indicates that the memory switching observed in Si-Te-Bi glasses is influenced by the thermally induced transitions (thermal mechanism). Scanning electron microscopy (SEM) studies on pre- switched and post switched samples reveal the morphological changes on the surface of the sample and serve as an experimental evidence for the formation of the crystalline filament between two electrodes during switching. We have investigated the crystallization kinetics of Si-Te-Bi chalcogenide glassy systems using differential scanning calorimetry (DSC) technique. Furthermore, thermal parameters such as change in specific heat (ΔC_p), fragility index (F), thermal stability (ΔT), enthalpy (ΔH_c), entropy (ΔS) are deduced to interpret distinct material behaviour as a function of composition. Structural evaluation like thermal devitrification studies and morphological changes elucidate on restricted glass formability of the studied glass system. Finally, the relationship has been established between the thermal parameters and electrical switching characteristics of $Si_{15}Te_{85-x}Bi_x$ ($0 \leq x \leq 2$) and $Si_{20}Te_{80-x}Bi_x$ ($0 \leq x \leq 3$) glasses.

4.1 INTRODUCTION

Chalcogenide compounds are of significant technological importance due to their electrical and optical properties(Chopra and Bahl 1970). They are potential materials used in several applications, such as photonic (Shiryaev and Churbanov 2017), thermoelectric(Tohge et al. 1980), energy(Bhat et al. 2017) and phase change memory devices (Wuttig 2005), out of which chalcogenide glassy alloys have been studied

extensively owing to their interesting phase change properties. Over the past four decades, attention has been devoted to the material properties of Te - based binary and ternary chalcogenide compounds because of their potential use memory switching devices. “Electrical switching” refers to an electric field driven transition exhibited by amorphous / glassy chalcogenides from a semiconducting OFF state to a conducting ON state (Fritzsche 1974). Chalcogenides exhibiting memory switching will retain their crystalline phase even after the input electric field has been removed. Hence, they are used as phase change memories (PCM).

Compounds made from the elements of the sixth main group of the periodic table are called chalcogenides: namely, oxides, selenides and tellurides, out of which Te - rich chalcogenides have been broadly studied since they own metallic bond properties (expressed as resonance bonds), contributing to their extremely rich variety of electronic properties (Waser et al. 2010). Usually, tellurides are easily prone to crystallization in comparison with sulfides and selenides. Further, the phase transition between amorphous and crystalline phases is found to be simpler in Te- based glassy alloys, thereby making them more useful materials for PCM applications (Das et al. 2011). Metal doped Ge-Te chalcogenides are some of the prominent materials studied for phase change memory applications. Meanwhile, investigations on Silicon (Si) containing binary or ternary glassy chalcogenides exhibit memory switching phenomenon, such as Si-Te (Murthy et al. 2005), As-Te-Si (Anbarasu and Asokan 2004), Ge-Te-Si (Anbarasu and Asokan 2007) and Si-Te-Sb (Lokesh et al. 2010). The possibility of replacing Ge from known compositions yields newer memory materials with varied electrical properties. The addition of metallic impurities brings about interesting changes in the properties of chalcogenides. For example, Bi and Pb added chalcogenide glasses are found to exhibit carrier type reversal (p to n) (Asha Bhat and Sangunni 2000; Bhatia et al. 1988; Tohge et al. 1980). Alloying Bi with other metal or metalloid elements is expected to enhance material properties, and this fact motivated us to investigate the electrical and thermal properties of $Si_{20}Te_{80-x}Bi_x$ ($0 \leq x \leq 3$) glassy alloys. Conventionally, it was thought that multicomponent bulk chalcogenide glasses have a homogeneous surface morphology, wherein there would be no specific morphological growth as metal atoms enter the glassy network (Singh 2012). Recent

studies suggest that chalcogenide alloys containing metal impurities can develop inhomogeneity within the structure. The metal-containing multicomponent chalcogenide glasses are identified with fractured surface morphology attributed to the micro scale crystallization, leading to inhomogeneity within the glassy structure (Abu-Sehly 2009; Piarristeguy et al. 2007). The inhomogeneity thus developed can improve the work performance of a glassy alloy. In this regard, analysis of surface morphologies becomes quite important.

It is observed that electrical switching in chalcogenides is due to the partial crystallization of the samples on application of high electric field. The repeated transitions between amorphous (OFF state) and crystallization (ON state) during electrical switching has profound effect on the thermal stability and lifetime of the device (Savage 1972; Titus et al. 1993). The dynamics involved in the devitrification of amorphous materials corresponding to time and temperature is called as crystallization kinetics(Singh 2013). Crystallization kinetics of chalcogenide glassy alloys involving quantitative analysis gives characteristic temperatures and their respective activation energy. The activation energy indicates the participation of molecular motions and reorganization of atoms around the critical transition temperatures (Singh 2012). Furthermore, kinetics of devitrification studies is interpreted based on thermal parameters such as thermal stability, fragility index, specific heat, etc. Hence, the knowledge of crystallization kinetics of chalcogenide glassy alloys is particularly important in identifying novel materials for memory applications.

Different methods such as electrical resistivity, X-ray diffraction, electron microscopy and differential scanning calorimetry (DSC) have been used to understand the crystallization of glassy chalcogenides (Raoux and Wuttig 2010). Out of those methods, DSC analysis is a versatile technique designed to obtain the structure of glass and related thermal properties for a wide range of applications. Crystallization kinetics parameters of the vitreous chalcogenides are generally deduced at glass transition temperature (T_g), onset crystallization temperature (T_c), peak crystallization temperature (T_p) and with the aid of several statistical approximations such as Hruby,

Ozawa, Augis - Bennet, Kissinger and Moynihan. It is worth to note that, the aforesaid statistical approximations are deduced based on the Johnson-Mehl-Avarami (JMA) model(Avarami 1941; Johnson and Mehl 1939) . These statistical approximations facilitate calculation of the activation energy for glass transition and crystallization.

In the following sections, electrical switching and thermal behavior of Si-Te-Bi chalcogenide glassy alloys over a narrow composition range ($0 \leq x \leq 3$) are discussed in detail. Thickness and temperature dependence of switching voltages have been studied. Compositional dependence of the thermal parameters is used to understand the effect of Bi on the crystallization of Si-Te glasses. Furthermore, surface morphology and structural studies lay emphasis on glass formability and phase separation in the glass matrix. An attempt has been made to correlate electrical switching studies and thermal properties.

4.2 EXPERIMENTAL TECHNIQUES

4.2.1 Sample preparation

Chalcogenide semiconducting glasses of Si-Te-Bi of four different compositions have been prepared by the well-established melt quenching method. The starting materials (99.99% purity) were weighed in the desired proportions and then transferred to the pre- cleaned flattened quartz ampoules and sealed under a vacuum of 10^{-5} Torr to avoid vaporization at higher temperature. Later, they were heated in an indigenously fabricated custom built furnace (Indfurr, India. patent pending). The ampoules were maintained at 1473 K and rotated continuously for 48 hours to ensure homogeneity of the melt. The ampoules were rapidly quenched into an ice bath containing NaOH and ice water. Amorphous nature of the melt quenched samples was confirmed by X-ray diffraction (XRD) technique.

4.2.2 Electrical switching and thermal properties

The electrical switching studies on the as- prepared Si-Te-Bi ternary chalcogenide glassy alloys were executed using Keithley 2410-C, a programmable source-meter. We

placed the samples of thickness 0.30 mm between a flat bottom electrode and pointed top electrode, making use of spring loaded mechanism. The switching experiments were repeated for at least five samples for each composition and the threshold voltages were found to be reproducible within ±5%. We have also studied the temperature dependence of switching in the range of 303-383K utilizing a specially made heater cell (Indfurr, India) installed with a thermocouple. Thermal properties were measured using DSC (Perkin Elmer, USA) instrument. The samples used for the experiments were of the range 10-20 mg and the operating temperature range of the range 350-600 K was selected at a scanning rate of 10 K/min. The estimated thermal parameters were later analyzed as a function of composition.

4.2.3 Structural and surface morphology studies

X-Ray diffraction (XRD) patterns of the as-synthesized glassy alloys were recorded using a benchtop X-ray diffractometer (Rigaku MiniFlex 600, Japan). Surface morphology and energy dispersive X-ray spectroscopy (EDS) studies were conducted using ZEISS SIGMA FE-SEM high quality imaging and advanced analytical microscopy (ZEISS SIGMA, USA). The samples used for the field emission SEM were gold coated on the surface in order to protect them from charging effect.

4.3 RESULTS AND DISCUSSIONS

4.3.1 XRD Studies

Figure 4.1 shows the XRD pattern of the as-prepared $Si_{15}Te_{85-x}Bi_x$ ($0 \leq x \leq 2$) and $Si_{20}Te_{80-x}Bi_x$ ($0 \leq x \leq 3$) glass samples. The amorphous nature of as-prepared samples is proved by the absence of sharp diffraction peaks in the XRD patterns.

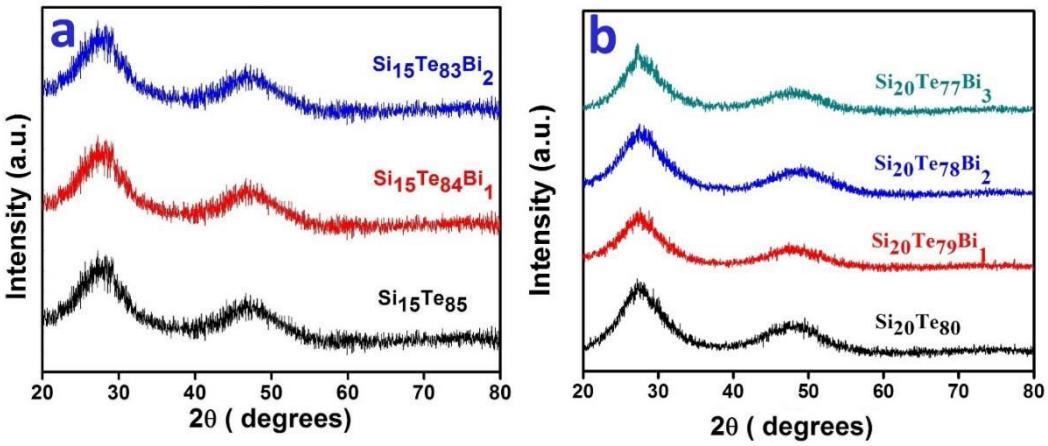

Figure 4.1 (a) XRD spectrum of $Si_{15}Te_{85-x}Bi_x$ ($0 \leq x \leq 2$) and (b) $Si_{20}Te_{80-x}Bi_x$ ($0 \leq x \leq 3$) chalcogenide glasses. Absence of sharp diffraction peaks in the X-Ray spectrum confirms the amorphous nature of the sample.

4.3.2 Current controlled negative resistance (CCNR) switching behavior and thermal mechanism

The distinct I-V characteristics displayed by $Si_{15}Te_{85-x}Bi_x$ ($0 \leq x \leq 2$) and $Si_{20}Te_{80-x}Bi_x$ ($0 \leq x \leq 3$) are shown in Figure 4.2 and Figure 4.3, respectively. The initial electrical resistivity values of the as prepared glasses are in the range of 10^6 Ω.cm. With increasing current, the voltage across the sample increases linearly, indicating an ohmic behavior. Near a threshold voltage V_T, the I-V curve shows a small nonlinearity, after which the voltage across the sample starts to decrease with current, indicating a negative resistance behavior. The negative resistance eventually leads to a low resistance state. As seen from the I-V plots, the samples exhibit swift switching from high resistance state (OFF) to low resistance state (ON). The samples did not revert back to their original high resistance state even after removal of the applied electrical field. This observation clearly indicates that Si-Te-Bi glassy alloys exhibit memory switching behavior at comparatively lower applied currents (≅ 2 mA). There are several factors which determine memory switching in chalcogenide glasses, out of which, formation of crystalline filament between the electrodes is a cause of major concern. When the voltage developed across a sample surpasses the threshold voltage, it is very difficult to cease switching at any point in the region of negative resistance which aids

the filament formation. Hence, the phenomenon of switching is mainly associated with the region of current controlled negative resistance (CCNR) (Owen and Robertson 1973). Many models have been used by researchers to best explain the switching and memory effects. Out of these models, the electro-thermal mechanism proposed by Warren (Warren 1970) suggests that during the switching process the current suddenly increases when the voltage reaches V_T. Here, V_T corresponds to the filling of charged defect states present in the mobility gap of the chalcogenide glasses.

Defects play a major role in the switching process. Structural defects, atomic defects and the electronic levels introduced by them are likely to influence the switching behavior in chalcogenides (Waser et al. 2010). Switching occurs when the lowest energy defect states, known as valence alteration pair (VAP) (Adler 1980) are filled by the field injected charge carriers by means of Poole -Frenkel effect (Ielmini and Zhang 2007; Xu et al. 2009). When the defect states are filled, carrier concentration increases suddenly to a higher value, thereby decreasing the resistivity of the material and allowing a large current to flow through the sample (Fernandes et al. 2016). As mentioned earlier, memory switching in chalcogenide glasses has a thermal origin which involves the formation of a conducting crystalline filament between the electrodes (Asokan and Lakshmi 2012). Generally, memory switching is observed in Te rich chalcogenide glassy alloys due to their greater electrical conductivity, leading to greater power dissipation which allows the easy formation of crystalline filament. It is worth noting that the energy required for crystallization is provided by the electric field. It is also known that weaker bonds, poor structural cross linking and more lone-pair interactions favor memory switching in telluride glasses (Phillips 1981). Formation of a conducting path is more drastic in those chalcogenide glassy alloys which are easily prone to devitrification (Owen and Robertson 1973). Normally, telluride glassy alloys show clean electrical switching without any fluctuation in their negative resistance region, which is evident in our current I-V plots.

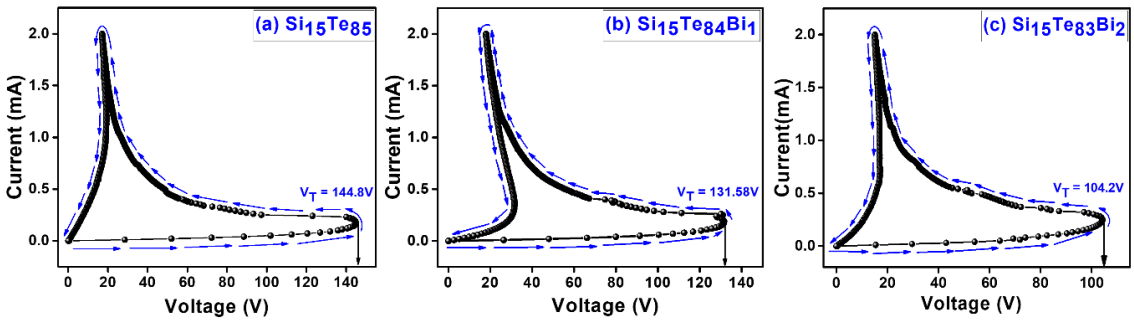

Figure 4.2 I-V characteristics of (a) $Si_{15}Te_{85}$, (b) $Si_{15}Te_{84}Bi_1$ and (c) $Si_{15}Te_{83}Bi_2$ chalcogenide glassy alloys. The arrow marks are guide to the eye representing the direction of current sweeping.

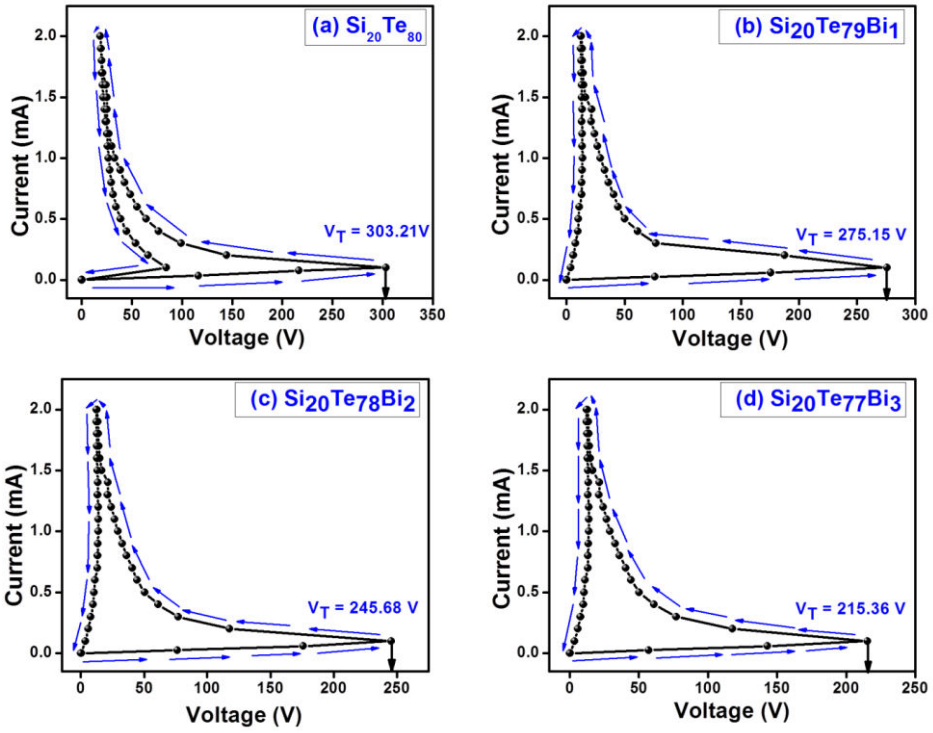

Figure 4.3 I-V characteristics of (a) $Si_{20}Te_{80}$, (b) $Si_{20}Te_{79}Bi_1$, (c) $Si_{20}Te_{78}Bi_2$ and (d) $Si_{20}Te_{77}Bi_3$ chalcogenide glassy alloys. The arrow marks are guide to the eye representing the direction of current sweeping.

4.3.3 Compositional dependence of threshold voltage V_T

The variation of the switching voltage and starting electrical resistance of $Si_{15}Te_{85-x}Bi_x$ ($0 \leq x \leq 2$) and $Si_{20}Te_{80-x}Bi_x$ ($0 \leq x \leq 3$) chalcogenide glassy alloys with respect to their composition is shown in Figure 4.4. The graph indicates a stepwise decrease in both V_T

and starting electrical resistance with an increase in the Bi concentration. The compositional dependence of threshold/ switching voltage in chalcogenide glassy alloys is determined mainly by the resistivity of the additive elements (Deringer et al. 2014), network connectivity/rigidity and chemical ordering (Phillips 1981). It is very important to understand the relationship between network connectivity/rigidity and threshold voltage.

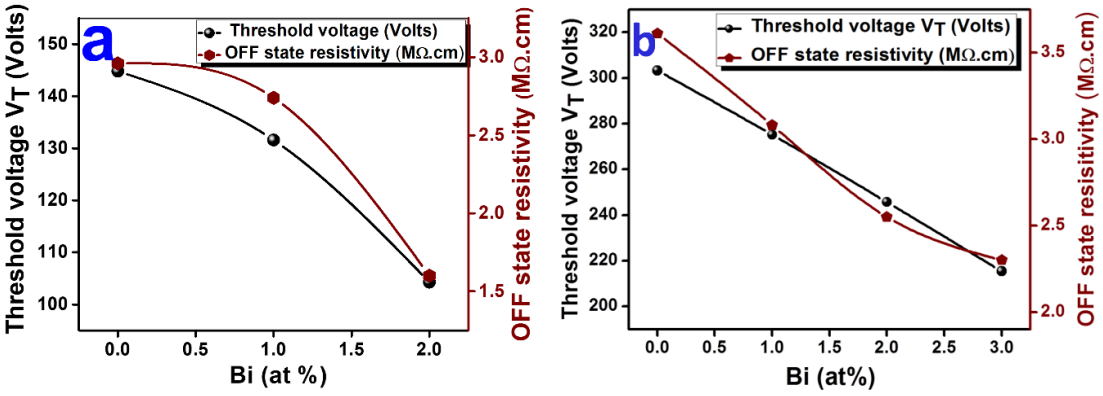

Figure 4.4 Compositional dependence of threshold voltage (V_T) and OFF state resistivity of (a) $Si_{15}Te_{85-x}Bi_x$ ($0 \leq x \leq 2$) and (b) $Si_{20}Te_{80-x}Bi_x$ ($0 \leq x \leq 3$) chalcogenide glassy alloys as a function of atomic percentage of Bi.

Basically, rigidity percolation theory deals with dimensionality and rigidity of a glassy network (Phillips and Thorpe 1985; Warren 1973). For a covalent network glass, the network connectivity and rigidity increases with the increase in average coordination number. This theory also proposes that the addition of higher coordinated atoms increases the network connectivity/rigidity which makes the structural reorganization difficult for the requirement of memory switching. This further implies that switching voltage should increase with increase in atomic concentration of higher coordinated atoms. In our present Si-Te-Bi chalcogenide system, one would expect the increase in switching voltage owing to the fact that the addition of Bi (coordination number of 3) at the expense of Te (coordination number of 2) results in a gradual increase in network connectivity and rigidity. However, the most interesting outcome of the present results is the remarkable decrease in V_T with increase in Bi concentration. Herein, the chalcogenide glassy alloys with a composition of $Si_{15}Te_{85-x}Bi_x$ ($0 \leq x \leq 2$) and $Si_{20}Te_{80-}$

$_{x}Bi_{x}$ ($0 \leq x \leq 3$) are synthesized by the addition of Bi metal to the base matrix $Si_{15}Te_{85}$ and $Si_{20}Te_{80,}$ respectively. The addition of Bi takes place at the cost of Te and decreases the resistivity of the compound due to the lower resistivity values compared to Te ($\rho_{Bi} = 1.29\ X\ 10^{-6}\ \Omega.m$ and $\rho_{Te} = 1\ X\ 10^{-4}\ \Omega.m$). The decrease in the resistivity values results in an increase in conductivity, allowing higher currents to flow through the samples. The higher current flow in the samples further increases the temperature due to Joule heating, favoring the structural transformation required for memory type of switching. These observations indicate that metallic dopants with lower resistivity values play a major role in the reduction of switching voltage, compared to network connectivity and rigidity. Furthermore, from Figure 4.4., we can also observe a decrease in the starting resistivity values with respect to the increase in Bi concentration, which establishes a direct correlation with the decreasing nature of switching voltages. Hence, results obtained for the chalcogenide glassy system Si-Te-Bi indicate that the effect of resistivity of the dopant is more distinct than the network connectivity and rigidity.

4.3.4 Thickness and temperature dependence of switching voltages

It is well known that samples with lower thermal diffusivity values and easy devitrification favor memory switching (Jones and Collins 1979). In order to clarify the aspects of thermal origin in memory switching effects, it is very important to understand the dependence of thickness and temperature on switching voltages. The sample thickness (d) is a significant parameter which provides clear perception of the switching mechanism. Literature reports suggest that, for samples exhibiting memory switching, the variation of V_T shows linear or square root dependence ($d^{1/2}$) with thickness, and square dependence (d^2) with sample thickness for threshold switching (Murugavel and Asokan 1998). The variation in V_T with respect to the thickness of a representative $Si_{15}Te_{83}Bi_2$ and $Si_{20}Te_{78}Bi_2$ sample is shown in Figure 4.5. There is no change in the overall feature of the S-Shaped nonlinear I-V curve. However, V_T is found to increase linearly with an increase in the thickness of $Si_{15}Te_{83}Bi_2$ and $Si_{20}Te_{78}Bi_2$, in agreement with theory. It is noteworthy to realize that heat loss through the electrode surface is determined by thermal conductivity (k) of the sample and external heat conductivity (λ), leading to the variation in switching voltage (Asokan and Lakshmi 2012). The

development of filament formation in the sample is associated with memory switching. In this case, if the sample is a thin slab, then the loss of heat generated from the filamentary channel to the surface of the electrode is less. Hence, V_T is less dependent on the thickness for thin samples. On the other hand, V_T increases with increase in thickness. Increase in V_T is usually observed with thickness greater than 0.30 mm. This is mainly because of large power consumption by the sample for filament formation. Therefore, we use samples of thickness (d = 0.30 mm) for our memory applications, which is optimized for most of the cases. It is very intricate to prepare samples of thickness less than 0.30 mm owing to their brittle nature.

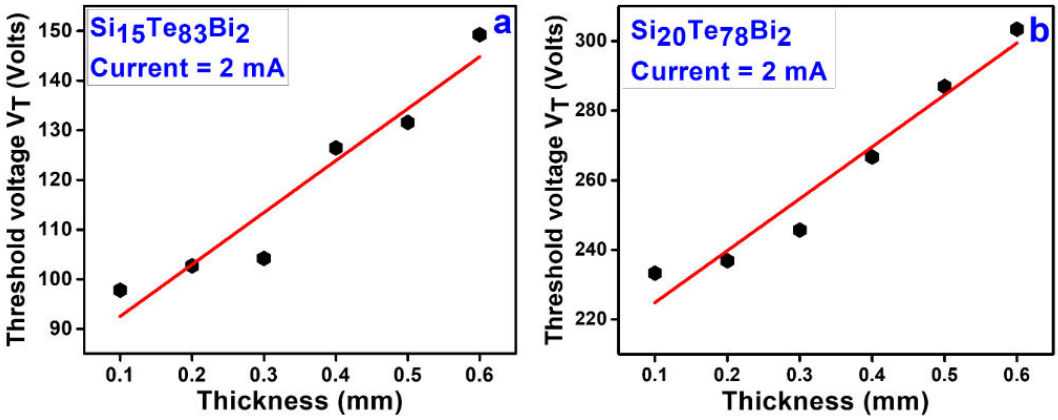

Figure 4.5 Variation of switching voltage (V_T) with respect to thickness of a representative (a)$Si_{15}Te_{83}Bi_2$ and (b) $Si_{20}Te_{78}Bi_2$ chalcogenide glass sample.

The variation of switching voltage with respect to different temperatures for a representative $Si_{15}Te_{83}Bi_2$ and $Si_{20}Te_{77}Bi_3$ chalcogenide glassy alloy is shown in Figure 4.6. I-V plots of the representative $Si_{20}Te_{77}Bi_3$ chalcogenide glassy alloy are shown in Figure 4.7. We observe a decrease in the value of V_T with the increase in temperature. As observed from the I-V plots of $Si_{20}Te_{77}Bi_3$, characteristic I-V curves look broader and sluggish at higher temperatures. It is evident from the switching plots that slope of the switching curve is narrowed down, indicating reduction of activation energy required for phase change phenomenon (Singh and Shimakawa 2003). Besides, at higher temperature, the charged defect centres are filled by thermally excited charge carriers contrary to the field injected charge carriers, resulting in the decrease in switching voltage. The above discussions suggest that there is an increase in electrical

conductivity with increase in temperature, confirming the semiconducting nature of the as- synthesized chalcogenide glassy alloys. For memory switching glasses, the reduction of V_T with temperature has been interpreted based on a configurational free-energy diagram, in which the reduction of V_T is due to the reduction in energy barrier requisite for the crystallization of a sample with elevating temperature (El-Khishin 1979).

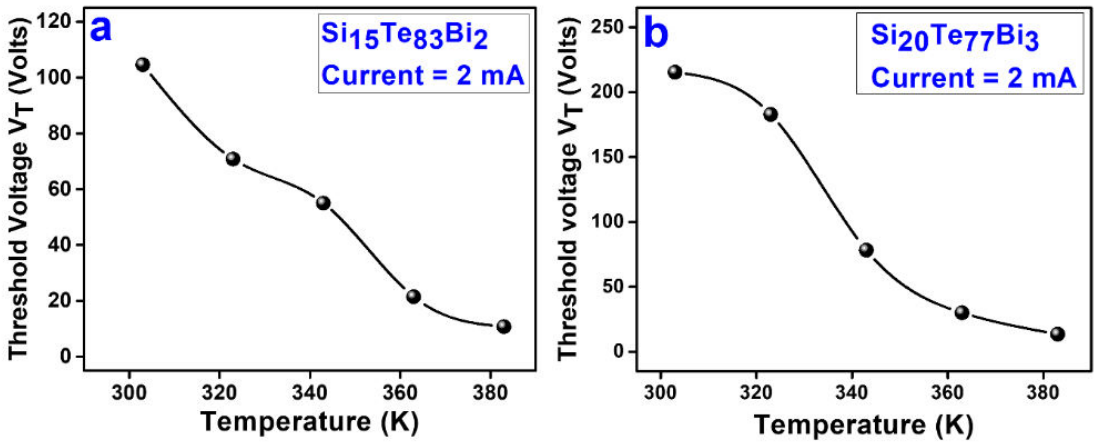

Figure 4.6 The variation of switching voltage with respect to different temperatures for a representative (a) $Si_{15}Te_{83}Bi_2$ and (b) $Si_{20}Te_{77}Bi_3$ chalcogenide glass sample.

The temperature dependence on V_T can be expressed as (Shimakawa et al. 1973),

$$V_T = V_0 exp\left(\frac{\varepsilon}{k_B T}\right) \tag{4.1}$$

where, V_T is the threshold switching voltage, ε is the threshold voltage - activation energy, k_B is the Boltzmann constant (8.617 X 10^{-5} eV K^{-1}) and T is the temperature in Kelvin. The threshold voltage – activation energy calculated from the equation (4.1) is tabulated in Table 4.1. The decrease in the values of the threshold voltage - activation energy at elevated temperatures validates our analysis on the temperature dependence on switching voltages. Generally, activation energy is termed as an input energy to initiate the reaction. Catalysts such as heat or pressure can lower the activation energy and increase the reaction rate without being consumed in the process. In our present experiment, along with the applied electric field, heat acts as an additional input, which further lowers the activation energy required for the electrical switching. Hence,

reduction in activation energy with an increase in temperature indicates positive nature of activation energy.

Table 4.1 Calculated activation energies in (eV) at different temperature ranges.

Temperature range (K)	Activation energy (eV)	
	$Si_{15}Te_{83}Bi_2$	$Si_{20}Te_{77}Bi_3$
303-323	0.16	0.14
323-343	0.11	0.12
343-363	0.02	0.10
363-383	0.01	0.08

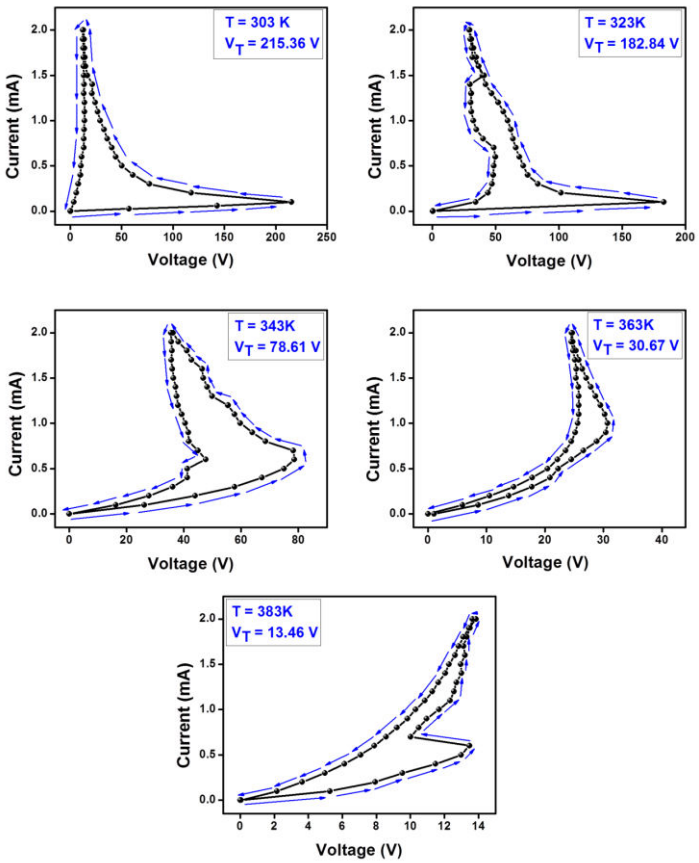

Figure 4.7 I-V characteristics of a representative $Si_{20}Te_{77}Bi_3$ chalcogenide glassy alloy measured at different temperatures from 303K to 383K. Increase in temperature exhibited a remarkable decrease in V_T. The arrow marks are guide to the eye representing the direction of current sweeping

4.3.5 Microscopic study of switched region

As the memory effect in chalcogenide glasses is an irreversible process and associated with filament formation, it is anticipated that the filament consisting of high conducting crystallites will remain unchanged in the post switching process. We have carried out SEM analysis on a representative sample of $Si_{20}Te_{78}Bi_2$ to examine the microstructural change before and after the switching studies. When the current is passed through the sample, the temperature of the sample at the electrode region is higher than the surrounding region of the electrode. Hence, a conducting channel is formed at the targeted region of the electrode. This channel will experience higher power dissipation (I^2R) owing to its lower resistance, thus allowing higher current density (Upadhyay and Murugavel 2013). It may be noted that higher current density increases the temperature at the electrode region, resulting in the formation of a high conducting crystalline filament (Karuppannan et al. 2011).

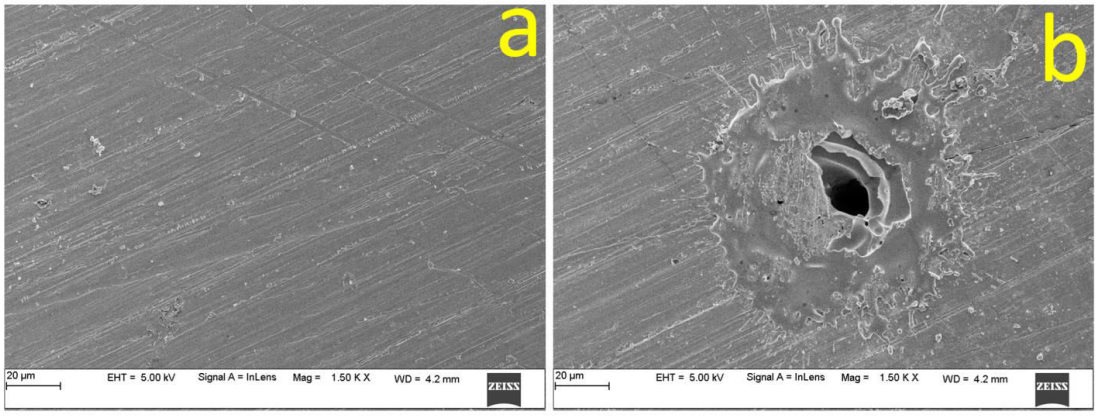

Figure 4.8 SEM micrographs of (a) unswitched (b) switched $Si_{20}Te_{78}Bi_2$ chalcogenide glassy sample. SEM image in (b) clearly shows a crystallized melt representing the conducting filament formed during switching.

The microstructural analysis carried herein for the sample before and after switching process is shown in Figure 4.8. It is interesting to see the splashing effect of the sample in the electrode region (Figure 4.8b). This indicates that the sample was in a liquid state during switching. Besides, the area other than the conducting filament is similar to the amorphous phase of pre-switched sample as shown in Figure 4.8b, and is distinguishable from the conducting filament. Energy dissipated by the current pulse was found be ~ 10^{-5} J, which is enough to induce melting (liquid phase) in the material

(Stocker 1970). Crystallization of a liquid phase is thermodynamically allowed once the material is cooled below the melting temperatures (Modgil and Rangra 2014). On removal of applied electric field (electric pulse), the heat generated at the electrode region also reduces. Hence, the free energy difference between the liquid and crystal helps in filament formation (Waser et al. 2010). In the process of filament (crystallized melt) formation, one may anticipate cracks at the surface of glassy materials. However, owing to higher coefficient of thermal expansion of chalcogenide glassy alloys, cracks are not observed. Cooled melt at the electrode region may consist of phase separated mixture of crystalline or amorphous domains (Nakashima and Kao 1979). Filament formation in chalcogenide glassy alloys is also associated with lower thermal diffusivity values. Heat generated at the electrode region is not removed at higher rate, hence structural transformation becomes easy. Thus, we can say that chalcogenide glassy alloys with lower thermal diffusivity values exhibit memory behavior (Asokan and Lakshmi 2012). These studies give additional experimental evidence on the thermal effects playing a key role in the switching process.

4.3.6 Compositional dependence of thermal parameters

Compositional dependence of thermal parameters deduced using DSC gives away significant evidence on material properties, thus suggesting their suitability for PCM application. Representative DSC thermogram of $Si_{20}Te_{77}Bi_3$ chalcogenide glassy alloy has been illustrated in the Figure 4.9. The glass transition T_g, onset crystallization temperature (T_c) and peak crystallization temperature (T_p) are measured. The variation of the characteristic temperatures at a heating rate of 10 K/min for the studied $Si_{15}Te_{85-x}Bi_x$ ($0 \leq x \leq 2$) and $Si_{20}Te_{80-x}Bi_x$ ($0 \leq x \leq 3$) glassy alloys is tabulated in the Table 4.2 and Table 4.3 respectively. All these glasses exhibit double crystallization as shown in (Figure 4.9a).

The appearance of double crystallization peaks is because of the partial phase separation in the material, owing to the disassociation of the initially homogeneous multicomponent material into two or more amorphous phases (Modgil and Rangra 2014). Tellurium crystallizes at lower temperature (T_{c1}) and the remaining amorphous matrix crystallizes into Si_2Te_3 at slightly higher temperature (T_{c2}) with a hexagonal

structure. From Table 4.2. and Table 4.3, we observe a decreasing trend in T_g, T_p and T_c . The decrease in T_g with the increase of Bi may be due to the reduction of rigidity in the amorphous network developed by the addition of metallic element Bi. Also, the increasing metallicity factor (more metallic in nature) may cause rupture of covalent bonds. It has also been reported (Tonchev and Kasap 1999) that larger atoms such as Bi, Sb and In entering glassy matrix break the chain length partially, thus increasing the concentration of weak Te rings (evident from section 4.3.8), resulting in the decrease of T_g. Hence, T_g is marked as an important thermal parameter, which reveals the rigidity and strength of vitreous material. But T_g alone is not sufficient to draw conclusions regarding thermal stability and glass formability. Therefore, knowledge of crystallization temperature marks its significance in explaining amorphous – crystalline phase transition. The reduced values of T_c of the studied compounds represent the presence of weak homopolar and heteropolar bonds in the glassy matrix (Singh and Shimakawa 2003). In this report, we consider crystallization temperature with respect to the first crystallization peak (FCP) for the analysis of crystallization kinetics. However, it is worth noting that values of crystallization temperatures in second crystallization peak (SCP) follow decreasing trend similar to that observed in FCP.

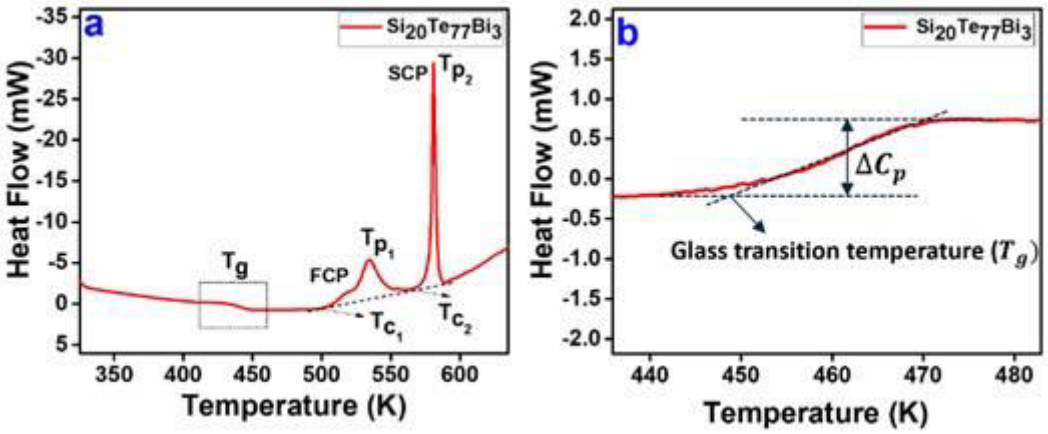

Figure 4.9 (a) Total heat flow curve of a representative $Si_{20}Te_{77}Bi_3$ glass sample displaying glass transition temperature (T_g) , peak crystallization temperature (T_p) (b) fig. 1a is expanded in the temperature range 430 to 490 K and between -2.0 and +2.0 mW to show the glass transition clearly.

Table 4.2. Characteristic temperatures and specific heat measurements of $Si_{15}Te_{85-x}Bi_x$ ($0 \leq x \leq 2$) chalcogenides at a heating rate of 10K/min

Composition	$T_g(K)$	$T_{c_1}(K)$	$T_{c_2}(K)$	$T_{p_1}(K)$	$T_{p_2}(K)$	ΔC_p(J/g-K)
$Si_{15}Te_{85}$	407.81	474.5	569.12	489.4	574.39	0.240
$Si_{15}Te_{84}Bi_1$	405.93	457.75	545.9	466.47	557.64	0.199
$Si_{15}Te_{83}Bi_2$	377.16	449.1	542.1	463.93	550.23	0.139

Table 4.3. Characteristic temperatures and specific heat measurements of $Si_{20}Te_{80-x}Bi_x$ ($0 \leq x \leq 3$) chalcogenides at a heating rate of 10K/min

Composition	$T_g(K)$	$T_{C_1}(K)$	$T_{p_1}(K)$	$T_{C_2}(K)$	$T_{p_2}(K)$	ΔC_p (J/g K)
$Si_{20}Te_{80}$	461.47	555.38	574.95	579.65	581.27	0.446
$Si_{20}Te_{79}Bi_1$	458.39	519.62	529.43	559.23	572.68	0.180
$Si_{20}Te_{78}Bi_2$	456.71	515.36	527.97	557.92	564.35	0.192
$Si_{20}Te_{77}Bi_3$	448.61	500.60	514.40	552.68	541.52	0.176

4.3.7 Crystallization kinetics

It is well known that addition of third element to the host matrix may expand glass forming ability or create configurational disorder. This extends ample prospects on tuning the alloy compositions for wide variety of applications. The glass transition response is usually referred to as 'swift mechanism' which is associated with the vibrational degrees of freedom and gradual relaxation related to the configurational changes of super cooled liquid (Málek 2000). Variation in T_g depends on quenching rate (rate at which molten alloy has been quenched), chemical alloying and entropy of mixing (the number of ways in which local units can combine) (Boolchand et al. 2002). Thus, the glass transition temperature turns out to be a very important thermal parameter as it not only expresses the strength and rigidity of the glassy alloy but also gives an insight into electrical properties (explained in section 4.3.9). The dependence of T_g on the heating rate with varying composition has been studied and the activation energy of thermal relaxation has been deduced on the basis of three different approaches as reported in the literature (El-Mously and El-Zaidia 1978; Kissinger 1957; Kotkata

and El-Mously 1983; Moynihan et al. 1976). First approach is given by Lasocka (Lasocka 1975, 1978), the empirical relationship is of the form

$$T_g = A + B ln\alpha \tag{4.2}$$

where A and B are the constants given for glassy alloy composition. The value of A can be deduced by extrapolating the heating rate (∝) to 1 K/min, whereas the value of constant B is equal to 0.693 times of the T_g corresponding to the heating rate at 10 K/min or the value of B is evaluated by taking slope from equation 4.2 . The value of B is associated with the cooling rate of the melt. Lower values of B suggest lower cooling rate of the melt, signifying rate dependence of structural modifications in the supercooled liquids (Debenedetti and Stillinger 2001). Values of A and B are evaluated by fitting the obtained experimental data to the least square as shown in Figure 4.10b and Figure 4.11b. These values are tabulated in the Table 4.4. and Table 4.5.

Evaluation of glass transition activation energy is useful in comparing the values obtained by adopting different models. The glass transition activation energy (E_g) of the chalcogenide glassy alloys under examination is evaluated using equation 4.3. and 4.4 given by Moynihan (Easteal et al. 1974; Moynihan et al. 1974; Moynihan and Gupta 1978) and Kissinger (Kissinger 1957), respectively.

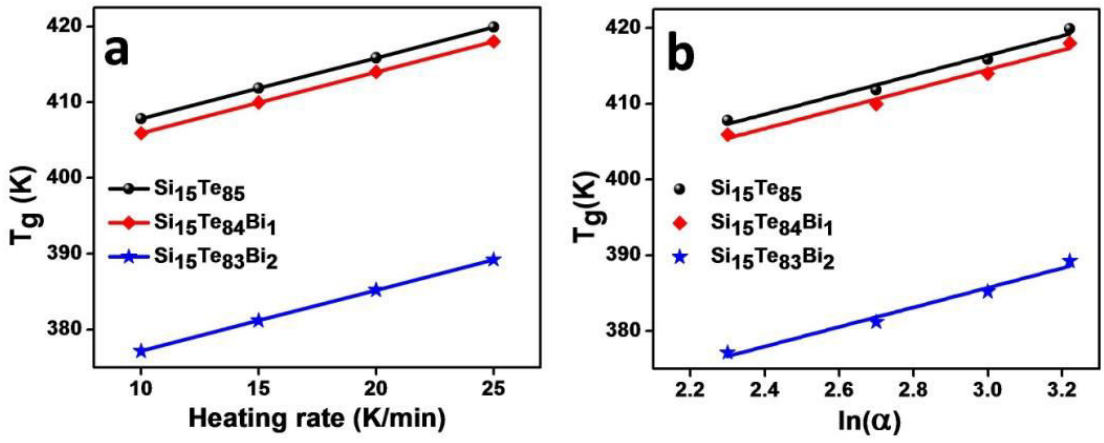

Figure 4.10 (a) The heating rate dependence of the glass transition temperature T_g. (b) Plot of glass transition temperature T_g against $ln(\alpha)$ for $Si_{15}Te_{85-x}Bi_x$ ($0 \leq x \leq 2$) chalcogenide glasses

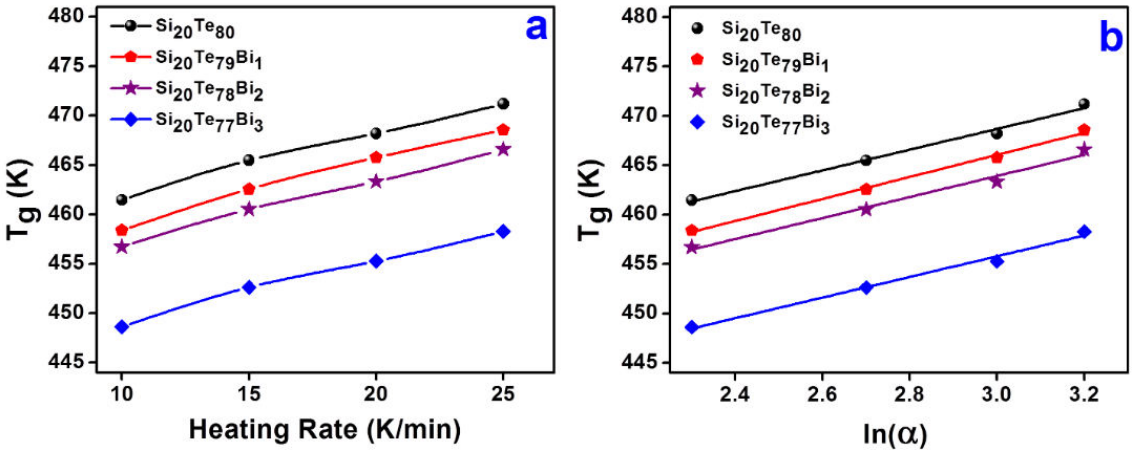

Figure 4.11 Plots showing the (a) dependence of heating rate on the glass transition temperature T_g and (b) glass transition temperature T_g against $ln(\alpha)$ for $Si_{20}Te_{80-x}Bi_x$ ($0 \leq x \leq 3$) chalcogenide glasses.

$$\ln(\alpha) = -\frac{E_g}{RT_g} + C \tag{4.3}$$

$$ln\left(\frac{\alpha}{T_g^2}\right) = -\frac{E_g}{RT_g} + C \tag{4.4}$$

Here α represents heating rate, R represents universal gas constant. The listed values of E_g in the Table. 4.4 and Table 4.5. are deduced using Kissinger and Moynihan models. The tabulated values are in good agreement with each other, implying effective means of calculating E_g. The calculated values of E_g represent the absorption of energy in the form of heat formed due to the molecular motion and rearrangement of atoms at T_g. In other words, T_g is a critical transition temperature comprising of different metastable states (excited state of an atom) isolated by energy barriers. Now the atoms in the metastable state try to achieve higher stable state by succeeding the energy barrier. This energy barrier around T_g is defined as activation energy of the glass transition

temperature (Imran et al. 2001; Kaswan et al. 2013). Aforesaid discussions indicate that E_g is related to the internal energy of the system. It is well known that internal energy is attributed to the mobility of the atoms and thermal relaxation. Interaction of third metallic element in the composition is expected to increase the internal energy of the system by doing work. This includes rupture of covalent bonds, thus partially breaking the chain length at the pre-crystallization temperature, leading to the increase in internal energy, thereby leading to the reduction in E_g values (Abd El Ghani et al. 2006; Deepika et al. 2012; Lafi et al. 2013).

Along with the kinetics related to T_g, it is also important to determine the nature of glass forming liquids. There are two types of glass forming liquids, namely fragile and strong. Fragile liquid indicates fewer stable configurations compared to strong liquid while solidifying into glass. Aforementioned details indicate that fragile liquid possesses a large difference in the specific heat. To understand the nature of the liquid we have carried out studies on the thermal parameters such as change in specific heat (ΔC_p) and fragility constant (F).

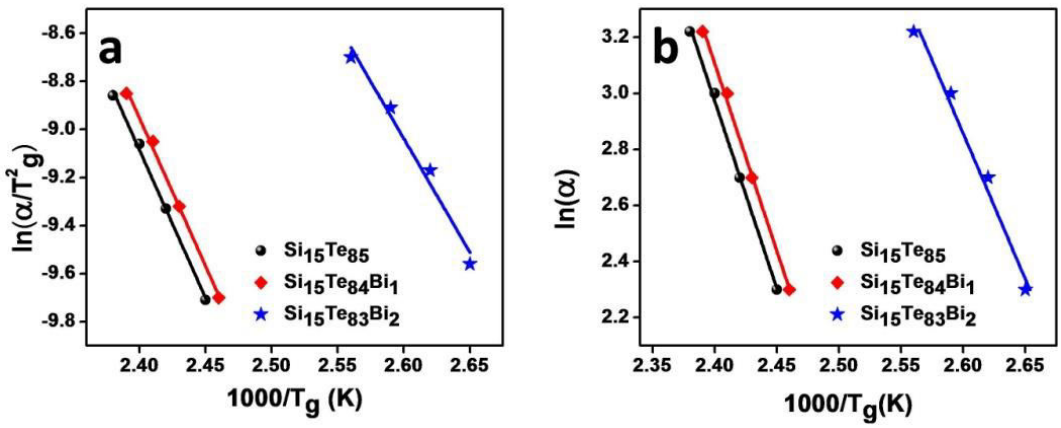

Figure 4.12 The plots exhibiting the variation of glass transition with respect to heating rate. (a) Plots of $\ln(\alpha)$ versus $1000/T_g$ according to Moynihan and (b) plots of $ln(\alpha/T_g^2)$ versus $1000/T_g$ according to Kissinger model, for $Si_{15}Te_{85-x}Bi_x$ ($0 \leq x \leq 2$) chalcogenide glasses.

Table 4.4 Lasocka parameters (A and B), fragility index and the glass transition activation energy determined using Moynihan and Kissinger model for $Si_{15}Te_{85-x}Bi_x$ ($0 \leq x \leq 2$) chalcogenide glasses

Composition	**Lasocka parameters**		**Activation energy (E_g) (kJ/mol)**		**Fragility**
	A(K)	B	Moynihan	Kissinger	**index (F)**
$Si_{15}Te_{85}$	377.54	12.95	110.74	102.17	13.62
$Si_{15}Te_{84}Bi_1$	375.66	12.94	110.74	102.17	13.68
$Si_{15}Te_{83}Bi_2$	346.91	12.91	84.80	78.65	11.29

Table 4.5 Lasocka parameters (A and B), fragility index and the glass transition activation energy determined using Moynihan and Kissinger model for $Si_{20}Te_{80-x}Bi_x$ ($0 \leq x \leq 3$) chalcogenide glasses

Composition	**Lasocka parameters**		**Activation Energy (E_g) (kJ/mol)**		**Fragility index (F)**
	A(K)	B	Moynihan	Kissinger	
$Si_{20}Te_{80}$	437.18	10.5	172.76	164.94	19.10
$Si_{20}Te_{79}Bi_1$	432.59	11.15	166.28	158.63	18.50
$Si_{20}Te_{78}Bi_2$	432.00	10.63	164.11	156.63	18.33
$Si_{20}Te_{77}Bi_3$	424.45	10.44	161.29	153.55	18.32

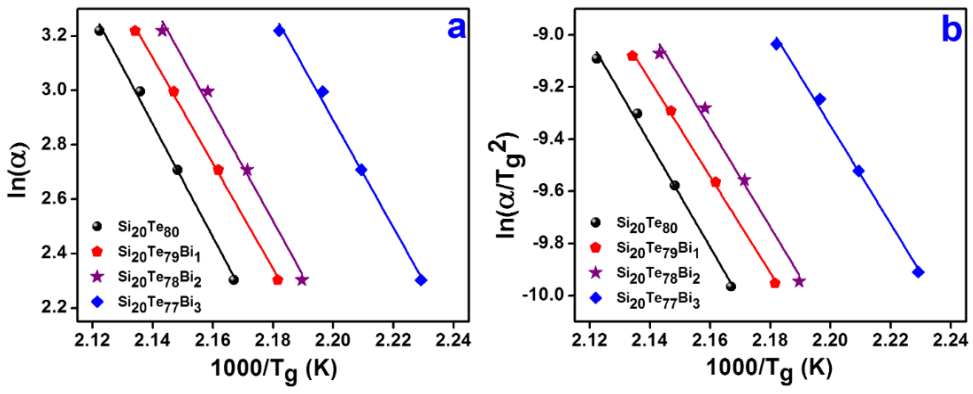

Figure 4.13 Plots exhibiting the variation of glass transition with respect to heating rate in $Si_{20}Te_{80-x}Bi_x$ ($0 \leq x \leq 3$) chalcogenide glasses based on (a) Moynihan [$ln(\alpha)$ versus $1000/T_g$] and (b) Kissinger [$ln(\alpha/T_g^2)$ versus $1000/T_g$] models.

The glass transition of a vitreous material is nothing but structurally arrested state from a viscous liquid. Hence, it is obvious that vitreous material will achieve different structural configurations above T_g, and the glassy network will possess a stable state below T_g (Angell 1997; Sharma et al. 2012). Therefore, change in specific heat(ΔC_p) around T_g is considered as the measure of stiffness transition (depicted in Figure 4.9b.). We know that glass formed by fragile liquids has less stable state structure. As a result, we can expect larger specific heat jump around T_g. The contradiction must be true for the glass formed by strong liquids. From the values of ΔC_p (Table.4.2 and 4.3), it is apparent that glassy alloys are formed by strong liquids. Similar results on metal doped chalcogenide systems validate our results(Imran 2011; Lafi and Imran 2011).

Fragility can be deduced using the relation given below (Böhmer et al. 1993)

$$F = \frac{E_g}{2.303RT_g} \tag{4.5}$$

As reported by Vilgils (Vilgis 1993), strong and fragile glass forming liquids are distinguished by a lower and higher value of F. Strong liquids are identified with a low value of F (F =16), whereas fragile glass forming liquids are defined by a higher value of F (F=200) (Böhmer and Angell 1994). It is evident from the listed values of F in the Table. 4.4. and Table 4.5. that the values of F fall within the border of 16, confirming that $Si_{20}Te_{80-x}Bi_x$ $(0 \leq x \leq 3)$ ternary chalcogenide glassy alloys are obtained from strong glass forming liquids. The deduced values of F and ΔC_p corroborate with the former discussions.

Based on the JMA model, various statistical models have been evolved enabling us to calculate the activation energy for crystallization E_c. We have used four different methods to evaluate E_c. Out of these, first three models consider peak crystallization temperature and the fourth model considers onset crystallization temperature to evaluate E_c. The four different approaches to find E_c were given by Kissinger (Kissinger 1957), Takhor (Takhor 1972), Augis-Bennett (Augis and Bennett 1978) and Ozawa (Ozawa 1965, 1971) as shown below. Equations (4.6 – 4.9) given below follow the respective trends of the methods mentioned above.

$$ln\left(\frac{\alpha}{T_p^2}\right) = -\frac{E_p}{RT_p} + C \quad (4.6)$$

$$ln(\alpha) = -\frac{E_p}{RT_p} + C \quad (4.7)$$

$$ln\left(\frac{\alpha}{T_p}\right) = -\frac{E_p}{RT_p} + C \quad (4.8)$$

$$\ln(\alpha) = -\frac{E_c}{RT_c} + C \quad (4.9)$$

Here T_p represents peak crystallization temperature, T_c represents onset crystallization temperature, α represents heating rate, R represents universal gas constant, $E_p and\ E_c$ represent activation energies of $T_p and\ T_c$, respectively. From the equations 4.6 - 4.9, the data for $Si_{15}Te_{85-x}Bi_x$ ($0 \leq x \leq 2$) and $Si_{20}Te_{80-x}Bi_x$ ($0 \leq x \leq 3$) glassy alloys was fitted to linear functions employing the least square fitting function as shown in Figure 4.15 and Figure 4.16, respectively. The values of activation energy of the $Si_{15}Te_{85-x}Bi_x$ and $Si_{20}Te_{80-x}Bi_x$ glasses were calculated from the corresponding slopes as listed in Table 4.6 and Table 4.7. Although we have deduced activation energy values for both $T_p and\ T_c$, the term E_c has been used for convenient explanation. We can see from the Table 4.6 and Table 4.7, that the values of E_c are found to decrease with the increase in Bi content. The decrease of T_c and T_p values is mainly due to the decrease in the viscosity, leading to the decrease in E_c. E_c not only signifies the rate of crystallization, but also the energy requisite for phase transition (Mullin 2001). We have found that the listed values slightly differ from each other within experimental errors. The large variation between Ozawa method and the other three methods employed herein, is basically due to the use of different thermal parameters. Ozawa uses onset crystallization temperature (T_c) in order to deduce E_c, reflecting on the amount of thermal energy required to start the devitrification process. On the other hand, statistical methods such as Kissinger, Takhor and Augis -Bennett employ peak crystallization temperature (T_p) to deduce E_c which expresses the amount of heat energy required for the maximum crystallization.

Thermal stability$(\Delta T = T_c - T_g)$ (Dietzel 1968) indicates resistance offered by the vitreous chalcogenides to crystallization during the hot forming process. As a rule of thumb, a minimum of $\Delta T = 100\ K$ temperature window is required for hot forming process without affecting vitreous nature of the alloys (Rocca et al. 2009). Highly stable chalcogenide glassy alloys are usually used in applications such as optical recording and fiber drawing. Meanwhile, lower values of ΔT signify easy devitrification of chalcogenide glassy alloys, substantiating their suitability for use in PCM devices. Hence, both lower and higher values of ΔT have technological importance and they can find applications in various fields. ΔT values for the examined $Si_{15}Te_{85-x}Bi_x$ and $Si_{20}Te_{80-x}Bi_x$ chalcogenide glassy alloys have been calculated and listed in the Table 4.6 and Table 4.7 respectively. A stepwise decrease in the ΔT values has been observed with the increase in the atomic percentage of Bi. Saad and Poulin (1987) have introduced another important parameter for thermal stability (S) as defined in the equation 4.10. T_p is an additional parameter considered in this equation while comparing it with the equation given by Dietzel (1968).

$$S = \frac{(T_p - T_c)(T_c - T_g)}{T_g} \tag{4.10}$$

$T_p - T_c$ is related to the complete crystallization transformation of the amorphous phase. The obtained values of S show stepwise decreasing mode concurring with the values of ΔT. Enthalpy (ΔH_c) released during crystallization process of an amorphous phase is analogous to thermal stability. Higher value of ΔH_c corresponds to lower value of ΔT and vice versa (Jain et al. 2009; Mahadevan et al. 1986; Predeep et al. 1997). The values of ΔH_c deduced using equation 4.11.

$$\Delta H_c = \frac{\eta A}{m} \tag{4.11}$$

(η is an instrumental constant $\cong$ 1.12; A is the area under the crystallization peak and m is the mass of the sample). Deduced values of ΔH_c for $Si_{15}Te_{85-x}Bi_x$ and $Si_{20}Te_{80-x}Bi_x$ glassy alloys tabulated in Table. 4.6 and Table 4.7 precisely portray an escalation in the

values with the increase in Bi content. The stability of the glassy alloys can be interpreted by another thermal parameter called as entropy(ΔS), which represents the degree of disorder in the vitreous alloy (Aji and Johari 2010; Dalvi et al. 2003; Kumar et al. 2011). Higher value of ΔS indicates a stable glassy state as it acquires a huge energy, owing to unstable atomic configuration. The entropy change during the devitrification can be calculated as (Dalvi et al. 2003),

$$\Delta S = \frac{\Delta H_c}{T_c} \tag{4.12}$$

The values of ΔH_c and ΔS display a decreasing trend with the addition of Bi in $Si_{15}Te_{85-x}Bi_x$ and $Si_{20}Te_{80-x}Bi_x$ chalcogenide glassy alloys as seen from the Table 4.6 and Table 4.7. The listed values of thermal parameters concur with each other, thereby validating the discussions made herein.

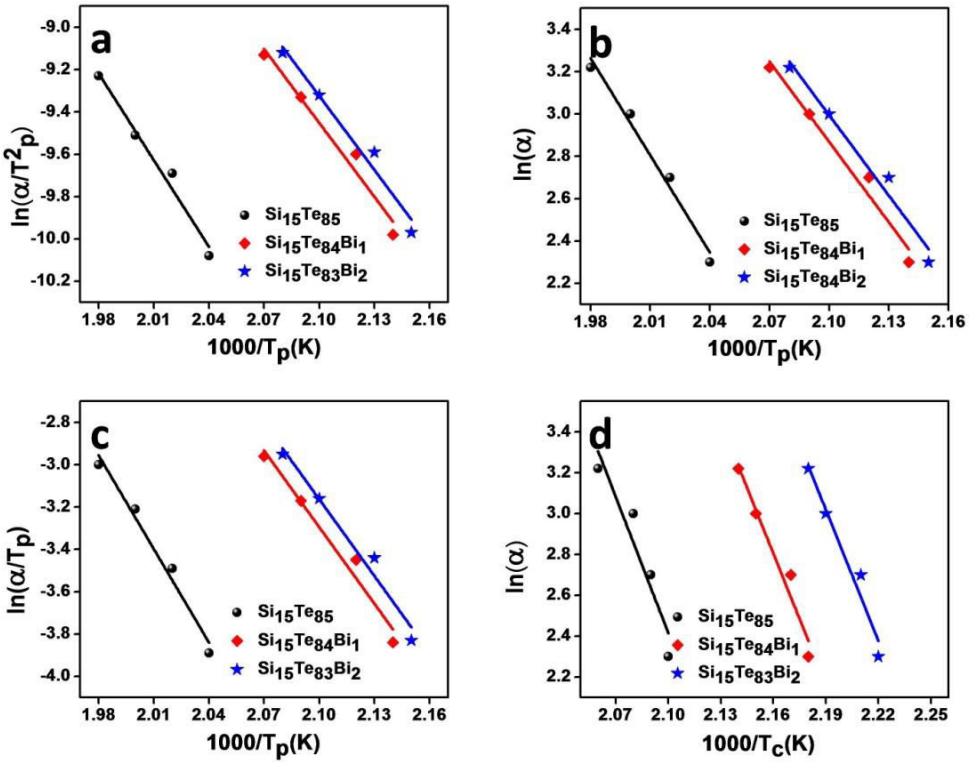

Figure 4.14 Plots used to calculated crystallization activation energy using (a) Kissinger, (b) Takhor, (c) Augis-Bennett and (d) Ozawa model. (a) Plots of $ln(\alpha/T_p^2)$ versus $1000/T_p$, (b) Plots of $\ln(\alpha)$versus $1000/T_p$, (c) Plots of $ln(\alpha/T_p)$ versus

$1000/T_p$ and (d) Plots of $\ln(\alpha)$versus $1000/T_c$ for $Si_{15}Te_{85-x}Bi_x$ ($0 \leq x \leq 2$) chalcogenide glasses.

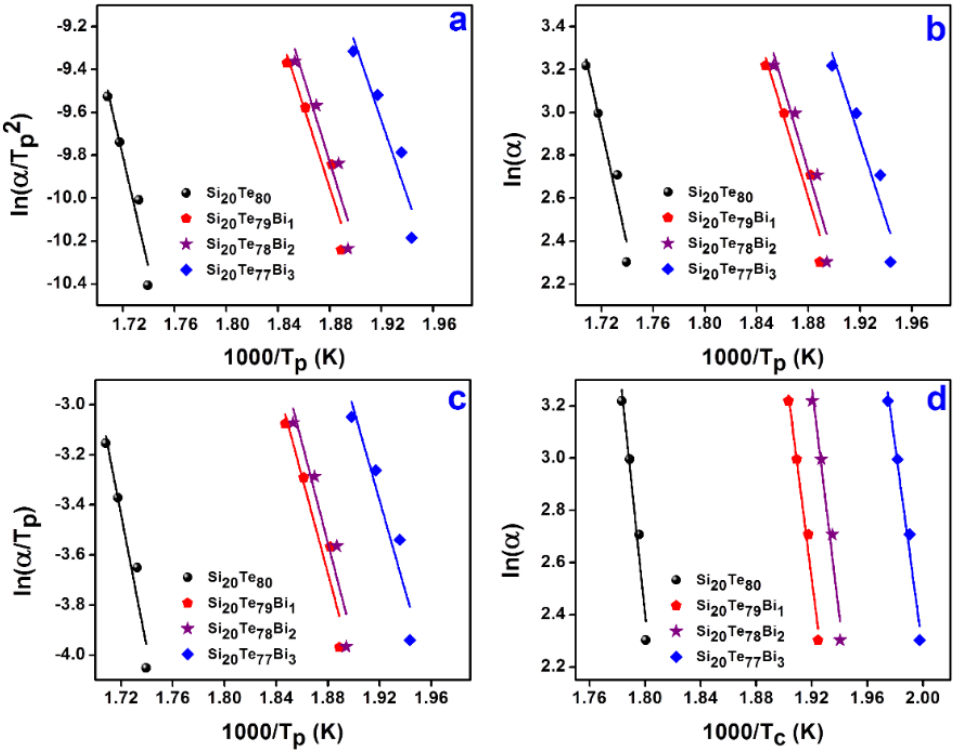

Figure 4.15 Plots of (a) $ln(\alpha/T_p^2)$ versus $1000/T_p$, (b) $ln(\alpha)$ versus $1000/T_p$, (c) $ln(\alpha/T_p)$ versus $1000/T_p$ and (d) $ln(\alpha)$ versus $1000/T_c$ for $Si_{20}Te_{80-x}Bi_x$ ($0 \leq x \leq 3$) glasses corresponding to Kissinger, Takhor, Augis-Bennett and Ozawa models for the calculation of the crystallization activation energy.

Table 4.6 Calculated values of crystallization activation energies (E_c) using Kissinger, Takhor, Augis-Bennett, Ozawa model and thermal parameters for $Si_{15}Te_{85-x}Bi_x$ ($0 \leq x \leq 2$) chalcogenide glasses.

Composition	**Crystallization activation energy (E_c) kJ/mol**				**Thermal parameters**			
	Kissinger	Takhor	Augis-Bennett	Ozawa	ΔT(K)	S	ΔH_c (J/g-K)	ΔS (J/g-K)
$Si_{15}Te_{85}$	113.48	127.20	122.63	184.73	66.69	2.43	-24.58	0.051
$Si_{15}Te_{84}Bi_1$	96.85	105.17	100.26	177.91	51.82	1.11	-24.02	0.052
$Si_{15}Te_{83}Bi_2$	96.85	105.17	100.26	177.91	71.94	2.69	-19.43	0.043

Table 4.7 Calculated values of crystallization activation energies (E_c) using Kissinger, Takhor, Augis-Bennett , Ozawa model and thermal parameters for $Si_{20}Te_{80-x}Bi_x$ ($0 \leq x \leq 3$) chalcogenide glasses.

Composition	Crystallization activation energy (E_c) kJ/mol				Thermal parameters			
	Kissinger	Takhor	Augis-Bennett	Ozawa	ΔT(K)	S	ΔH_c (J/g-K)	ΔS (J/g-K)
$Si_{20}Te_{80}$	216.91	226.55	221.73	259.47	93.91	3.98	-10.36	-0.018
$Si_{20}Te_{79}Bi_1$	162.03	170.85	166.44	200.61	61.23	1.31	-7.14	-0.013
$Si_{20}Te_{78}Bi_2$	155.63	164.53	160.44	183.40	58.65	1.61	-4.78	-0.009
$Si_{20}Te_{77}Bi_3$	146.99	155.63	151.31	160.12	51.99	1.59	-1.86	-0.003

4.3.8 Thermal crystallization and structural studies

It is obvious that when atoms of the third element are added to the host matrix, they are expected to change the atomic arrangement of the network. If the additive enters the network without interacting with the parent matrix, then the network connectivity will not improve. The additive will remain as a micro-inclusion in the structural network (Borisova 2013). If it interacts with the parent matrix and takes active part in the network formation then there will be an increase in the network connectivity and rigidity. In order to explore the possible interaction of Bi into the base matrix, $Si_{20}Te_{78}Bi_2$ glass was thermally crystallized by annealing at its crystallization temperature of 673 K for 5 h under a vacuum of 10^{-5} Torr. The XRD pattern of the annealed sample is shown in Figure 4.16a. It can be seen that the major phases which crystallize out are hexagonal Te (JCPDS card no. 00-036-1452) and Si_2Te_3 (JCPDS card no. 01-086-2268). There is no indication of Bi involved crystalline phases in the annealed sample. It indicates that the interaction of Bi with host $Si_{20}Te_{80}$ matrix is minimal. Generally, the interaction of metal atoms with chalcogenide glass matrix is complex and differs very much from system to system. For example, in Cu-As-Se, about 30 at% of Cu can be incorporated when Se content is low. For Se rich glasses, the glass formation is very much limited as the added Cu does not interact with the host

matrix and remains in the network as a micro-inclusion(Ramesh et al. 2006). The network continuity is obstructed, leading to the depolymerization of the network which results in limited glass formation in Se rich As-Se-Cu system (Ramesh et al. 2006). Glass formation in Cu-Ge-Te system is limited to about 10 at% of Cu. Atomic size, electronegativity and coordination of Cu and Ge are similar in Cu-Ge-Te glasses and it was proposed that the added Cu randomly replaces Ge sites. Hence, the network connectivity does not improve in Cu-Ge-Te glasses with the increase of Cu (Ramesh et al. 2000). Moreover, in Ge-Te-Sn system, the added Sn does not interact with the host Ge-Te matrix, correspondingly glass formation is limited (Fernandes et al. 2016). Interestingly, in Ag-Ge-Te system, glass formation is found to be good (24 at% of Ag can be added) as Ag interacts with the host Ge-Te matrix and polymerizes the network by forming structural species involving Ag, Ge and Te (Ramesh et al. 1999). It has also been reported (Tonchev and Kasap 1999) that larger atoms such as Bi, Sb and In entering glassy matrix break the chain length partially, thus increasing the concentration of weak Te rings. However, it is worth noting that higher concentration of Bi in Si-Te-Bi system is likely to get involved with weak Te rings, thus forming BiTe phase as shown in Figure 4.16b. In the present $Si_{20}Te_{80-x}Bi_x$ glasses, the non-interaction of Bi with Si-Te matrix and depolymerization of the network limits the glass formation, This feature is also mirrored in the variation of switching voltages, in which we observe a decrease in V_T with addition of Bi content. In Al-As-Te glasses, Al resides in 4 and 6 fold coordination (Pumlianmunga and Ramesh 2017). The higher coordination of Al increases the connectivity, cross-linking and rigidity in the network. Correspondingly, an increase in glass transition, crystallization and threshold switching voltage is observed. Thus, the combined effect of the void of network connectivity and the lower electrical resistivity of the additive Bi in the $Si_{20}Te_{80-x}Bi_x$ glasses results in the decrease of switching voltage. Concurrently, it is interesting to find similar results on Bi doped chalcogenide systems such as Ge-Te-Bi (Das et al. 2011) and Ge-Se-Te-Bi (Bhatia et al. 1988).

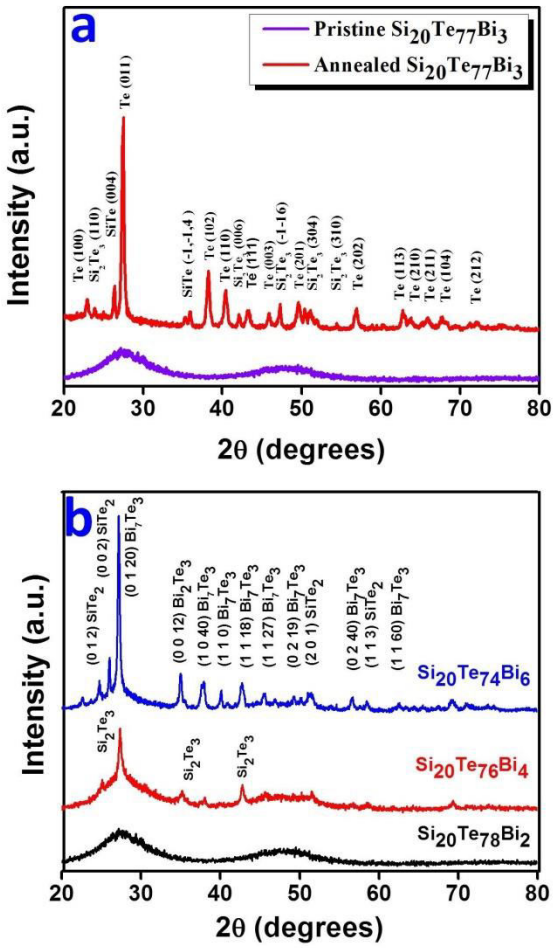

Figure 4.16 (a) XRD patterns of pristine and annealed $Si_{20}Te_{77}Sn_3$ chalcogenide sample. (b) XRD analysis of as-prepared $Si_{20}Te_{78}Sn_2$, $Si_{20}Te_{76}Sn_4$ and $Si_{20}Te_{74}Sn_6$ chalcogenide samples clearly indicating transition from amorphous to crystalline.

From the preceding discussions, it is obvious that one can anticipate morphological modifications in the Si-Te-Bi chalcogenide system as a function of composition. Hence, it is worth investigating surface morphology of $Si_{20}Te_{80-x}Bi_x$ chalcogenide glasses. We have also carried out elemental analysis of $Si_{20}Te_{80-x}Bi_x$ chalcogenide glasses, which shows presence of starting material (See Appendix VIII - XI). Images obtained from field emission scanning electron microscope (FESEM) give interesting information regarding glass formability, phase separation and electron conduction of the glassy alloys. Microscopic surface morphologies of the as-prepared chalcogenide glasses along with the corresponding X-ray spectrum are shown in the Figure 4.18. We find significant changes in the microstructures with change in composition. We observe a

clear transition from lush and shiny microstructures to fractured, rough, dry and random microstructures. Dry and rough surface morphologies indicate higher electronic conduction of the glassy material, whereas, lush and shiny morphologies indicate lesser electronic conduction of the material (Singh 2012). In general, we know that crystalline metallic alloys are more conducting than amorphous alloys. From Figure 4.17, it is clearly evident that the sample microstructure of $Si_{20}Te_{80-x}Bi_x$ glasses drastically change from amorphous to crystalline structure for x > 3. This suggests the poor role of Bi in the glass formability and also possible growth of microstructures in the amorphous background. Aforementioned details also disclose the reason for increase in electrical conductivity with the increase of Bi, resulting in the decrease of V_T. Similar reports for the metal containing chalcogenide glassy alloys complement our results (Fernandes et al. 2016; Sharmila and Asokan 2005).

4.3.9 Correlation between electrical and thermal parameters

Electrical switching characteristics of $Si_{15}Te_{85-x}Bi_x$ and $Si_{20}Te_{80-x}Bi_x$ show profound decrease in V_T and electrical resistivity as a function of composition. In this section, effort has been made to correlate the obtained thermal parameters with the electrical switching behavior. Out of all the thermal parameters, T_g is considered as one of the important parameters of vitreous chalcogenides as it expresses strength and rigidity of the glassy alloys. Change in the values of T_g with composition displays a monotonous decrease with Bi content.

Empirical relation between switching field (E_t) and T_g is given by (Prakash et al. 1994)

$$E_t^2 = C_1 \exp[C_2 * k(T_g - T)/kT] \quad (4.13)$$

where C_1, and C_2 are constants, T is the ambient temperature and k is the Boltzmann constant. Aforementioned relation states that variation of T_g is directly proportional to the change in switching field (E_t), thus establishing a relationship between T_g and E_t. Lower values of T_c indicate ease of devitrification, suggesting swift phase change mechanism of the studied chalcogenides. Hence, the reduced values of E_c as a function of composition reciprocate with the decreasing values of V_T. In this way, the obtained

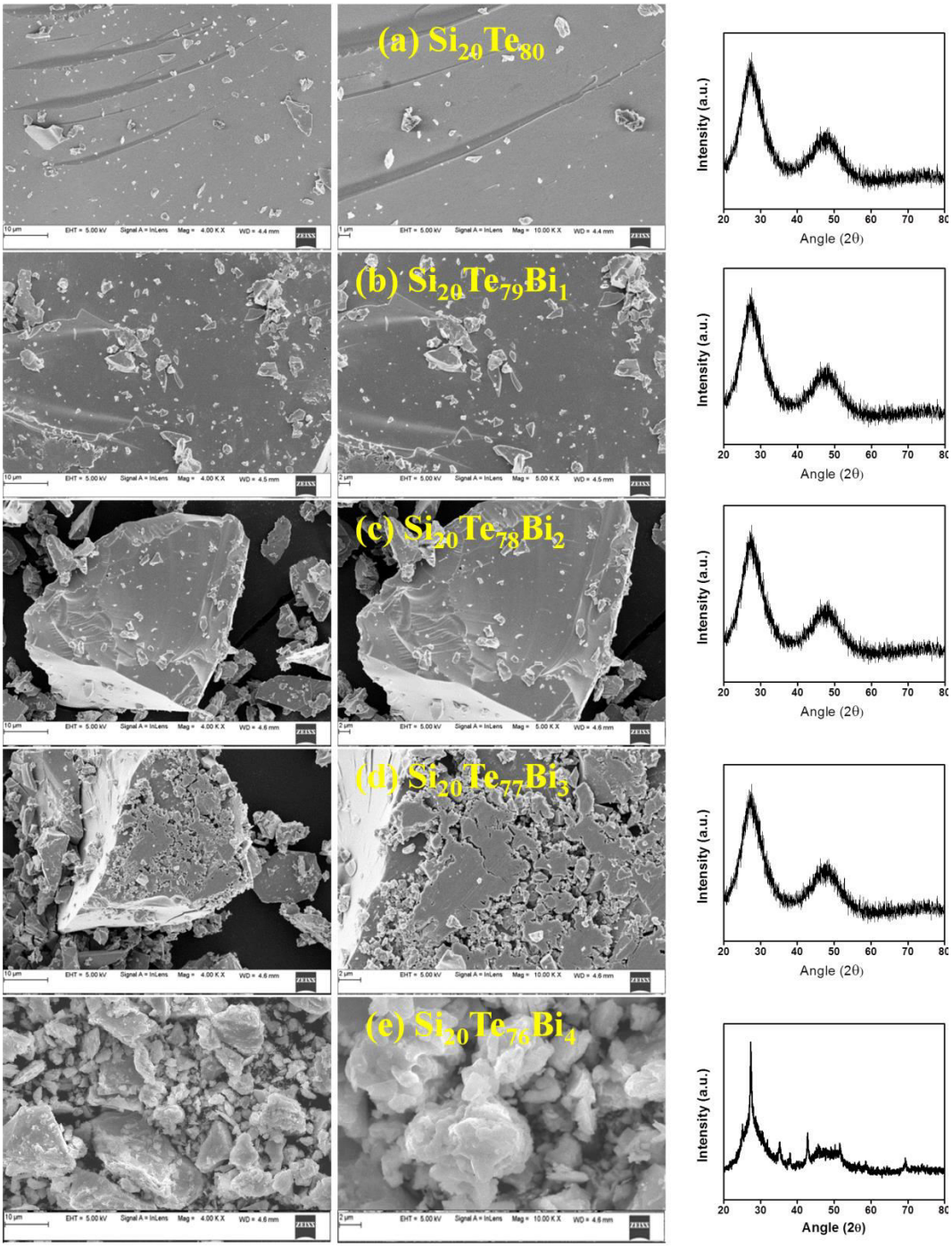

Figure 4.17 Morphology and structural changes in $Si_{20}Te_{80}$ host matrix with respect to the interaction of Bi. With an increase in Bi content, the sample micro-structure drastically changed from amorphous to crystalline, which is reflected in the micrograph in (e) as a dry-rough surface, confirmed from the corresponding XRD pattern.

values of thermal parameters T_g, T_c and E_c are compatible with the decreasing trend of switching voltage. Similar results have been observed for chalcogenide systems such as Ge-Te- Bi (Das et al. 2011), validating our results. Systematic variation of $\Delta T, S, H_c$, ΔS will best explain the possibility of memory switching in the studied composition.

4.4 CONCLSIONS

Memory type of electrical switching behavior is observed from as-prepared bulk semiconducting $Si_{20}Te_{80-x}Bi_x$ ($0 \leq x \leq 3$) chalcogenide glassy alloys. Compositional dependence of V_T is understood on the basis of the decreasing trend of starting electrical resistivity values and thermal stability. Linear increase in V_T with sample thickness is found to be consistent with the memory type of electrical switching. Also, the decrease in V_T with the increase in temperature is attributed to the decrease in activation energy required for devitrification at elevated temperatures. SEM studies on the pre-switched and post switched sections of Si-Te-Bi sample clearly illustrate morphological changes on the surface of the switched sample. This gives an experimental proof for filament formation during the switching process. Decrease in ΔT values indicates that Si-Te glasses become easily de-vitrifiable with addition of Bi, and are in good agreement with the observed decrease in V_T with composition. Non-isothermal calorimetry measurements have been conducted for melt-quenched $Si_{20}Te_{80-x}Bi_x$ ($0 \leq x \leq 3$) chalcogenide glassy alloys using differential scanning calorimetry (DSC) . These glasses are found to exhibit single T_g and double T_c. The obtained values of characteristic temperatures such as T_g, T_c and T_p display a decreasing trend as a function of composition. Various quantitative methods according to well-known JMA model have been utilized to calculate E_g and E_c. It is worth noting that the acquired values of activation energy are found to match with each other pertaining to the validity of the methods used herein. In addition to the activation energy, thermal parameters such as change in specific heat (ΔC_p), fragility index (F), thermal stability (ΔT) & (S), enthalpy (ΔH_c), entropy (ΔS) are deduced using different statistical formulae as a function of composition and are found to shed light on various material aspects and the glass forming difficulty of Bi added Si-Te. Finally, thermal crystallization and morphological studies on Si-Te-Bi system disclose the non- cooperation of Bi in the

network formation, consequently leading to poor network connectivity and rigidity which result in narrow range of glass formation ($0 \leq x \leq 3$).

CHAPTER 5
SUMMARY AND CONCLUSIONS

5.1 SUMMARY AND CONCLUSIONS

In the present thesis work, electrical switching studies and differential scanning calorimetric (DSC) studies have been undertaken on two series of chalcogenide systems, namely Ge-Te-Sn and Si-Te-Bi. The main motivation behind these investigations is to understand the effect of addition of metallic dopants on switching voltages and thermal properties. Thermal properties have been investigated using DSC, as the thermal parameters such as glass transition temperature (T_g), crystallization temperature (T_c), thermal stability (ΔT), etc., have a direct relationship with the local structural ordering of these glasses which can influence the switching phenomena. Studies on thermal devitrification studies and morphological changes elucidate more on narrow glass forming ability of the studied compositions. A relationship has been established between the obtained thermal parameters and electrical switching characteristics. Rapid quenching of the ampoules containing chalcogenide melt has been achieved using modifications in the working chamber of furnace, and the design of ampoule holder is the highlight of this thesis.

The significant results obtained from the studies are as follows:

- Ge-Te-Sn, Si-Te-Bi ternary chalcogenide glassy alloys synthesized by the melt-quenching method has shown smooth memory type switching behavior.

- Composition dependence on switching studies on Ge-Te-Sn and Si-Te-Bi chalcogenide glassy alloys show decreasing trend of switching voltages. This suggests dominance of metallicity factor, leading to the decrease in electrical resistivity values which guides reduction in switching voltages.

- Linear increase in V_T with sample thickness is found to be consistent with the memory type of electrical switching and reveals thermal origin for the switching mechanism. Also, the decrease in V_T with the increase in

temperature is attributed to the decrease in activation energy required for devitrification at elevated temperatures, which also indicates moderate thermal stability of the studied samples.

- SEM studies on the pre-switched and post switched sections of Ge-Te-Sn and Si-Te-Bi sample illustrate morphological changes on the surface of the switched sample. This gives an experimental proof for the filament formation during the switching process.

- Compositional dependence on thermal parameters of Ge-Te-Sn and Si-Te-Bi chalcogenide glassy alloys shows decrease in the values of characteristic temperatures such as glass transition temperature (T_g), crystallization temperature (T_c), activation energy of glass transition (E_g), and crystallization (E_c). These observations indicate some reduction in network connectivity of the glassy system favoring decrease in switching voltages, guiding us to draw a correlation between obtained thermal parameters and the electrical switching behavior.

- Investigations on thermal stability (ΔT) and glass forming ability (GFA) reveal the applicability of the synthesized materials in phase change memory (PCM) applications. The thermal parameters of Ge-Te-Sn and Si-Te-Bi glasses indicate that the moderate thermal stability and easy devitrifiability are favorable for phase-change memory device applications. Furthermore, thermal parameters such as change in specific heat (ΔC_p), fragility index (F), enthalpy (ΔH_c), entropy (ΔS) are deduced to interpret distinct material behaviour as a function of composition.

- Narrow glass formability of the Ge-Te-Sn and Si-Te-Bi chalcogenide system is understood by thermal devitrification studies and morphological changes. They disclose the void of Sn and Bi in the network formation, consequently

leading to poor network connectivity and rigidity which result in narrow range glass formation.

- Decreasing trend of thermal stability indicates that as-prepared chalcogenide glassy alloys are prone to vitrification. This results in reduced glass formability of the studied chalcogenide system

- Newly designed furnace for the preparation of chalcogenide glassy alloys ensures safety, repeatability, proper mixing of starting material and rapid quenching. Owing to its merits it can replace conventional furnace systems.

5.2 SCOPE FOR THE FUTURE WORK

The investigations of the present research work can be extended further in the following directions:

- The structural studies such as Raman, Extended X-ray Absorption Fine Structure (EXAFS) and FTIR need to be performed in order to get information about the bonding and coordination environment of the atoms present in the glasses. These results are necessary as local structural effects play a very important role in the switching phenomena.

- Since Si-Te-Bi glasses are found to exhibit strong memory switching behavior, other low resistivity compositions can be synthesized in bulk/thin film form, and investigated for suitability in PCM applications.

- Investigations on the ac conduction properties of amorphous chalcogenide semiconductors are important because they contribute to the charge transport mechanism in these materials. In particular, the study on ac conduction mechanism is important to understand the nature and the origin of dielectric losses, which in turn may be useful in the determination of structure and defects in solids.

- The electrical and thermal characterization were carried out on bulk chalcogenide glasses. It can be prepared in the thin film form, which can exhibit large number of SET-RESET cycles.

APPENDIX I : Energy dispersive X-Ray spectrum (EDS) of $Ge_{20}Te_{80}$ chalcogenide glassy alloy

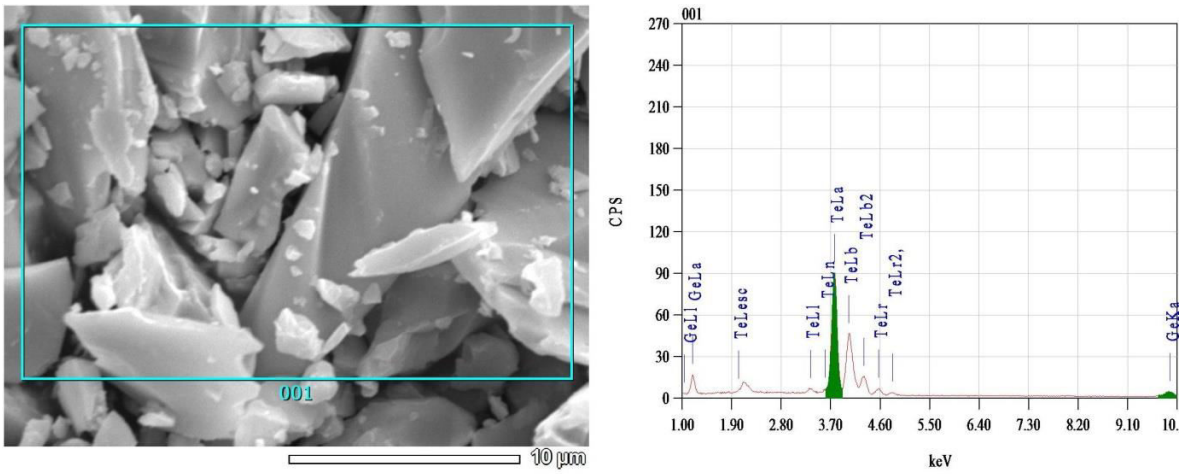

Element	(kev)	Mass%	Error%	At%
Ge K	9.874	10.88	1.20	17.67
Te L	3.768	89.12	0.33	82.33
Total		100.00		100.00

Figure I Energy dispersive X-Ray spectrum (EDS) obtained by scanning the area marked in the SEM image corresponding to $Ge_{20}Te_{80}$ (host matrix) chalcogenide. No impurities were detected and the composition of Ge and Te are confirmed through elemental analysis.

APPENDIX II : Energy dispersive X-Ray spectrum (EDS) of $Ge_{20}Te_{79}Sn_1$ chalcogenide glassy alloy

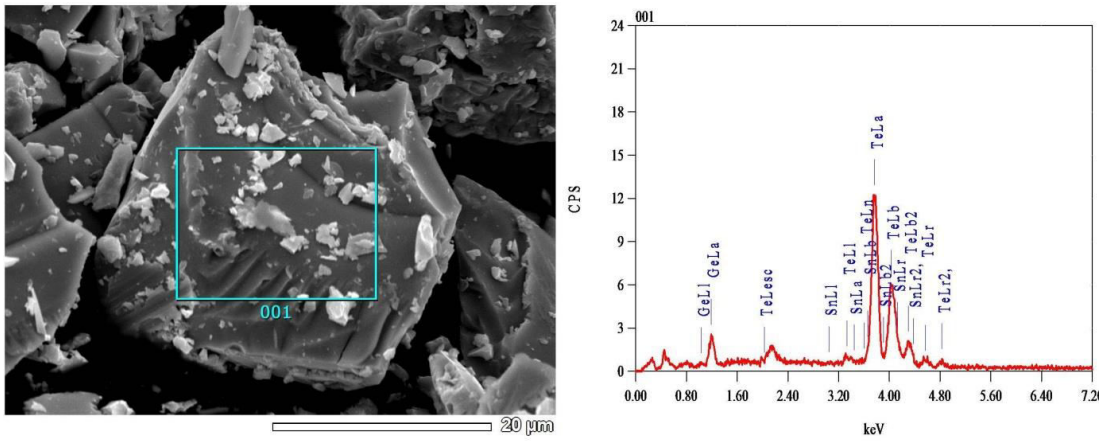

Element	(kev)	Mass%	Error%	At%
Ge K	9.874	10.67	1.04	17.34
SnL	3.442	1.29	0.25	1.28
Te L	3.768	88.04	0.29	81.38
Total		100.00		100.00

Figure II Energy dispersive X-Ray spectrum (EDS) obtained by scanning the area marked in the SEM image corresponding to $Ge_{20}Te_{79}Sn_1$ chalcogenide. No impurities were detected and the composition of Ge, Te and Sn are confirmed through elemental analysis.

APPENDIX III : Energy dispersive X-Ray spectrum (EDS) of $Ge_{20}Te_{78}Sn_2$ chalcogenide glassy alloy

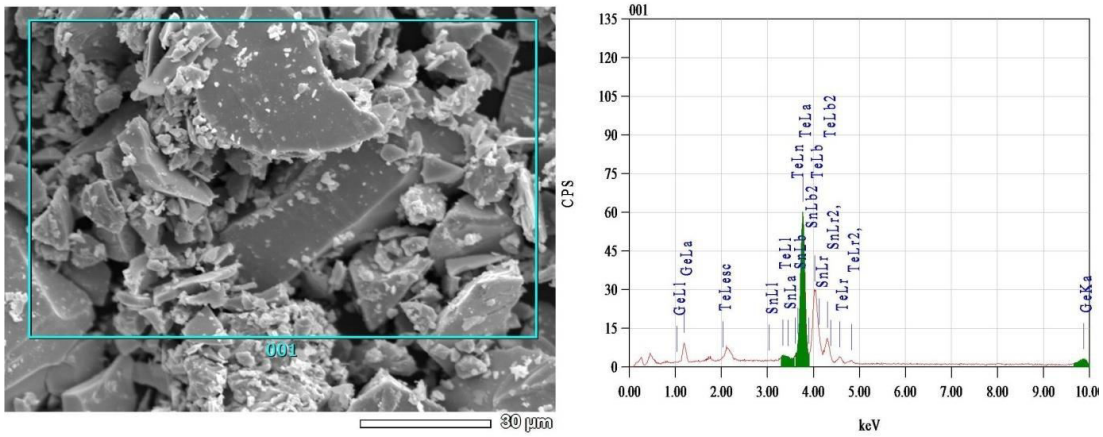

Element	(kev)	Mass%	Error%	At%
Ge K	9.874	10.34	1.12	16.82
SnL	3.442	2.92	0.27	2.91
Te L	3.768	86.74	0.31	80.27
Total		100.00		100.00

Figure III Energy dispersive X-Ray spectrum (EDS) obtained by scanning the area marked in the SEM image corresponding to $Ge_{20}Te_{78}Sn_2$ chalcogenide. No impurities were detected and the composition of Ge, Te and Sn are confirmed through elemental analysis.

APPENDIX IV : Energy dispersive X-Ray spectrum (EDS) of $Ge_{20}Te_{77}Sn_3$ chalcogenide glassy alloy

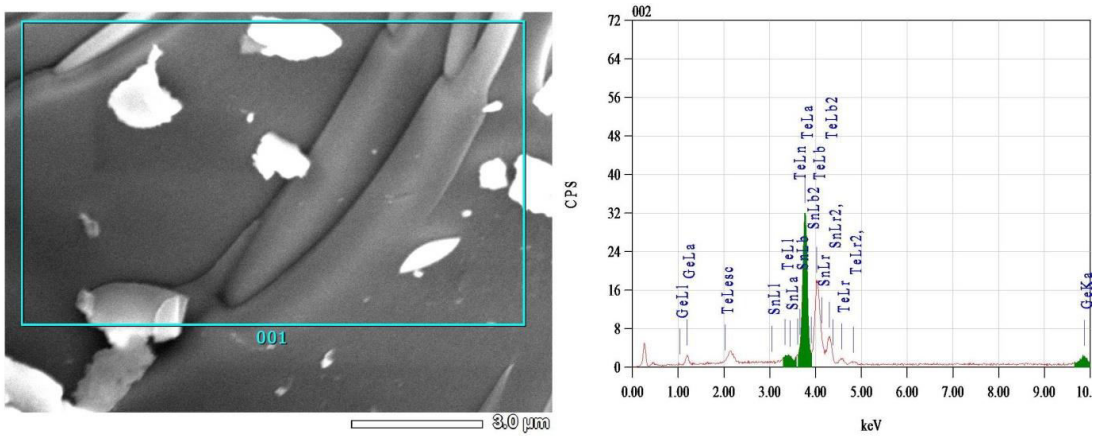

Element	(kev)	Mass%	Error%	At%
Ge K	9.874	13.38	1.25	21.31
SnL	3.442	3.21	0.30	3.13
Te L	3.768	83.41	0.35	75.56
Total		100.00		100.00

Figure IV Energy dispersive X-Ray spectrum (EDS) obtained by scanning the area marked in the SEM image corresponding to $Ge_{20}Te_{77}Sn_3$ chalcogenide. No impurities were detected and the composition of Ge, Te and Sn are confirmed through elemental analysis.

APPENDIX V : Energy dispersive X-Ray spectrum (EDS) of $Ge_{20}Te_{76}Sn_4$ chalcogenide glassy alloy

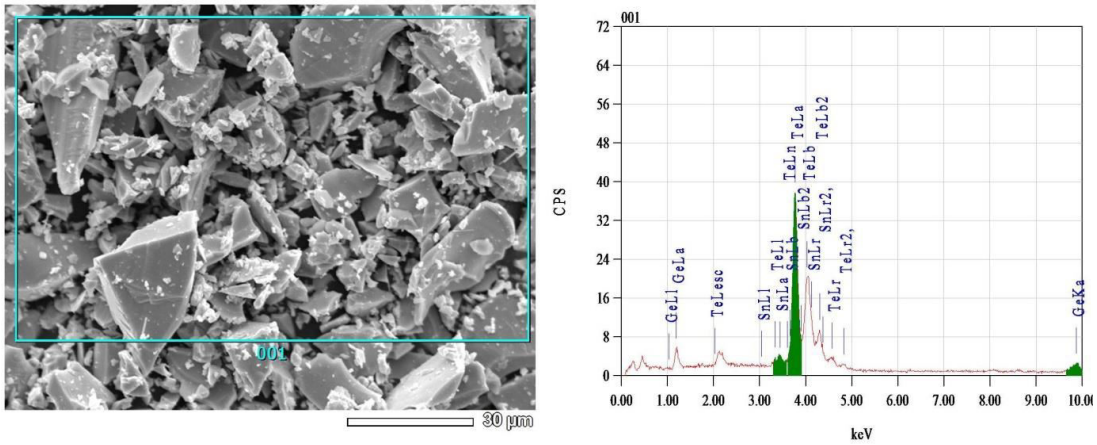

Element	(kev)	Mass%	Error%	At%
Ge K	9.874	11.96	0.96	19.22
Sn L	3.442	4.62	0.23	4.54
Te L	3.768	83.41	0.27	76.24
Total		100.00		100.00

Figure V Energy dispersive X-Ray spectrum (EDS) obtained by scanning the area marked in the SEM image corresponding to $Ge_{20}Te_{76}Sn_4$ chalcogenide. No impurities were detected and the composition of Ge, Te and Sn are confirmed through elemental analysis.

APPENDIX VI : Energy dispersive X-Ray spectrum (EDS) of $Ge_{20}Te_{75}Sn_5$ chalcogenide glassy alloy

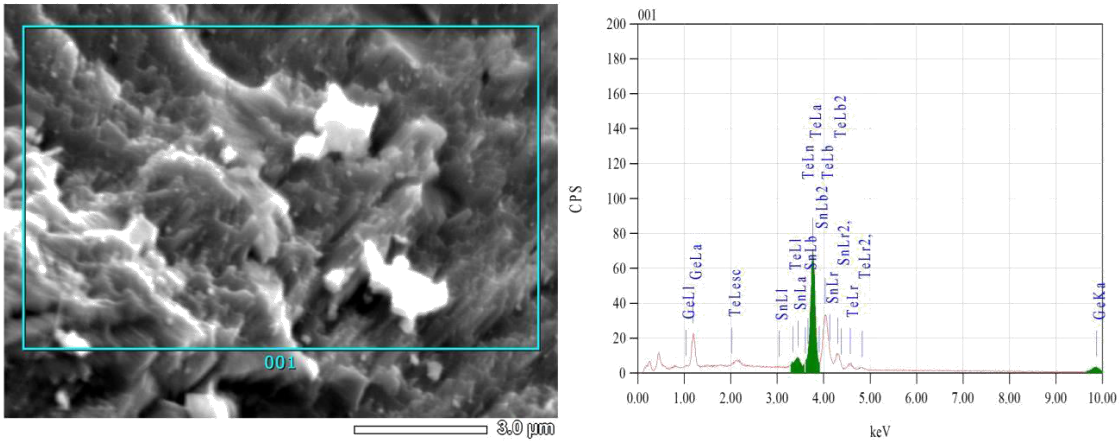

Element	(Kev)	Mass%	Error%	At%
Ge K	9.874	10.56	1.36	17.10
Sn L	3.442	6.93	0.32	6.87
Te L	3.768	82.51	0.38	76.84
Total		100.00		100.00

Figure VI Energy dispersive X-ray spectrum (EDS) obtained by scanning the area marked in the SEM image corresponding to $Ge_{20}Te_{75}Sn_5$ chalcogenide. No impurities were detected and the presence of Ge, Te and Sn and their corresponding composition are confirmed from the elemental analysis.

APPENDIX VII : Energy dispersive X-Ray spectrum (EDS) of $Ge_{20}Te_{73}Sn_7$ chalcogenide glassy alloy

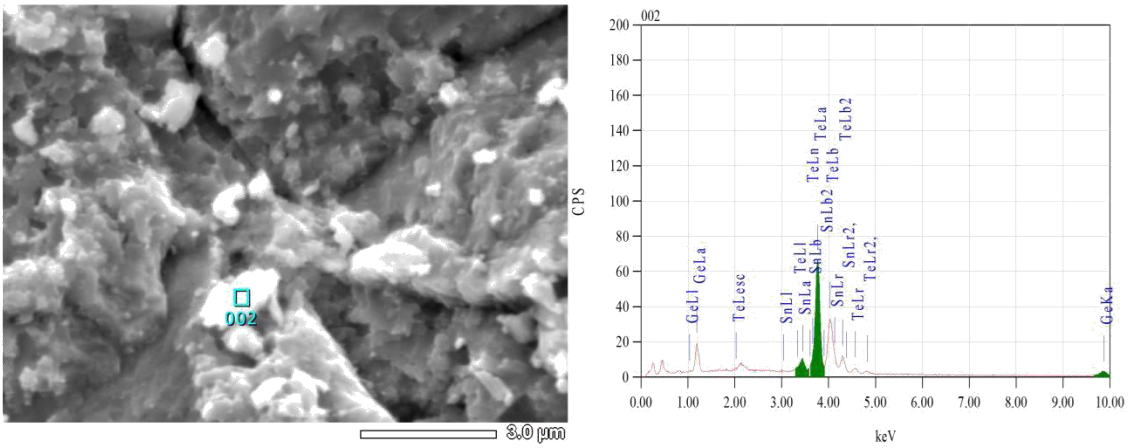

Element	(Kev)	Mass%	Error%	At%
Ge K	9.874	10.62	1.43	17.17
Sn L	3.442	8.65	0.34	8.56
Te L	3.768	80.73	0.40	74.27
Total		100.00		100.00

Figure VII Energy dispersive X-ray spectrum (EDS) obtained by scanning the area marked in the SEM image corresponding to $Ge_{20}Te_{73}Sn_7$ chalcogenide. No impurities were detected and the presence of Ge, Te and Sn and their corresponding composition are confirmed from the elemental analysis.

APPENDIX VIII : Energy dispersive X-Ray spectrum (EDS) of $Si_{20}Te_{80}$ chalcogenide glassy alloy

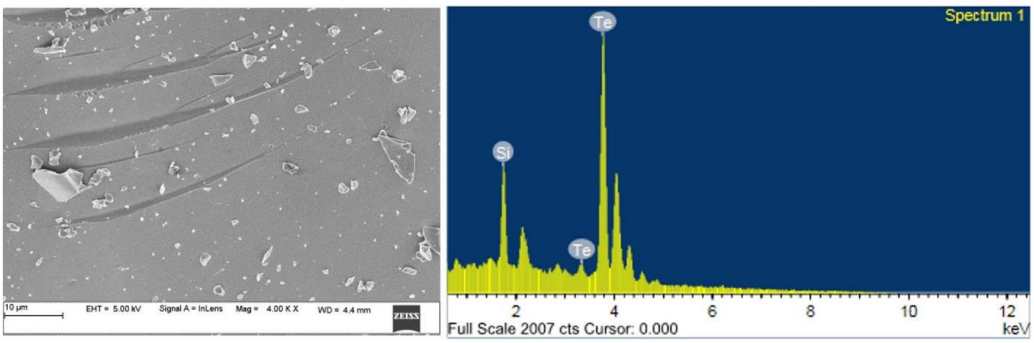

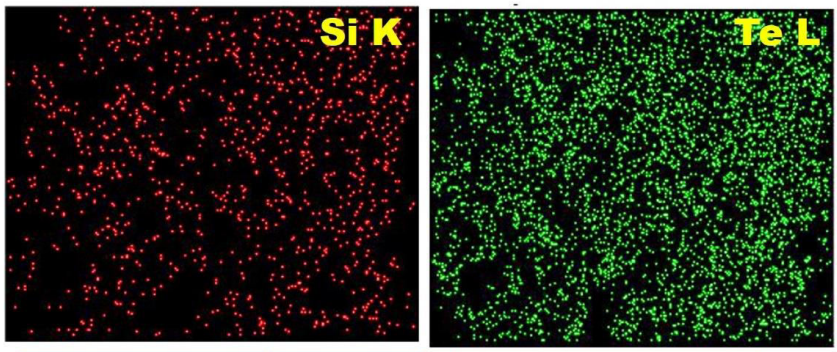

Element	At% (Theoretical)	At% (Practical)
Si K	20.00	18.16
Te L	80.00	81.84
Total	100.00	100.00

Figure VIII Energy dispersive X-Ray spectrum (EDS) obtained by scanning the area marked in the FESEM image corresponding to $Si_{20}Te_{80}$(host matrix) chalcogenide glassy alloy. No impurities were detected and the composition of Si and Te are confirmed through elemental analysis. EDS mapping analysis is employed to further confirm the starting materials and elemental distribution

APPENDIX IX : Energy dispersive X-Ray spectrum (EDS) of $Si_{20}Te_{79}Bi_1$ chalcogenide glassy alloy

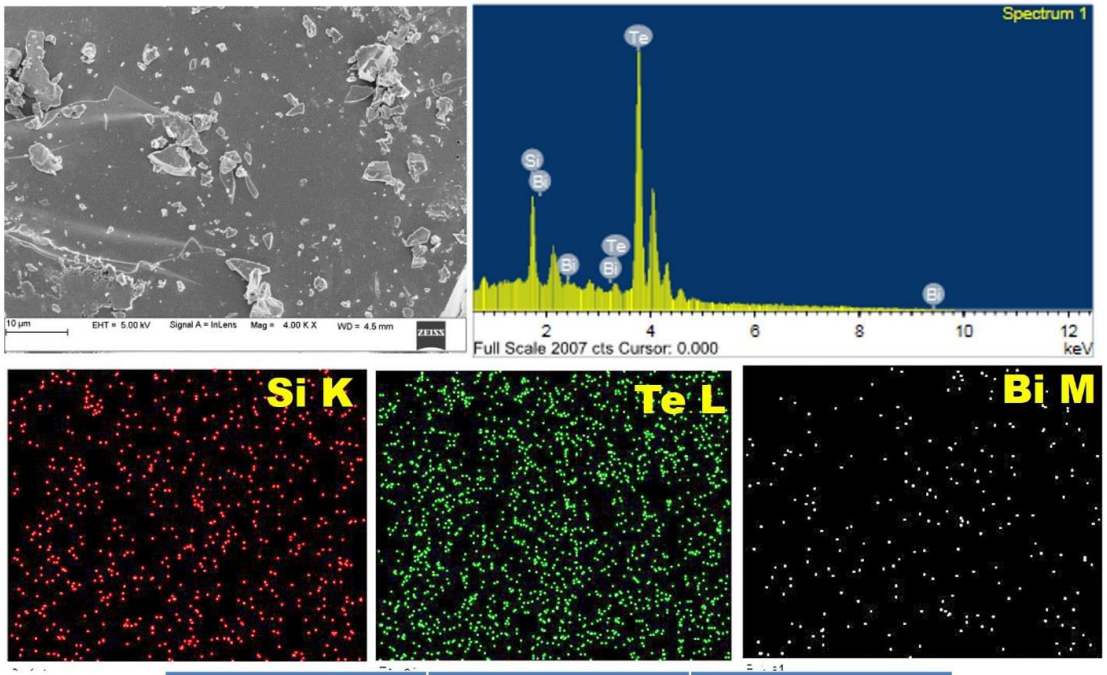

Element	At % (Theoretical)	At% (Practical)
Si K	20.00	18.51
Te L	79.00	80.31
Bi M	01.00	01.18
Total	100.00	100.00

Figure IX Energy dispersive X-Ray spectrum (EDS) obtained by scanning the area marked in the FESEM image corresponding to $Si_{20}Te_{79}Bi_1$ chalcogenide glassy alloy. No impurities were detected and the composition of Si, Te and Bi are confirmed through elemental analysis. EDS mapping analysis is employed to further confirm the starting materials and elemental distribution**.**

APPENDIX X : Energy dispersive X-Ray spectrum (EDS) of $Si_{20}Te_{78}Bi_2$ chalcogenide glassy alloy

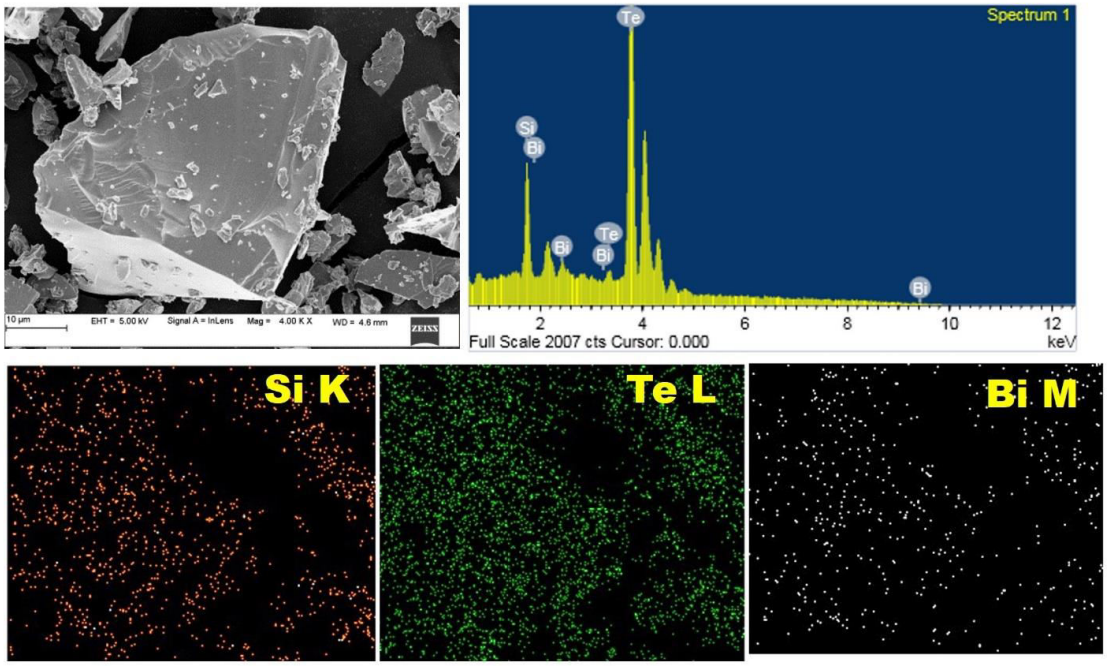

Element	At % (Theoretical)	At% (Practical)
Si K	20.00	19.46
Te L	78.00	78.52
Bi M	02.00	02.02
Total	100.00	100.00

Figure X Energy dispersive X-Ray spectrum (EDS) obtained by scanning the area marked in the FESEM image corresponding to $Si_{20}Te_{78}Bi_2$ chalcogenide glassy alloy. No impurities were detected and the composition of Si, Te and Bi are confirmed through elemental analysis. EDS mapping analysis is employed to further confirm the starting materials and elemental distribution

APPENDIX XI : Energy dispersive X-Ray spectrum (EDS) of $Si_{20}Te_{77}Bi_3$ chalcogenide glassy alloy

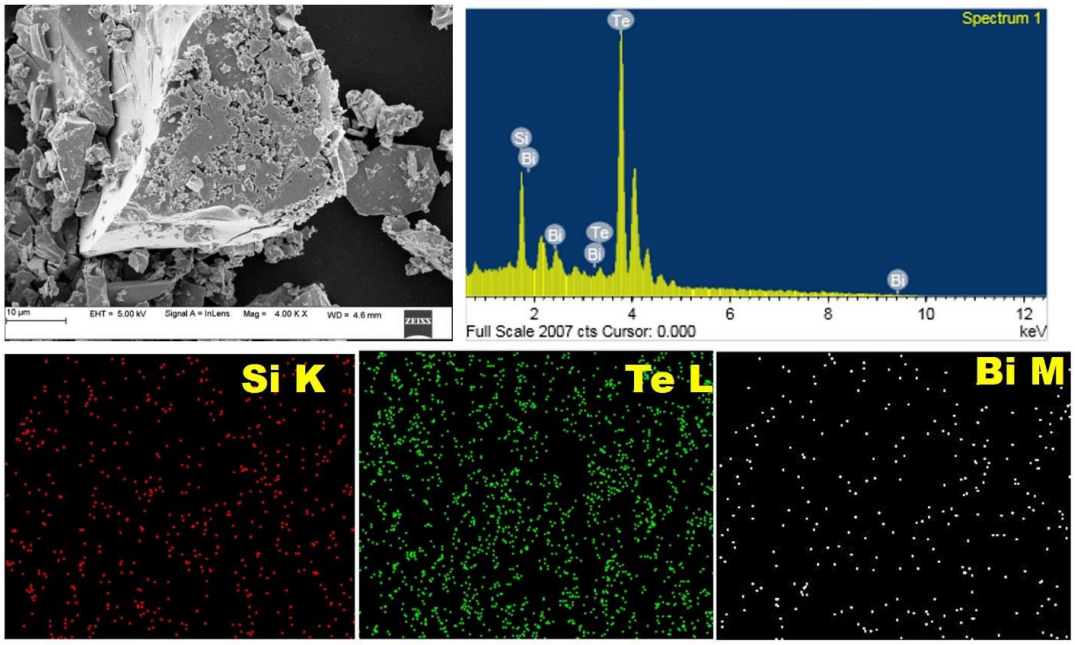

Element	At % (Theoretical)	At% (Practical)
Si K	20.00	18.62
Te L	77.00	78.33
Bi M	03.00	03.04
Total	100.00	100.00

Figure XI Energy dispersive X-Ray spectrum (EDS) obtained by scanning the area marked in the FESEM image corresponding to $Si_{20}Te_{77}Bi_3$ chalcogenide glassy alloy. No impurities were detected and the composition of Si, Te and Bi are confirmed through elemental analysis. EDS mapping analysis is employed to further confirm the starting materials and elemental distribution

REFERENCES

Abd El Ghani, H. A., Abd El Rahim, M. M., Wakkad, M. M., Abo Sehli, A., and Assraan, N. (2006). "Crystallization kinetics and thermal stability of some compositions of Ge–In–Se chalcogenide system." Phys. B Condens. Matter, 381(1–2), 156–163.

Abdel-Wahab, F. (2011). "Observation of phase separation in some Se–Te–Sn chalcogenide glasses." Phys. B Condens. Matter, 406(5), 1053–1059.

Abu-Sehly, A. A. (2009). "Structural and kinetic studies of crystallization of $Te_{51}As_{42}Cu_7$ chalcogenide glass." J. Alloys Compd., 486(1), 97–102.

Adam, J.-L., and Zhang, X. (2014). Chalcogenide Glasses: Preparation, Properties and Applications. Woodhead Publishing.

Adler, D. (1971). "Amorphous semiconductors." C R C Crit. Rev. Solid State Sci., 2(3), 317–465.

Adler, D. (1977). "Amorphous-Semiconductor Devices." Sci. Am., 236(5), 36–48.

Adler, D. (1980). "Defects in amorphous semiconductors." J. Non-Cryst. Solids, 35–36, Part 2, 819–824.

Aji, D. P. B., and Johari, G. P. (2010). "Enthalpy and entropy changes on structural relaxation of $Mg_{65}Cu_{25}Tb_{10}$ glass." Thermochim. Acta, 503–504, 121–131.

Anbarasu, M., and Asokan, S. (2004). "Electrical switching behavior of bulk As–Te–Si glasses: composition dependence and topological effects." Appl. Phys. A, 80(2), 249–252.

Anbarasu, M., and Asokan, S. (2007). "The influence of network rigidity on the electrical switching behaviour of Ge–Te–Si glasses suitable for phase change memory applications." J. Phys. Appl. Phys., 40(23), 7515.

Angell, C. A. (1985). "Spectroscopy simulation and scattering, and the medium range order problem in glass." J. Non-Cryst. Solids, Glass Science and Technology Problems and Prospects for 2004, 73(1), 1–17.

Angell, C. A. (1997). "Entropy and Fragility in Supercooling Liquids." J. Res. Natl. Inst. Stand. Technol., 102(2), 171–185.

Asha Bhat, N., and Sangunni, K. S. (2000). "A consistent approach towards Bi doping mechanism in chalcogenide glasses from Cp measurement in Ge–Se–Te–Bi system." Solid State Commun., 116(6), 297–302.

Asokan, S., and Lakshmi, K. P. (2012). "Electrical Switching and Other Properties of Chalcogenide Glasses." J. Indian Inst. Sci., 91(2), 319–330.

Augis, J., and Bennett, J. (1978). "Calculation of the Avrami parameters for heterogeneous solid state reactions using a modification of the Kissinger method." J. Therm. Anal. Calorim., 13(2), 283–292.

Avarami, M. (1941). "Granulation, phase change and microstructure III: kinetics of phase change." J Chem Phys, 9, 177–184.

Bhat, K. S., Barshilia, H. C., and Nagaraja, H. S. "Porous nickel telluride nanostructures as bifunctional electrocatalyst towards hydrogen and oxygen evolution reaction." Int. J. Hydrog. Energy.

Bhatia, K. L., Parthasarathy, G., Sharma, A., and Gopal, E. S. R. (1988). "Carrier-sign reversal in Bi-doped bulk amorphous semiconductors $Ge_{20}Te_{80-x}Bi_x$ Phys. Rev. B, 38(9), 6342–6344.

Bicerano, J., and Ovshinsky, S. R. (1985). "Chemical bond approach to the structures of chalcogenide glasses with reversible switching properties." J. Non-Cryst. Solids, 74(1), 75–84.

Böhmer, R., and Angell, C. A. (1994). "Global and local relaxations in glass-forming materials."

Böhmer, R., Ngai, K. L., Angell, C. A., and Plazek, D. J. (1993). "Nonexponential relaxations in strong and fragile glass formers." J. Chem. Phys., 99(5), 4201–4209.

Boolchand, P., Georgiev, D. G., and Micoulaut, M. (2002). "Nature of glass transition in chalcogenides." J Optoelectron Adv Mater, 4(4), 823.

Borisova, Z. (2013). Glassy Semiconductors. Springer Science & Business Media.

Campbell, K. A., and Anderson, C. M. (2007). "Phase-change memory devices with stacked Ge-chalcogenide/Sn-chalcogenide layers." Microelectron. J., 38(1), 52–59.

Chen, H. S. (1978). "A method for evaluating viscosities of metallic glasses from the rates of thermal transformations." J. Non-Cryst. Solids, 27(2), 257–263.

Chopra, K. L., and Bahl, S. K. (1970). "Structural, Electrical, and Optical Properties of Amorphous Germanium Films." Phys. Rev. B, 1(6), 2545–2556.

Colmenero, J., and Barandiaràn, J. M. (1979). "Crystallization of $Al_{23}Te_{77}$ glasses." J. Non-Cryst. Solids, 30(3), 263–271.

Cornet, J., and Rossier, D. (1973). "Properties and structure of As-Te glasses (II). Local order parameters and structural model." J. Non-Cryst. Solids, 12(1), 85–99.

Dalvi, A., Awasthi, A. M., Bharadwaj, S., and Shahi, K. (2003). "A comparative study of crystallization kinetics between conventionally melt quenched and mechanochemically synthesized $AgI–Ag_2O–CrO_3$ superionic system." Mater. Sci. Eng. B, 103(2), 162–169.

Das, C., Rao, G. M., and Asokan, S. (2011). "Electrical switching and thermal studies on bulk Ge–Te–Bi glasses." J. Non-Cryst. Solids, 357(1), 165–169.

Das, G. C., Bever, M. B., Uhlmann, D. R., and Moss, S. C. (1972). "Relaxation phenomena in amorphous selenium-tellurium alloys." J. Non-Cryst. Solids, 7(3), 251–270.

Debenedetti, P. G., and Stillinger, F. H. (2001). "Supercooled liquids and the glass transition." Nature, 410(6825), 259–267.

Deepika, Kuldeep Singh, R., and Narendra Sahai, S. (2012). "Kinetics of Phase Transformations and Thermal Stability of $Se_{58}Ge_{42-x}Pb_x$ (x = 15, 18 & 20) Glasses." New J. Glass Ceram., 2012.

Deringer, V. L., Zhang, W., Lumeij, M., Maintz, S., Wuttig, M., Mazzarello, R., and Dronskowski, R. (2014). "Bonding Nature of Local Structural Motifs in Amorphous GeTe." Angew. Chem. Int. Ed., 53(40), 10817–10820.

Dietzel, A. (1968). "Glass structure and glass properties." Glasstech, 22, 41.

Easteal, A. J., Sare, E. J., Moynihan, C. T., and Angell, C. A. (1974). "Glass-transition temperature, electrical conductance, viscosity, molar volume, refractive index, and proton magnetic resonance study of chlorozinc complexation in the system ZnCl2+LiCl+H2O." J. Solut. Chem., 3(11), 807–821.

Eckert, M. (2012). "Max von Laue and the discovery of X-ray diffraction in 1912." Ann. Phys., 524(5), A83–A85.

El-Khishin, A. T. (1979). "Memory switching processes in chalcogenide glasses."

Elliott, S. R. (1983). "Physics of amorphous materials." Longman Group Longman House Burnt Mill Harlow Essex CM 20 2 JE Engl. 1983.

Elliott, S. R. (1991). "Medium-range structural order in covalent amorphous solids." Nature, 354(6353), 445–452.

El-Mously, M. K., and El-Zaidia, M. M. (1978). "Thermal and electrical conductivities during the devitrification of $Te_{87.5}Se_{12.5}$ amorphous alloy." J. Non-Cryst. Solids, 27(2), 265–271.

Farid, A. S., and Atyia, H. E. (2015). "Glass transition and crystallization study of Te additive SeBi chalcogenide glass." J. Non-Cryst. Solids, 408, 123–129.

Fernandes, B. J., Sridharan, K., Munga, P., Ramesh, K., and Udayashankar, N. K. (2016). "Memory type switching behavior of ternary $Ge_{20}Te_{80-x}Sn_x$ ($0 \leqslant x \leqslant 4$) chalcogenide compounds." J. Phys. Appl. Phys., 49(29), 295104.

Frerichs, R. (1953). "New Optical Glasses with Good Transparency in the Infrared*." JOSA, 43(12), 1153–1157.

Fritzsche, H. (1974). "Switching and Memory in Amorphous Semiconductors." Amorph. Liq. Semicond., J. Tauc, ed., Springer US, 313–359.

Gill, P. S., Sauerbrunn, S. R., and Reading, M. (1993). "Modulated differential scanning calorimetry." J. Therm. Anal., 40(3), 931–939.

Gilman, J. J. (1975). "Mechanical behavior of metallic glasses." J. Appl. Phys., 46(4), 1625–1633.

Grenet, J., Larmagnac, J. P., Michon, P., and Vautier, C. (1981). "Relaxation structurelle dans les couches minces de sélénium amorphe au dessous de la température de transition vitreuse." Thin Solid Films, 76(1), 53–60.

Heera, P., Kumar, A., and Sharma, R. (2012). "Physical and dielectric properties of Sn doped Se-Te glassy system." J. Ovonic Res. Vol, 8(2), 29–40.

Hilton, A. R. (1970). "Optical properties of chalcogenide glasses." J. Non-Cryst. Solids, Proceedings of the Symposium on Semiconductor Effects in Amorphous Solids, 2, 28–39.

Howell, F. S., Bose, R. A., Macedo, P. B., and Moynihan, C. T. (1974). "Electrical relaxation in a glass-forming molten salt." J. Phys. Chem., 78(6), 639–648.

Hrubý, A. (1972). "Evaluation of glass-forming tendency by means of DTA." Czechoslov. J. Phys. B, 22(11), 1187–1193.

Ielmini, D., and Zhang, Y. (2007). "Evidence for trap-limited transport in the subthreshold conduction regime of chalcogenide glasses." Appl. Phys. Lett., 90(19), 192102.

Imran, M. M. A. (2011). "Thermal characterization of $Se_{85-x}Sb_{15}Sn_x(10\leq x\leq 13)$ chalcogenide glasses." Phys. B Condens. Matter, 406(22), 4289–4295.

Imran, M. M. A., Bhandari, D., and Saxena, N. S. (2001). "Enthalpy recovery during structural relaxation of $Se_{96}In_4$ chalcogenide glass." Phys. B Condens. Matter, 293 (3–4), 394–401.

Jain, P. K., Deepika, and Saxena, N. S. (2009). "Glass transition, thermal stability and glass-forming ability of $Se_{90}In_{10-x}Sb_x$ (x = 0, 2, 4, 6, 8, 10) chalcogenide glasses." Philos. Mag., 89(7), 641–650.

Johnson, W. A., and Mehl, R. F. (1939). "Reaction kinetics in processes of nucleation and growth." Trans Aime, 135(8), 396–415.

Jones, G., and Collins, R. A. (1979). "Threshold and memory switching in amorphous selenium thin films." Phys. Status Solidi A, 53(1), 339–350.

Karuppannan, R., Ganesan, V., and Asokan, S. (2011). "Electrical Switching in Cu–As–Se Glasses." Int. J. Appl. Glass Sci., 2(1), 52–62.

Kasap, S. O., and Juhasz, C. (1986). "Kinematical transformations in amorphous selenium alloys used in xerography." J. Mater. Sci., 21(4), 1329–1340.

Kaswan, A., Kumari, V., Patidar, D., Saxena, N. S., and Sharma, K. (2013). "Kinetics of Phase Transformations and Thermal Stability of $Ge_xSe_{70}Sb_{30-x}$ (x = 5, 10, 15, 20) Chalcogenide Glasses." New J. Glass Ceram., 2013.

Kato, N., Takeda, Y., Fukano, T., Motohiro, T., Kawai, S., and Kuno, H. (1999). "Compositional Dependence of Optical Constants and Microstructures of GeSbTe Thin Films for Compact-Disc-Rewritable (CD-RW) Readable with Conventional CD-ROM Drives." Jpn. J. Appl. Phys., 38(3S), 1707.

Kauzmann, W. (1948). "The Nature of the Glassy State and the Behavior of Liquids at Low Temperatures." Chem. Rev., 43(2), 219–256.

Kissinger, H. E. (1957). "Reaction Kinetics in Differential Thermal Analysis." Anal. Chem., 29(11), 1702–1706.

Kolomiets, B. T., and Lebedev, E. A. (1963). "Current-Voltage Characteristics of a Point Contact with Vitreous Semiconductors." Radiotekh Elektron, 8, 2097–2098.

Kotkata, M. F., and El-Mously, M. K. (1983). "A survey of amorphous Se- Te semiconductors and their characteristic aspects of crystallization." Acta Phys. Hung., 54(3–4), 303–312.

Kumar, S., and Singh, K. (2011). "The effect of indium additive on crystallization kinetics and thermal stability of Se–Te–Sn chalcogenide glasses." Phys. B Condens. Matter, 406(8), 1519–1524.

Lafi, O. A., and Imran, M. M. A. (2011). "Compositional dependence of thermal stability, glass-forming ability and fragility index in some Se–Te–Sn glasses." J. Alloys Compd., 509(16), 5090–5094.

Lafi, O. A., Imran, M. M. A., Abdullah, M. K., and Al-Sakhel, S. A. (2013). "Thermal characterization of $Se_{100-x}Sn_x$ (x = 4, 6 and 8) chalcogenide glasses using differential scanning calorimeter." Thermochim. Acta, 560, 71–75.

Larmagnac, J. P., Grenet, J., and Michon, P. (1981). "Glass transition temperature dependence on heating rate and on ageing for amorphous selenium films." J. Non-Cryst. Solids, 45(2), 157–168.

Lasocka, M. (1978). "Thermal evidence of overlapping effects of glass transition and crystallization, derived from two different glassy phases in the phase-separated system $Te_{80}Ge_{12.5}Pb_{7.5}$." J. Mater. Sci., 13(9), 2055–2059.

Lencer, D., Salinga, M., and Wuttig, M. (2011). "Design Rules for Phase-Change Materials in Data Storage Applications." Adv. Mater., 23(18), 2030–2058.

Lezal, D. (2003). "Chalcogenide glasses-survey and progress." J. Optoelectron. Adv. Mater., 5(1), 23–34.

Lokesh, R., Udayashankar, N. K., and Asokan, S. (2010). "Electrical switching behavior of bulk $Si_{15}Te_{85-x}Sb_x$ chalcogenide glasses – A study of compositional dependence." J. Non-Cryst. Solids, 356(6–8), 321–325.

Macmillan, J. A. (1965). "Crystallization kinetics in new Sb-As-Se-Te amorphous glasses." J Phys Chem, 42, 3497.

Mahadevan, S., Giridhar, A., and Singh, A. K. (1986). "Calorimetric measurements on as-sb-se glasses." J. Non-Cryst. Solids, 88(1), 11–34.

Maimon, J., Spall, E., Quinn, R., and Schnur, S. (2001). "Chalcogenide-based non-volatile memory technology." 2001 IEEE Aerosp. Conf. Proc. Cat No01TH8542, 2289–2294 vol.5.

Málek, J. (2000). "Kinetic analysis of crystallization processes in amorphous materials." Thermochim. Acta, 355(1), 239–253.

Mehta, N. (2006). "Applications of chalcogenide glasses in electronics and optoelectronics: A review." JSIR Vol6510 Oct. 2006.

Modgil, V., and Rangra, V. S. (2014). "Effect of Sn Addition on Thermal and Optical Properties of Glass." J. Mater., 2014, e318262.

Mott, N. F., and Davis, E. A. (1979). "Electronic processes in non-crystalline solids." Clarendon Oxf., 465.

Moynihan, C. T., Easteal, A. J., Wilder, J., and Tucker, J. (1974). "Dependence of the glass transition temperature on heating and cooling rate." J. Phys. Chem., 78(26), 2673–2677.

Moynihan, C. T., and Gupta, P. K. (1978). "The order parameter model for structural relaxation in glass." J. Non-Cryst. Solids, 29(2), 143–158.

Moynihan, C. T., Macedo, P. B., Montrose, C. J., Montrose, C. J., Gupta, P. K., DeBolt, M. A., Dill, J. F., Dom, B. E., Drake, P. W., Easteal, A. J., Elterman, P. B., Moeller, R. P., Sasabe, H., and Wilder, J. A. (1976). "Structural Relaxation in Vitreous Materials*." Ann. N. Y. Acad. Sci., 279(1), 15–35.

Mullin, J. W. (2001). Crystallization. Butterworth-Heinemann.

Murthy, C. N., Ganesan, V., and Asokan, S. (2005). "Electrical switching and topological thresholds in Ge-Te and Si-Te glasses." Appl. Phys. A, 81(5), 939–942.

Murugavel, S., and Asokan, S. (1998). "Composition tunable memory and threshold switching in $Al_{20}As_xTe_{80-x}$ semiconducting glasses." J. Mater. Res., 13(10), 2982–2987.

Nagels, P. (1979). "Electronic transport in amorphous semiconductors." Amorph. Semicond., Topics in Applied Physics, Springer, Berlin, Heidelberg, 113–158.

Nakashima, K., and Kao, K. C. (1979). "Conducting filaments and switching phenomena in chalcogenide semiconductors." J. Non-Cryst. Solids, 33(2), 189–204.

Naqvi, S. F., and Saxena, N. S. (2011). "Kinetics of phase transition and thermal stability in $Se_{80-x}Te_{20}Zn_x$ (x = 2, 4, 6, 8, and 10) glasses." J. Therm. Anal. Calorim., 108(3), 1161–1169.

Nascimento, M. L. F., Souza, L. A., Ferreira, E. B., and Zanotto, E. D. (2005). "Can glass stability parameters infer glass forming ability?" J. Non-Cryst. Solids, 351(40–42), 3296–3308.

O'Dwyer, J. J. (1969). "Theory of Dielectric Breakdown in Solids." J. Electrochem. Soc., 116(2), 239–242.

Ovshinsky, S. R. (1968). "Reversible Electrical Switching Phenomena in Disordered Structures." Phys. Rev. Lett., 21(20), 1450–1453.

Owen, A. E., and Robertson, J. M. (1973). "Electronic conduction and switching in chalcogenide glasses." IEEE Trans. Electron Devices, 20(2), 105–122.

Ozawa, T. (1965). "A new method of analyzing thermogravimetric data." Bull. Chem. Soc. Jpn., 38(11), 1881–1886.

Ozawa, T. (1971). "Kinetics of non-isothermal crystallization." Polymer, 12(3), 150–158.

Phillips, J. C. (1979). "Topology of covalent non-crystalline solids I: Short-range order in chalcogenide alloys." J. Non-Cryst. Solids, 34(2), 153–181.

Phillips, J. C. (1981). "Topology of covalent non-crystalline solids II: Medium-range order in chalcogenide alloys and A-Si(Ge)." J. Non-Cryst. Solids, 43(1), 37–77.

Phillips, J. C., and Thorpe, M. F. (1985). "Constraint theory, vector percolation and glass formation." Solid State Commun., 53(8), 699–702.

Piarristeguy, A., Ramonda, M., Ureña, A., Pradel, A., and Ribes, M. (2007). "Phase separation in Ag–Ge–Se glasses." J. Non-Cryst. Solids, 353(13), 1261–1263.

Popescu, C. (1975). "The effect of local non-uniformities on thermal switching and high field behaviour of structures with chalcogenide glasses." Solid-State Electron., 18(7), 671–681.

Prakash, S., Asokan, S., and Ghare, D. B. (1994). "Electrical switching behaviour of semiconducting aluminium telluride glasses." Semicond. Sci. Technol., 9(8), 1484.

Prakash, S., Asokan, S., and Ghare, D. B. (1996). "Easily reversible memory switching in Ge - As - Te glasses." J. Phys. Appl. Phys., 29(7), 2004.

Predeep, P., Saxena, N. S., and Kumar, A. (1997). "Crystallization and specific heat studies of $Se_{100-x}Sb_x$ (x = 0, 2 and 4) glass." J. Phys. Chem. Solids, 58(3), 385–389.

Pumlianmunga, and Ramesh, K. (2016). "Electrical switching and aluminium speciation in Al-As-Te glasses." J. Non-Cryst. Solids, 452, 253–258.

Pumlianmunga, and Ramesh, K. (2017). "Electrical switching in Sb doped $Al_{23}Te_{77}$ glasses." J. Phys. Chem. Solids, 107, 68–74.

Rahman, M. M., Rukmani, K., and Asokan, S. (2011). "Electrical switching studies on Ge–Te–Tl chalcogenide glasses: Effect of thallium on the composition dependence of switching voltages." J. Non-Cryst. Solids, 357(3), 946–950.

Ramesh, K., Asokan, S., and Gopal, E. S. R. (2006). "Chemical ordering and fragility minimum in Cu–As–Se glasses." J. Non-Cryst. Solids, 352(26), 2905–2912.

Ramesh, K., Asokan, S., Sangunni, K. S., and Gopal, E. S. R. (1999). "Electrical switching in germanium telluride glasses doped with Cu and Ag." Appl. Phys. A, 69(4), 421–425.

Ramesh, K., Asokan, S., Sangunni, K. S., and Gopal, E. S. R. (2000). "Glass formation in germanium telluride glasses containing metallic additives." J. Phys. Chem. Solids, 61(1), 95–101.

Raoux, S., and Wuttig, M. (2010). Phase Change Materials: Science and Applications. Springer Science & Business Media.

Reinberg, A. R. (1998). "Chalcogenide memory cell with a plurality of chalcogenide electrodes."

Rocca, J., Erazú, M., Fontana, M., and Arcondo, B. (2009). "Crystallization process on amorphous GeTeSb samples near to eutectic point $Ge_{15}Te_{85}$." J. Non-Cryst. Solids, Non-Oxide and New Optical Glasses 16Proceedings of the 16th International Symposium on Non-Oxide and New Optical Glasses16th International Symposium on Non-Oxide and New Optical Glasses Materials, 355(37–42), 2068–2073.

Saad, M., and Poulain, M. (1987). "Glass forming ability criterion." Mater. Sci. Forum, Trans Tech Publ, 11–18.

Savage, J. A. (1972). "Glass formation and D.S.C. data in the Ge-Te and As-Te memory glass systems." J. Non-Cryst. Solids, 11(2), 121–130.

Schultz-Sellack, C. (n.d.). "Diathermansie einer Reihe von Stoffen für Wärme sehr geringer Brechbarkeit." Ann. Phys., 215(1), 182–187.

Selvaraju, V. C., Asokan, S., and Srinivasan, V. (2003). "Electrical switching studies on $As_{40}Te_{60-x}Se_x$ and $As_{35}Te_{65-x}Se_x$ glasses." Appl. Phys. A, 77(1), 149–153.

Sharma, A., Kumar, H., and Mehta, N. (2012). "Determination of specific heat in multi-component chalcogenide glasses of Se–Te–Sn–Pb system using modulated differential scanning calorimetry." Mater. Lett., 86, 54–57.

Sharmila, B. H., and Asokan, S. (2005). "Studies on electrical switching behavior of As-Te-Tl glasses – effect of local structure on switching type and composition dependence of switching voltages." Appl. Phys. A, 82(2), 345–348.

Shelby, J. E. (1979). "Thermal expansion of amorphous metals." J. Non-Cryst. Solids, 34(1), 111–119.

Sherchenkov, A., Kozyukhin, S., and Babich, A. (2014). "Estimation of kinetic parameters for the phase change memory materials by DSC measurements." J. Therm. Anal. Calorim., 117(3), 1509–1516.

Shimakawa, K., Inagaki, Y., and Arizumi, T. (1973). "Thermal Switching in Chalcogenide Glass Semiconductors." Jpn. J. Appl. Phys., 12(7), 1043–1046.

Shiryaev, V. S., and Churbanov, M. F. (2017). "Recent advances in preparation of high-purity chalcogenide glasses for mid-IR photonics." J. Non-Cryst. Solids, 475(Supplement C), 1–9.

Singh, A. K. (2012). "Surface Morphology and Crystallization Kinetics of Multicomponent Chalcogenide Glasses." Mater. Focus, 1(1), 50–56.

Singh, A. K. (2013). "Crystallization kinetics of Se–Zn–Sb nano composites chalcogenide alloys." J. Alloys Compd., 552, 166–172.

Singh, J., and Shimakawa, K. (2003). Advances in amorphous semiconductors. CRC Press.

Stocker, H. J. (1970). "Phenomenology of switching and memory effects in semiconducting chalcogenide glasses." J. Non-Cryst. Solids, 2, 371–381.

Takhor, R. L. (1972). "Determining the suitability of nucleating agents for glass-ceramics." Adv. Nucleation Cryst. Glas., 166–172.

Titus, S. S. K., Chatterjee, R., Asokan, S., and Kumar, A. (1993). "Electrical switching and short-range order in As-Te glasses." Phys. Rev. B, 48(19), 14650–14652.

Tohge, N., Minami, T., Yamamoto, Y., and Tanaka, M. (1980). "Electrical and optical properties of n-type semiconducting chalcogenide glasses in the system Ge-Bi-Se." J. Appl. Phys., 51(2), 1048–1053.

Tonchev, D., and Kasap, S. O. (1999). "Thermal properties of SbxSe100−x glasses studied by modulated temperature differential scanning calorimetry." J. Non-Cryst. Solids, 248(1), 28–36.

Upadhyay, M., and Murugavel, S. (2013). "Correlation between crystallization behavior, electrical switching and local atomic structure of Ge–Te glasses." J. Non-Cryst. Solids, 368, 34–39.

Vilgis, T. A. (1993). "Strong and fragile glasses: A powerful classification and its consequences." Phys. Rev. B, 47(5), 2882–2885.

Warren, A. C. (1970). "Thermal switching in semiconducting glasses." J. Non-Cryst. Solids, 4, 613–616.

Waser, R., Dittmann, R., Salinga, M., and Wuttig, M. (2010). "The role of defects in resistively switching chalcogenides." Int. J. Mater. Res., 101(2), 182–198.

Wright, A. C., Hulme, R. A., Grimley, D. I., Sinclair, R. N., Martin, S. W., Price, D. L., and Galeener, F. L. (1991). "The structure of some simple amorphous network solids revisited." J. Non-Cryst. Solids, 129(1), 213–232.

Wuttig, M. (2005). "Phase-change materials: Towards a universal memory?" Nat. Mater., 4(4), 265–266.

Xu, M., Cheng, Y. Q., Sheng, H. W., and Ma, E. (2009). "Nature of Atomic Bonding and Atomic Structure in the Phase-Change $Ge_2Sb_2Te_5$ Glass." Phys. Rev. Lett., 103(19), 195502.

Zallen, R. (2008). The Physics of Amorphous Solids. John Wiley & Sons.

Zhang, S. N., Zhu, T. J., and Zhao, X. B. (2008). "Crystallization kinetics of Si15Te85 and Si20Te80 chalcogenide glasses." Phys. B Condens. Matter, 403(19–20), 3459–3463.

Zhou, G.-F. (2001). "Materials aspects in phase change optical recording." Mater. Sci. Eng. A, RQ10, Tenth International Conference on Rapidly Quenched and Metastable Materials, 304, 73–80.

LIST OF PUBLICATIONS BASED ON PhD RESEARCH WORK

Indian Patent

Brian Jeevan Fernandes, N K Udayashankar and S Harish, High temperature melt quenching system for preparing glassy alloys and a method thereof, Patent Application No. **201641044209**, (2016), Complete patent has been filed. Date of filing : 24-12-2016, Publication date : 29-06-2018.

International Journals

Brian Jeevan Fernandes, Kishore Sridharan, Pumlian Munga, K Ramesh and N K Udayashankar, Memory type switching behavior of $Ge_{20}Te_{80-x}Sn_x$ ($0 \leq x \leq 4$) chalcogenide compounds, **J. Phys. D: Appl. Phys**. 49, (2016) IOP Publishing. doi:10.1088/0022-3727/49/29/295104

Brian Jeevan Fernandes, N Naresh, K Ramesh, Kishore Sridharan and N K Udayashankar, Crystallization kinetics of Sn doped $Ge_{20}Te_{80-x}Sn_x$ ($0 \leq x \leq 4$) chalcogenide glassy alloys, **J. Alloys Compd.** 721, (2017) Elsvier Publishing, doi.org/10.1016/j.jallcom.2017.06.070

Brian Jeevan Fernandes, K Ramesh and N K Udayashankar, "Electrical switching in $Si_{20}Te_{80-x}Bi_x$ ($0 \leq x \leq 3$) chalcogenide glassy alloys." **J. Non-Cryst. Solids.**(2018) Elsvier Publishing, doi.org/10.1016/j.jnoncrysol.2018.01.001

Brian Jeevan Fernandes, Pumlian Munga, K Ramesh and N K Udayashankar, "Electrical switching and thermal behavior of ternary $Si_{15}Te_{85-x}Bi_x$ ($0 \leq x \leq 2$) chalcogenide glasses" **Materials Today: Proceedings** (2018) 5 (10), 21292-21298

Brian Jeevan Fernandes, Pumlian Munga, K Ramesh and N K Udayashankar, "Thermal stability and crystallization kinetics of Bi doped Si15Te85-xBix ($0 \leq x \leq 2$) chalcogenide glassy alloys" **Materials Today: Proceedings** (2018) 5 (8), 16237-16245

Brian Jeevan Fernandes, K Ramesh and N K Udayashankar, "Crystallization kinetics in $Si_{20}Te_{80-x}Bi_x$ ($0 \leq x \leq 3$) chalcogenide glasses." Submitted to **Journal of Material Science and Engineering: B**, Elsvier Publishing.

Presentations in the International Conferences

Brian Jeevan Fernandes and N K Udayashankar, Synthesis and studies on surface morphology of Te-based chalcogenide glasses. International Conference on Electron Microscopy **EMSI -2014**, University of Delhi, Delhi, (POSTER)

Brian Jeevan Fernandes, Pumlian Munga, K Ramesh and N K Udayashankar, Electrical switching studies of ternary $Si_{15}Te_{85-x}Bi_x$ ($0 \leq x \leq 2$) chalcogenide glasses. International Conference on Smart Engineering Materials **ICSEM - 2016**, RV College of Engineering Bengaluru (ORAL).

Brian Jeevan Fernandes, Pumlian Munga, K Ramesh and N K Udayashankar, Thermal stability and crystallization kinetics of Bi doped $Si_{15}Te_{85-x}Bi_x$ ($0 \leq x \leq 2$) chalcogenide glassy alloys. International Conference on Advanced Materials **SCICON - 2016**, Amrita Vishwa Vidyapeetham, Coimbatore, (ORAL).

Brian Jeevan Fernandes

Research Scholar

(+91) 9945362005
brainjf.ph11f06@nitk.edu.in

"Success is always sweet, but the secret of success is sweat"

Education

2012–2018 **PhD in Physics**, *National Institute of Technology Karnataka*, Surathkal.

2006–2008 **MSc in Electronics**, *Mangalore University*, Mangalore.

2003–2006 **BSc in Physics, Electronics, and Maths**, *St. Aloysius Degree College*, Mangalore.

Experience

2012 - 2017 **Teaching Assistant**, *National Institute of Technology Karnataka*, Surathkal.
I worked as a tutor for MSc students, teaching them electronics.Handled Engg. Physics Laboratory course for B.Tech students and M.Sc students.

Nov 2008 - Jan 2012 **Electronics Lecturer**, *Sharada PU College*, Mangalore.
Taught electronics to I and II PUC classes, with incredible success.

2009 - 2011 **Electronics Lecturer**, *Cosmos Tutorials*, Mangalore.
I worked as a tutor in analog electronic circuits, microprocessors, linear ICs and applications. I taught students of engineering.

Jan 2008 - Aug 2008 **Project Trainee**, *WEP Peripherals*, Mysore.
I worked in the R & D department, on the subject of power electronics

Jul 2005 - Apr 2006 **Volunteer Kannada Tutor**, *St. Aloysius College*, Mangalore.
I volunteered to teach Kannada to students from the Social Service department in St. Aloysius College.

Honours and Awards

2006 **The Best Volunteer**, *The best volunteer at the university level*, Mangalore.

2006 **NSS Special Award**, *For excellent service towards the college*, Mangalore.

2006 **Meritorious Service Award**, *For an overall contribution towards the college*, St. Aloysius Degree College, Mangalore.

2003 **Constructive Activity Award**, *For the best overall student*, St. Aloysius Degree College, Mangalore.

Extra-Curricular Activities

National Service Scheme(NSS), Mangalore.
I served as the secretary for NSS St. Aloysius College section from 2004 to 2005. I have served with the NSS with numerous distinctions, in addition to having given talks on AIDS, and Malaria.

Computer Skills

Langages (Beginner) C, MATLAB

Software Packages Microsoft Office, NI Multisim, Origin

Languages

Fluent English, Kannada, Hindi, Tulu, Konkani

Patent

High temperature melt quenching system for preparing glassy alloys and a method thereof. *Brian Jeevan Fernandes, N K Udayashankar and S Harish.* **Indian Patent Application No.201641044209**. *Complete Patent has been Published*

Publications

Memory type switching behavior of $Ge_{20}Te_{80-x}Sn_x$ ($0 \leq x \leq 4$) chalcogenide compounds. *Brian Jeevan Fernandes, Kishore Sridharan, Pumlian Munga, K Ramesh and N K Udayashankar.* **J. Phys. D: Appl.Phys. 49 (2016) IOP Publishing.**

Crystallization kinetics of Sn doped Ge20Te80-xSnx chalcogenide glassy alloys. *Brian Jeevan Fernandes, N Naresh, K Ramesh, Kishore Sridaran and N K Udayashankar.* **J. Alloys Compd, 721, (2017) Elsevier Publication**

Electrical switching in Si20Te80-xBix chalcogenide glassy alloys. *Brian Jeevan Fernandes, K Ramesh and N K Udayashankar.* **J. Non-Cryst Solids, 483, (2018), Elsevier Publication**

Electrical switching and thermal behavior of ternary Si15Te85-xBix chalcogenide glasses. *Brian Jeevan Fernandes, Pumlianmunga, K Ramesh and N K Udayashankar* **Materials Today: Proceedings 5(10), 21292-21298, Elsevier Publication**

Thermal stability and crystalization kinetics of Bi doped Si15Te85-xBix chalcogenide glassy alloys. *Brian Jeevan Fernandes, Pumlianmunga, K Ramesh and N K Udayashankar* **Materials Today: Proceedings 5(10), 21292-21298, Elsevier Publication**

Gamma irradiation effect on structural,optical and electical properties of organometallic potassium hydrogen oxalate oxalic acids dihydrate single crystal. *K Mahendra, K K Nayak, Brian Jeevan Fernandes and N K Udayashankar* **Journal of Materials Science: Materials in Electronics 29(22), 18905-18912, Springer Publication**

Presentations at International Conferences

Synthesis and studies on surface morphology of Te-based chalcogenide glasses. *Brian Jeevan Fernandes and N K Udayashankar*, **International Conference on Electron Microscopy EMSI - 2014** , University of Delhi, Delhi.(POSTER)

Electrical switching studies of ternary $Si_{15}\ Te_{85-x}\ Bi_x$ ($0 \leq x \leq 2$) chalcogenide glasses. *Brian Jeevan Fernandes, Pumlian Munga, K Ramesh and N. K. Udayashankar*, **International Conference on Smart Engineering Materials ICSEM-2016**, RV College Bengaluru, Bengaluru .(ORAL)

Thermal stability and crystallization kinetics of Bi doped Si15Te85-xBix chalcogenide glassy alloys. *Brian Jeevan Fernandes, Pumlian Munga, K Ramesh and N K Udayashankar*, **International Conference on Advanced Materials SCICON-2016**,Amrita Vishwa Vidyapeetham, Coimbatore. (ORAL)

AC conductivity and dielectric properties of Si20Te80-xBix (x=1,2) chalcogenide semiconductors. *Brian Jeevan Fernandes, Achyutha Kodibailu, M N Satyanarayam and N K Udayashankar* **International Conference on Recent Advances in Material Science and BioPhysics RAMSB -2018** Mangalore University, Mangalagangothri, Mangalore.(ORAL)

References

Dr. Leela Upadhyaya, *Former Principal*, Sharada Pre-University College.
Phone : (+91) 9900329259

Prof. N K Udayashankar, *Dept of Physics*, NITK - Surathkal.
Phone : (+91) 99020 64124